'THE ELECTRICAL PROPERTIES OF WET BONE'

by

Christopher Eriksson, B.Sc. , A.R.C.S

A Thesis submitted for the degree of
Doctor of Philosophy in the
University of London.

Department of Electrical Engineering,
Imperial College of Science and Technology,
London

Dec. 1968

Abstract

The electrical signals resulting from the stressing of human tendon collagen have been investigated as a function of pH. The isoelectric point for this collagen was measured by micro-cell electrophoresis.It is concluded that fully wet tendon collagen is not piezoelectric, and that the electrical signals produced upon stressing the tendon are streaming potentials.

The piezoelectric properties of dry and wet, human and beef bone specimens have been quantitatively investigated in the direct and converse piezoelectric effects at low audio frequencies.The wet measurements have been determined as a function of pH. Quantitative evaporation measurements have been conducted on wet bone pieces where the mass is continously measured as a function of water content.The directional resistivities of stressed and unstressed wet bone pieces have been measured as the water content is lowered from natural evaporation.

It is concluded that the electrical signals arising from the stressing of wet bone are mainly streaming potentials, although the bone collagen is piezoelectric.The evaporation measurements identify two different types of bound water in bone.Both these are interpreted as protein water, and are associated with the bone collagen

A and B bands.The resistivity results show that when the collagen fibres are sheared the collagen A band water molecules re-orientate from the bone long to a transverse direction.It is suggested that loss of skeletal stress may reduce the protein-mineral binding force by virtue of this reorientation, and that the primary mineral seeding may occur in the collagen A bands. It is tentatively suggested that this reorientation may be responsible for the occurrence of mineralization of the protein in connective tissues when sudden changes in direction occur.

CONTENTS

ACKNOWLEDGEMENTS

The author thanks Professor J.C.Anderson of Imperial College, for originally suggesting the problem, supervising this work and many useful discussions.Financial support from the Medical Research Council is gratefully acknowledged in the form of a Research Assistantship.Thanks are also extended to Dr. R.W.B.Stophens of Imperial College(in whose laboratory the initial apparatus was built) for helpful suggestions.

Chapter One

Review of Previous Work

The majority of experiments carried out in this general field have been post-war and conducted in two countries, the United States of America and Japan. The work in Japan has been done by Fukada and Yasuda, whereas in the United States many more people have contributed. Two schools of thought have arisen from these experiments. The first supports Fukada's general observations that the stress-generated electrical potentials in dried bone and collagen [1,2,3,4] are classically piezoelectric and therefore highly directional. The other school holds that the potentials in bone derive from the stressing of a myriad of P-N junctions, formed from collagen P-type and apatite N-type crystals, with no mention of directionality. The former school has demonstrated that dried tendon collagen itself is piezoelectric [2], its greatest coefficient being of the same order as the d_{11} of quartz. Dainora [5] quotes that he obtained nearly 80% of the stress-generated potentials in bone when the apatite was removed by formic acid, and remarks that ' it is difficult to conceive of P-N junctions being formed when the N part has been

removed' . The PN junction school of thought has conducted many experiments to look for free electron sites in bone. These include extensive qualitative Electron Paramagnetic Resonance measurements on bone and its main constituents [6,7,8], and also experiments designed to investigate photoelectric effects [9], and fluorescence under ultra-violet excitation.[10] They conclude from the EPR measurements that the bone g-2 resonance signal is not attributable to a simple combination of that obtained for collagen and apatite separately, and that a direct physical bond exists between the collagen and the apatite. They note that there is a distinct difference in the results betwwen dry and wet collagen, and they attribute this to the ability of the collagen fibre to structure absorbed water to an high degree.

Becker and Brown [9] conclude in their paper on the ' Photoelectric Effects in human bone ' that the results support the P-N junction theory. However Spruch and Shamos [11] in a later paper conclude that the effect of light on bone is simple heating. Becker, Marino, and Bachman [12] have measured the dielectric constant of human cortical bone in varying degrees of wetness, at 1, 10, and 100 kHz, in a direction perpendicular to the long direction, and observed a ' critical hydration point ', which they interpret as the

bound water of the system at 37mg H_2O to 48mg H_2O/gm bone.

S.B. Lang[13] investigated the pyroelectric effect in cow bone and tendon specimens all of which had been dried by heating to temperatures between 50 and 105°C.He observed that voltages only appeared in a direction parallel to the collagen fibres.He gives the pyroelectric coefficient for hoof tendon as approximately 4.1×10^{-13} coulomb $cm^{-3}/°C$ and that for the phalanx as 2.5×10^{-13} coulomb $cm^{-3}/°C$.It is not stated whether the observed effect is primary pyroelectricity, that is at constant strain when the sample is clamped, or whether the effect is secondary pyroelectricity at constant stress when the sample is free to strain.What is observed in secondary pyroelectricity is the primary effect plus the piezoelectric voltage caused by the thermal strain in the material.The difference between the two effects is approximately 100% and therefore not trivial.It would appear from the experimental details that what was observed was secondary pyroelectricity. In crystals for which piezoelectricity is permitted but not pyroelectricity,secondary pyroelectricity cannot occur.Hence we may conclude from this experiment that both heated collagen and heated bone are pyroelectric.It is possible that the observed effect would be larger for unheated bone, since the bone denaturation temperature is approximately 65°C [12].

(Protein Denaturation refers to the irreversible breaking down of the molecular structure.When the bone protein denatures, the triple helix of the collagen macromolecule collapses.This structure is described in Chapter Three.)
He concludes that the existence of a pyroelectric effect indicates that bone should possess symmetry of the (∞) type texture and not (∞ : 2) as originally found by Fukada.That is that bone should possess the same polar symmetry as collagen.
(An account of piezoelectric textures is given in the next chapter.)

Dainora[5] measured the elastic modulus in the long direction of three human femurs in the wet condition, and determined a piezoelectric constant for bone specimens that had been dried in an oven at 105°C for one week.The specific gravity and microhardness were determined for the same specimens. He observed that the piezoelectric voltage decreased with increasing specific gravity,microhardness, and modulus of elasticity.He states that:-

' When the piezoelectric specimen was loaded parallel to the long axis of the bone, a negative charge appeared on the outer surface of the compacta.This is in agreement with what was found by Fukada....' Subsequently he gives the values found for this piezoelectric modulus and states that these are

the magnitudes of the d_{14} constant. We are not in complete accord with what is implied in this remark. This is discussed in Chapter Five.

Dainora also measured the piezoelectric voltage on the same bone specimens after they had been demineralized in 5% formic acid until flexibility was achieved. As before they were dried in an oven for one week at a temperature of 105°C. In the discussion of the results he states that the piezoelectric voltage generated for such specimens was approximately 80% of the normal undemineralized specimens, and yet in the Abstract the average value of 0.3×10^{-8} c.g.s is given for both types of specimen. He concludes that the observed potentials can best be explained by the classical theory of piezoelectricity.

Fukada[2] measured the piezoelectric properties of vacuum-dried cow and horse Achilles tendon specimens in the converse effect using his own apparatus, where the specimens are electrically driven at a low audio frequency, (see Chapter 5). These and his bone results are discussed in detail in the above-mentioned chapter.

Basset and Becker[14] could detect no stress-induced potentials in wood and fresh cat Achilles tendon, whereas Bazhenov[15] has extensively studied and measured the piezoelectric

and elastic properties of wood, which are concordant with the symmetry group $(\infty : 2)T$ [16], and Fukada confirmed the equality of the direct and converse effects in wood. In referring to wood, Bazhenov states that the piezoelectric modulus is increased two or three times when treated by H-bond breaking chemicals, such as liquid NH_3 . NaOH, and ethylene diamine. He concludes that this is due to the liquid being 'texturised'. Considering the results of Chapter 4 this increase seems likely to be due to streaming potentials.

An account of the PN junction theory of Becker, Bassett, and Bachman is given in 'Bone Biodynamics'[17] . They state at one point that ' considerable differences from the single crystal piezoelectric effects were observed, including a tendency towards a non-symmetrical output and a steady-state output during the period of steady stress application.' In the previous paragraph they dismiss piezoelectricity as a possible explanation of their results on the grounds that the classic concept of single crystal piezoelectricity requires the absence of either a plane or axis of symmetry in the crystal structure. In the addendum of the same paper they give the experimental details for the measurement of the electrical characteristics of the ' collagen apatite ' PN junction. One electrode is placed

on the face perpendicular to the long direction and the other is placed on a side face parallel to this direction. The forward and reverse bias currents are then measured for these contacts, on the assumption that the first electrode makes contact with P type semiconductor and the other electrode with N type semiconductor.They find that the 'forward current ' is greater than the 'reverse current'.

Shamos and Lavine [18] carried out several experiments on the electrical properties of dry bone and other mineralized tissues, and commented on previous work.They measured the temperature variation of the resistivities of various materials, including wood, dry bone, dry bone collagen, and marble, and showed that it is more correct to regard such substances as poor insulators rather than as semiconductors.They obtained a value of 2.4 eV for the energy gap of dry bone from these resistivity-temperature measurements, and concluded that this was much too high for appreciable semiconductor effects to occur at body temperatures, near to .03eV, if these dry results are relevant to the wet case.In commenting upon Becker et al's statement on the nature and duration of the signals compared with of quartz, they showed that it was incorrect to regard the bone signals as non-piezoelectric because the quartz signal decayed rapidly whereas the bone signals did not.They pointed out that

the measured electrical signal depends upon the circuit constants such as the bone leakage resistance and the input impedance of the measuring apparatus.They also observed that the signal produced upon releasing the applied stress was not a piezoelectric signal, and that because this signal was often less than that produced upon the application of the stress, one was not justified in saying that rectification was taking place in a reverse direction.

In an article on the electrical and piezoelectrical properties of dental hard tissues[19], the authors give an account of their work on elephant dentin and enamel.They measured the electrical potentials arising from compressive stresses by connecting the specimen through an electrometer valve to an oscilloscope.The electrical resistance of 'parallel' specimens was also measured at 50 c/s using an R-C bridge.They state:-

' We were unable to discern any piezoelectric effect with the mineral apatite $Ca_{10}(PO_4)_6(OH)_2$ as expected, or with enamel.'

No information is given on the specimen orientations used so that we are not in a position to know whether all the piezoelectric coefficients for enamel and apatite were measured to be zero.However we assume that several orientations were used so that this is the case.They report that results were obtained

for dentin comparable with those found for bone, but that 'the electrical response appears to vary non-linearly with stress, contrary to the findings of Fukada and Yasuda.They show that the resistivity of dried dentin varies exponentially with the reciprocal of temperature in the range 50°C to 120°C, in a similar way to that suggested by Shamos and Lavine[18], and they conclude that there is nothing to suggest that dried dentin is a semiconductor.

The experiments described in this thesis were undertaken primarily to determine the electrical properties of wet bone, that is bone bathed in an ionic fluid as it is in vivo.Because of the confusion existing in the literature it was thought necessary first to examine the properties of pure collagen in the wet state. The results from these experiments were then used to interpret measurements made on wet bone.The piezoelectrical properties of dry bone were also investigated, and these show that the bone collagen is responsible for the observed properties. The work on collagen shows that fully-wet, pure collagen is not piezoelectric and that potentials obtained from it when strained can be ascribed to ionic streaming effects.The measurements on wet bone demonstrate that streaming potentials are by far the greatest source of electrical signals in stressed wet bone, in the long direction, but that the bone collagen still retains piezoelectric properties.

Chapter Two

Theory of Piezoelectricity

2.1 Introduction.

Direct Piezoelectricity is the physical phenomenon which occurs in some insulating solids, of the production of an electric moment which is proportional to, and derives from applied stress.The converse effect is the strain produced in the solid resulting from an applied electric field.The phenomenon is commonly associated with single crystals, because their anisotropy is readily apparent,and a solid must be be anisotropic if it is to be piezoelectric.This condition is a necessary one, but not sufficient for the existence of the effect.The criterion that determines whether a crystal is piezoelectric or not is the possession of a centre of symmetry in its structure.A crystal that possesses a centre of symmetry cannot be piezoelectric, because no combination of uniform stresses will produce a separation of the centres of gravity of the positive and negative charges that is necessary for the occurrence of a dipole moment.Crystals can be divided into thirty two classes on the basis of the symmetry they possess, and of these thirty two classes twenty may be piezoelectric and twelve cannot.

Piezoelectricity is distinguished from electrostriction,

(which is another effect that causes a dielectric to deform on the application of an electric field) in that a reversal of the applied electric field causes the strain to be reversed. For electrostrictive effects the resulting deformation is independent of the sign of the electric field. Because the electrostrictive coefficients do not vanish for isotropic materials the phenomenon may occur in all materials, including liquids. However for non-ferroelectric piezoelectric crystals, the electrostrictive terms may be ignored as they are orders of magnitude less in value.

If the piezoelectric properties of any material are to be investigated quantitatively the phenomenon must be treated mathematically. Authoritative accounts of the subject are given by Cady[48], and by Mason[49], so that only the barest outline will be presented here as is pertinent to the work of this thesis.

2.2 A short note on the Piezoelectric Coefficients.

There are many ways in which the piezoelectric properties of a crystal may be given. The coefficient that will be used in this thesis is the 'd' coefficient. When referred to Cartesian coordinates ijk, the d_{ijk} coefficient in the direct effect measures the electric polarization per unit area P_i produced in the i direction, resulting from an applied stress T_{jk} ;

when all other stresses are constant. In the converse effect it relates the strain S_{jk} in a free crystal produced by an applied electric field E_i in the i direction. In tensor notation the two effects are written,

$$P_i = d_{ijk} T_{jk} \qquad i,j,k = 1,2,3$$
$$S_{jk} = d_{ijk} E_i$$

The above d coefficients may be shown to be the same using the Thermodynamical Gibbs Function. d_{ijk} is a third rank matter tensor(and so must conform to the symmetry of the point group), and T_{jk} and S_{jk} are both symmetrical second rank field tensors which do not represent therefore the group symmetry. T_{jk} represents a force in the j direction acting on the k plane, so that T_{11} is a tensile force in the 1 direction. Likewise the components of strain S_{ii} are the tensile strains. They are the extensions which elements of unit length, drawn originally parallel to the i axis, undergo during the strain. As an example of a shear strain, S_{23} equals half the change in angle between two elements drawn parallel to the 2 and 3 axes before deformation, and is considered positive if the angle decreases. For the derivation of these symmetrical second rank tensors the reader is referred to Mason. Fig 2.1 shows a unit cube with

stresses T_{jk} marked on the forward faces.

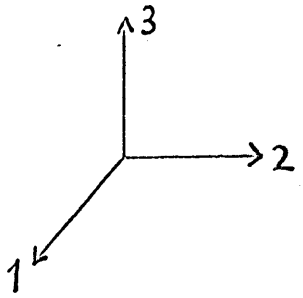

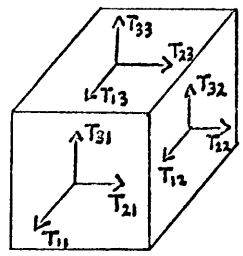

As long as body torques are not present $T_{ij} = T_{ji}$. This makes the stress tensor symmetrical.The stress and strain tensors are written,

$$\begin{matrix} T_{11} & T_{12} & T_{13} \\ T_{12} & T_{22} & T_{23} \\ T_{13} & T_{23} & T_{33} \end{matrix} \qquad \text{and} \qquad \begin{matrix} S_{11} & S_{12} & S_{13} \\ S_{12} & S_{22} & S_{23} \\ S_{13} & S_{23} & S_{33} \end{matrix}$$

The diagonal symmetry of these second rank tensors allows them to be represented by a one suffix matrix notation shown below.

$$\begin{matrix} T_1 & T_6 & T_5 \\ T_6 & T_2 & T_4 \\ T_5 & T_4 & T_3 \end{matrix} \qquad \text{and} \qquad \begin{matrix} S_1 & \frac{1}{2}S_6 & \frac{1}{2}S_5 \\ \frac{1}{2}S_6 & S_2 & \frac{1}{2}S_4 \\ \frac{1}{2}S_5 & \frac{1}{2}S_4 & S_3 \end{matrix}$$

When these changes are incorporated into the definition of the d coefficient the direct and converse effects are written in matrix notation,

$$P_i = d_{ij} T_j$$
$$S_j = d_{ij} E_i \qquad i = 1,2,3; \quad j = 1,2, \ldots 6.$$

As an example of this notation $d_{123} = d_{132}$ becomes $\frac{1}{2}d_{14}$, and d_{211} becomes d_{21}. The array of d_{ij} written out as a matrix is

$$\left[\begin{array}{ccc|ccc} d_{11} & d_{12} & d_{13} & d_{14} & d_{15} & d_{16} \\ d_{21} & d_{22} & d_{23} & d_{24} & d_{25} & d_{26} \\ d_{31} & d_{32} & d_{33} & d_{34} & d_{35} & d_{36} \end{array}\right]$$

There are 18 matrix coefficients compared with 27 tensor coefficients, so that when possible it is more convenient to handle the matrix notation. All the terms with second suffices greater than 3 represent shear terms in this frame of reference; '4' is equivalent to a shear around the 1 axis, '5' around the

2 axis, and '6' around the 3 axis. Hence the piezoelectric matrix may be split into two halves, shear and non-shear terms.

By using the Thermodynamical Gibbs Function, and treating the strains, electric displacements, and entropy, as the fundamental variables, and the stresses, electric fields, and changes in temperature, as the dependent variables, general expressions may be developed for the first three in terms of the others. For adiabatic conditions the resulting equations are

$$S_i = \sum_{j=1}^{6} s_{ij}\, T_j + \sum_{k=1}^{3} d_{ki}\, E_k$$

$$\delta_m = D_m/4 = \sum_{n=1}^{6} d_{mn}\, T_n + 1/4\pi \sum_{p=1}^{3} \epsilon^{T}_{mp}\, E_p$$

where D_m = a component of electric displacement.

δ_m = the surface charge at a boundary.

ϵ^{T}_{mp} = a free dielectric constant.

s^{E}_{ij} = the elastic compliance at constant electric field.

The first equation incorporates the converse piezoelectric effect and the second, the direct effect. It is these equations which are used in analysing Fukada's apparatus in Chapter Five.

2.3 The Symmetry Theory of Polycrystalline Materials or Textures. The theoretical footing of this subject is entirely due to A.V.Shubnikov[52], and the reader is referred to the textbook for further information.

A texture is defined as any homogeneous body lacking a lattice structure, which consists of a multitude of elementary particles of undefined physical nature that are oriented in space according to symmetry laws. Among the examples of textures are fibrous substances such as wood, polarized dielectrics consisting of dipoles oriented in the same sense, and magnets presenting aligned electron spins. What interests us are the textures containing axes of infinite order, that is those textures which possess one axis or more around which rotations of any magnitude leave the body in a position which is indistinguishable from that before the rotation. It may be helpful to remark here that a polar vector, (which is commonly represented by the arrow sign ⟶), belongs to the above limiting point group textures, as does an axial vector (normally drawn ⟲). In Shubnikov's notation the polar vector belongs to the point group $\infty \cdot m$ and the axial vector to the point group $\infty : m$. The dot in the $\infty \cdot m$ representation signifies parallelism between the infinity axis and the mirror planes, and the two dots in the $\infty : m$ formula represent

perpendicularity between the axis and the single mirror plane.The limiting point groups are seven in number and are written.

∞ , ∞.m , ∞:m , ∞:2 , m.∞:m , ∞/∞ , and ∞/∞.m

The stroke in the last two groups indicates an oblique relation between the two infinity axes. We shall only discuss three of these groups, since only these may show piezoelectric behaviour. These are

∞ , ∞.m , and ∞:2 .

The first group possesses no elements of symmetry other than the infinity axis.Textures of the type (∞)T may be formed by submitting a right-handed or left-handed asymmetric particle to all possible translations of the group T, and then rotating the particle through an arbitrary angle, but always in the same sense, around an arbitrary axis.An example of a texture so formed is illustrated below.

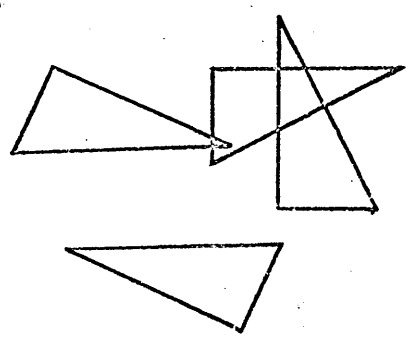

The ∞ axis is perpendicular to the plane of the drawing. Such a texture consists of all right-handed or all left-handed particles.It therefore has two enantiomorphic forms. The ∞ axis is polar-axial.

The ∞.m group contains besides the ∞ axis symmetry element, an infinite number of longitudinal mirror planes. Textures of the type (∞.m)T may be realised with any such polar particles of whatever orientation as long as the particles are directed with the same polarity parallel to each other. The axis in this case is polar.An example of such a texture is drawn below.

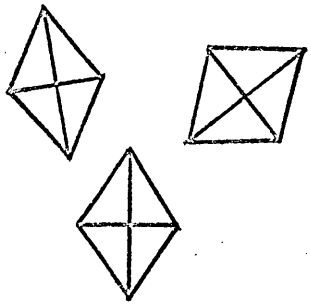

The ∞:2 group possesses besides the ∞ order axis an infinite number of transverse diad axes.It may be formed from particles of symmetry 2:2 as long as all the longitudinal diad axes are parallel to each other.As for the group there are two enantiomorphic forms.An example of such a texture is shown at the top of the next page.The shaded areas depict regions of

of opposite polarity.

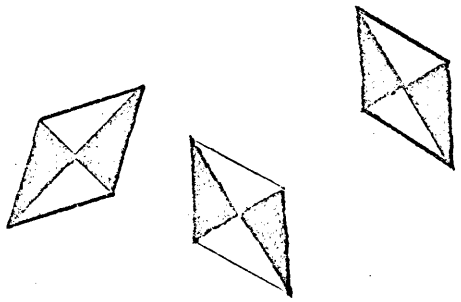

A texture which belongs to the ∞ limiting point group must possess the piezoelectric matrix shown below, if the axis is along the 3 axis .This may be seen by recalling that the form of the matrix is independent of rotations about the 3 axis.

$$\infty\,(T) = \begin{matrix} 0 & 0 & 0 & d_{14} & d_{15} & 0 \\ 0 & 0 & 0 & d_{15} & -d_{14} & 0 \\ d_{31} & d_{31} & d_{33} & 0 & 0 & 0 \end{matrix}$$

For textures of the ∞.m group the form is similar except that the longitudinal mirror planes do not permit the d_{14} and d_{25} terms.Hence the piezoelectric matrix of this group is

$$(\infty.m)T = \begin{matrix} 0 & 0 & 0 & 0 & d_{15} & 0 \\ 0 & 0 & 0 & d_{15} & 0 & 0 \\ d_{31} & d_{31} & d_{33} & 0 & 0 & 0 \end{matrix}$$

If one operates on the $(\infty)T$ matrix with a transverse diad axis one arrives at the matrix for the $(\infty:2)T$ textures. This is

$$(\infty:2)T = \begin{matrix} 0 & 0 & 0 & d_{14} & 0 & 0 \\ 0 & 0 & 0 & 0 & -d_{14} & 0 \\ 0 & 0 & 0 & 0 & 0 & 0 \end{matrix}$$

These matices are the only irreducible representations for an homogeneous piezoelectric texture which belongs to the limiting point groups. Reference to Chapter Five shows that an Achilles tendon that consists of parallel collagen fibres belongs to the ∞ point group.

Chapter Three

The structure of Bone and its Protein Collagen

3.1 The structure of Bone

A bone such as a femur is approximately cylindrical in shape possessing a soft centre which is termed the marrow. To the naked eye it appears homogeneous. Viewed with an optical microscope the bone appears to consist of smaller nearly cylindrical units called osteons running parallel to the long axis of the bone. The osteon is sometimes referred to as the building block of bone, but it would appear from the literature that it is controversial to regard it as such. Bassett[23] in his article in Scientific American on 'Electrical Effects in Bone', depicts a piece of bone as consisting of perfectly cylindrical osteons in close-packed hexagonal arrangement lying along the long direction of the bone. He shows the osteon consisting of the central Haversian canal, which contains the blood vessels, surrounded by concentric layers of hydroxyapatite crystals, $Ca_{10}(PO_4)_6(OH_2)$, embedded in collagen fibres that are ' alternatively turned to the left and the right ' in the neighbouring lamellae. On this model the collagen fibres in one layer spiral around the axis of the osteon in the opposite sense to that of the neighbouring layer, and since the axis of the osteon is shown as running parallel to the long

axis of the femur, the picture is of collagen fibres spiralling around the long axis of the femur.The osteocytes, which are the bone producing cells, are located in small cavities throughout the cross-section, and are linked by very fine capillaries to the central blood canal.

Cooper and Robinson [24] state that'.... While it is true that many of the Haversian canals are orientated in a longitudinal manner with respect to the long axis of the bone, textbook diagrams showing straight Haversian canals which connect by transverse Volkmann canals are definitely misleading. The three-dimensional reconstruction of osteons by Cohen and Harris demonstrated the intricate branching, spiralling, and interconnection of osteons and their vessels.' Fig 3.11 shows the structure of bone as illustrated by Bassett.

Cooper and Robinson later remark, '..... The lamellar pattern was evident in both mineralized and unmineralized sections.Individual lamellae averaged about three micra in width. Adjacent lamellae had their collagen oriented in different directions. In many osteons, lamellae with their collagen fibres circumferentially oriented alternated with lamellae in which the collagen was parallel or oblique to, the long axis of the Haversian canal. No cellular layer or

Fig. 3.11

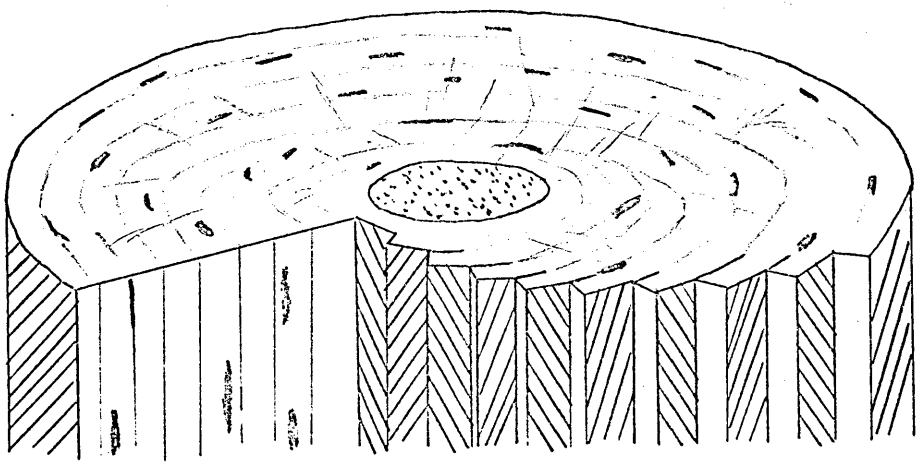

Structure of the Osteon

In the middle is the canal that contains the blood vessels. It is connected by much finer canals to cavities that contain osteocytes. The concentric layers are composed mainly of of hydroxyapatite embedded in variously oriented layers of collagen fibres(depicted above).

amorphous zone separated the various lamellae, and in fact the collagen fibrils of adjacent layers were seen to intermingle .....'

J.W.Smith [25] classifies the bone fibre pattern into three types of different maturity, the third group representing the most mature bone.

Type 1 consists of an alternation of lamellae which contain approximately longitudinal and approximately transverse circumferential fibres respectively, and in which the concentration of fibres in adjacent lamellae is nearly equal.

Type two consists of distinct lamellae, concentrically arranged about a vascular canal, and as for the first type alternate lamellae contain approximately longitudinal and approximately circumferential fibres respectively. However, contrary to the first type adjacent lamellae concentrations are markedly unequal. The longitudinal fibres are densely packed together so that in the transverse directions they form darker layers than the circumferential fibres which are loosely dispersed.

The feature if the third group is the non-abundance of the lamellae. This is due to the small number of circumferential fibres.Under low magnification a transverse section

does not show concentric layers. At higher magnifications the cut ends of longitudinal oriented fibres are visible.

Thus in going from type one to type three the number of longitudinally oriented fibres increases and fewer fibres are arranged in lamellae. J.W.Smith states that the first two types are characteristic of immature bone, and that as the osteons become older the longitudinal fibres increase in number until they are no longer confined in lamellae.

Hence for a large specimen in which all orientations are included, the most general description of the structure of bone collagen is that the protein fibres may be said to exibit, statistically speaking, conical symmetry with respect to the long direction of the bone.The apical angle will depend upon how many fibres lie parallel to the axis of the osteon, how many lie circumferentially, and whether the osteons themselves spiral along the direction of the long axis.However, for specimens of size comparable with or less than the pitch of the spiral, the fibres will in general strike an oblique angle with the long direction.

The positioning and size of the hydroxyapatite crystals in bone seems less controversial than that of the protein fibres. Engström and Finean [26], using X-ray techniques,

found that the apatite crystals of bone were rod-shaped, and uniform in their dimensions of 210 Å and 50 Å. Fernandez-moran and Engström[27] confirmed this using the electron microscope. They give the average dimensions as 200 Å and 30 – 60 Å. The c- axis of the crystals was observed to be in the fibre direction. It is pertinent to remark here that the point group symmetry of the apatite structure is 6/m, that is a mirror plane perpendicular to an hexad axis . This is a centro - symmetrical group so that apatite is not piezoelectric. Glimcher[28] has shown that not only are the crystals attached to the surface of the fibrils but that the bulk of the apatite is within the fibrils. Fitton-Jackson[29] showed that electron-dense particles are arranged in a regular periodic pattern along the fibril, and electron diffraction identified these particles as apatite crystals of diameter less than 100 Å. The observation that the length of the crystals is a sub-period of the collagen 640 Å band - inter band unit forms the basis of the ' collagen seeding theory '.

Cooper and Robinson[24] state that it is generally accepted that the inorganic component of bone is hydroxy-apatite and that the c-axis of the crystallites is parallel to the fibril axis. They state that the crystals vary in

thickness from about 25 to 40 Å and length from 200 to 400 Å, with occasional crystals up to 1000 Å in length. They give the surface area of the crystals as varying from 100 to 300 sq m/gm, and they state that the crystals are deposited over about 400 Å of every 640 Å of the fibril length.

Thus in conclusion, there seems to be general agreement that the inorganic crystals of bone are hydroxy-apatite, that they are needle or rod-shaped with average dimensions of approximately 210 Å in length and 30 to 60 Å in thickness.

An account of the structure of bone would not be complete without reference to the nature and size of the water which forms an integral part of the living material. The work of Berendsen[22] indicates a possible interpretation, but without experimental evidence it cannot be assumed that the structure of the collagen water is relevant to bone which is a rigid body, largely consisting of apatite which itself takes up water. The problem of bone hydration seems to have received relatively little attention. The main work on this subject appears to be that of Marino, Becker, and Bachman,[12] who measured the dielectric constant and dielectric loss of bone at various frequencies and humidities. All their measurements were carried out on human cortical bone in a direction

perpendicular to the long axis, so that to a first approximation we might say that the dielectric constant transverse to the collagen fibres was measured. These measurements were made at 100,50,10, and 1kc/sec, employing a capacitance ' measuring assembly ' and a micrometer – driven dielectric sample cell. A typical curve resulting from their measurements is shown in Fig 3.12. It shows the variation of the dielectric constant with hydration, the latter quantity being in units of mg H_2O / gm bone. The point at which the slope of the curve appears to change is termed the ' critical hydration point ' and occurs in the region 37 to 48 mg H_2O / bone, the actual figure for a specimen depending upon the density. The authors interpret this as the amount of water necessary to occupy the ' primary absorption sites ' in bone, that is the bound water of bone. They note that absorption isotherms for synthetic hydroxyapatite [30] and hide collagen [31] have been determined, and when fitted to the B.E.T equation, values of 17.6 mg H_2O / gm and 95.2 mg H_2O / gm are obtained for the amount of water necessary to complete the 'monolayer' in apatite and collagen respectively. (The B.E.T equation and its general applicability are discussed in Chapter 6 in connection with the interpretation of the evaporation curves.)

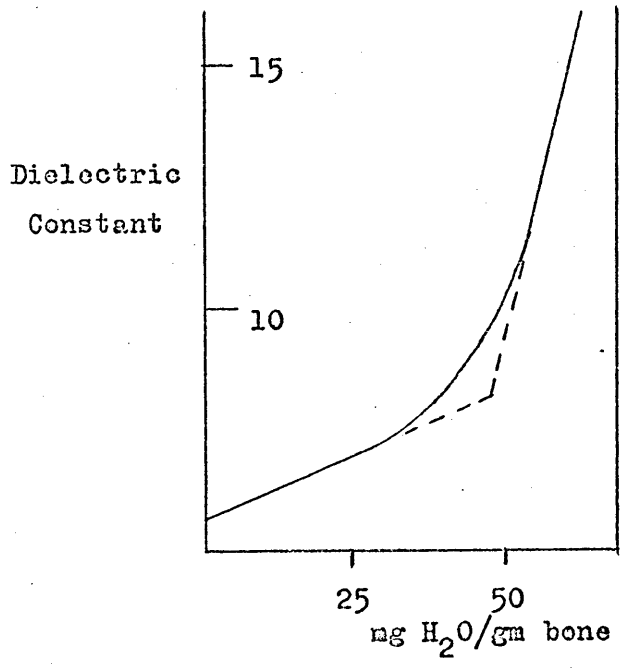

Fig. 3.12

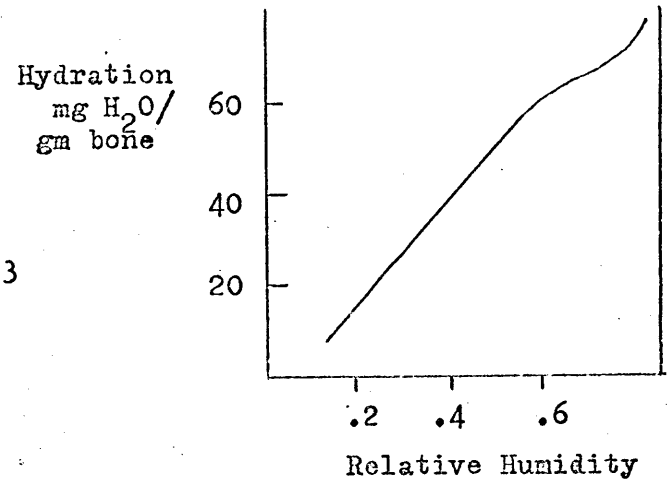

Fig. 3.13

Using the fact that bone by weight consists of 65% apatite and 35% collagen, they obtain a figure of approximately 45 mg H_2O / gm bone for the water necessary to occupy the ' primary absorption sites ' in bone.This compares with their experimental value of 37 to 48 mg H_2O / gm bone.

They comment that even though absorption on collagen and apatite has been interpreted (and presumably they imply can be) using the B.E.T equation , and that their own results can be interpreted using this equation, this does not necessarily mean that absorption on bone follows a B.E.T equation. The absorption isotherm which they determined for bone,(see Fig 3.13) is in their own opinion not sufficiently accurate to the point. They remark that that a system of two B.E.T absorbers will not in general follow a B.E.T equation, except in the case where the heats of absorption are the same. They conclude that if the absorption on bone is found to obey a B.E.T equation then the ' monolayer capacity ' should be expected to agree with their value of 37 to 48 mg H_2O / gm bone for the critical hydration.It should be remarked that Rougvie and constructed a moisture sorption isotherm for collagen and found that the primary sorption amounted to about 13 gm H_2O / 100 gm of collagen, when analysed by the B.E.T equation.

Clearly this is not consistent with the figure of 9.52mgm H_2O /gm of collagen used by these authors in the interpretation of their data.

When the later figure of 13.0 gms H_2O/100 gm collagen is used for the primary sorption in collagen one obtains a value of approximately 58 mg H_2O/gm bone for the ' bound water of bone'. This figure is not consistent with the value of their ' critical hydration point' as determined by bone's dielectric behaviour.However, this observed ' critical hydration point' is consistent theoretically and numerically with what is termed in Chapter Six, the first discontinuity.This marks the end of free water evaporation and the start of evaporation from the collagen B bands.(see 3.3)

3.2 The Structure of dry Collagen

We shall only present a brief outline here. For a critical review the reader is referred to the article by Harrington and Von Hippel.[43]

3.21 The collagen molecular structure

The collagen macromolecule is a triple helix built from three polypeptide chains that are minor helices themselves. It is approximately 2800Å in length and 15Å in diameter. The three constituent chains are hydrogen-bonded to each other by bonds that are essentially perpendicular to the axis of the helix. (A polypeptide chain is a repeating structure made up of identical peptide groups (CCONHC). The chain is formed by amino acids or residues, each of which contributes an identical group to the backbone, plus a distinguishing radical (R) as a side group. Fig 3.21 depicts a polypeptide chain and three of the amino acids that occur in collagen). Fig 3.22 shows the basic structure of the collagen macromolecule as proposed by Rich and Crick.[47] Only the amino acids are shown on each chain as the backbone is common throughout. This model is known as the 'Collagen 21' model, and is built on the assumption that every third residue is the amino acid glycine, and that the sequence glycine, proline, hydroxyproline can be incorporated

Fig. 3.21

Planar Projections of a)Polypeptide Chain , b)Glycine c)Proline, d) Hydroxyproline

a)

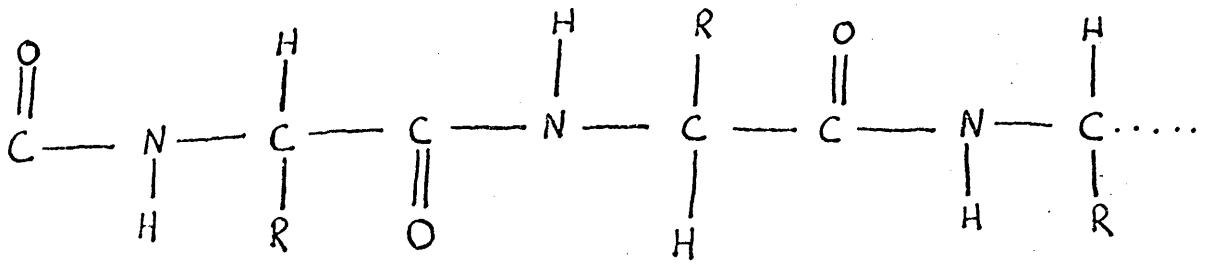

b)

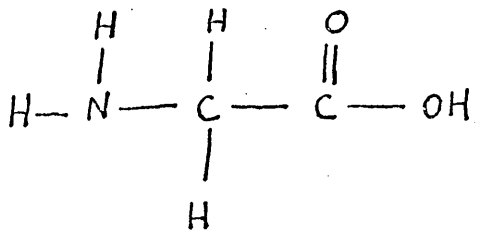

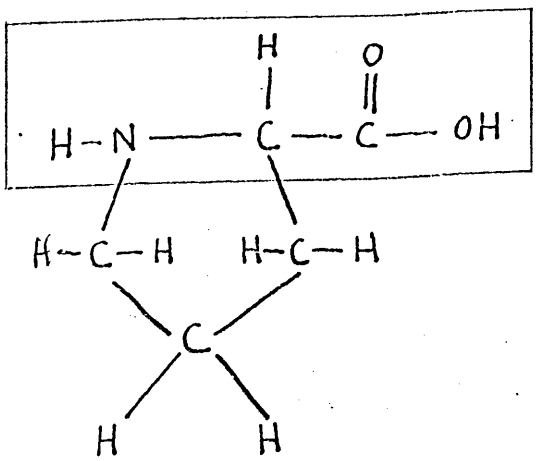

d)

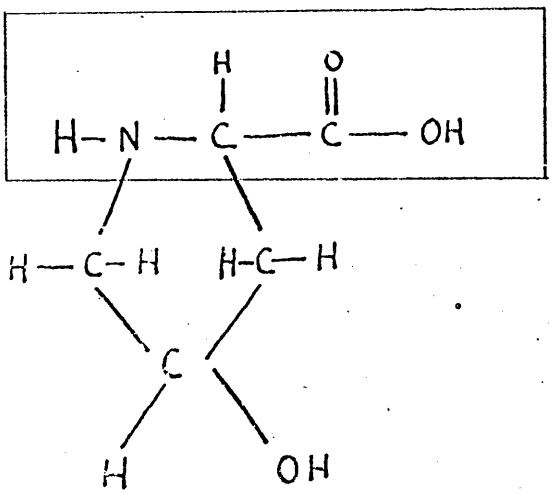

The ringed structure is contributed to the backbone.

Fig. 3.22

Structure of the Collagen Macromolecule according to Rich and Crick (1961)

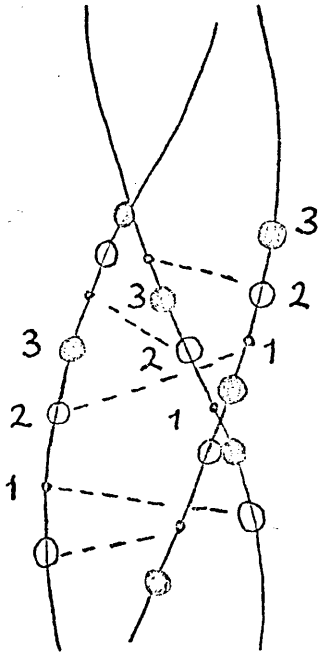

a) 1 = glycine
2 = proline
3 = hydroxyproline

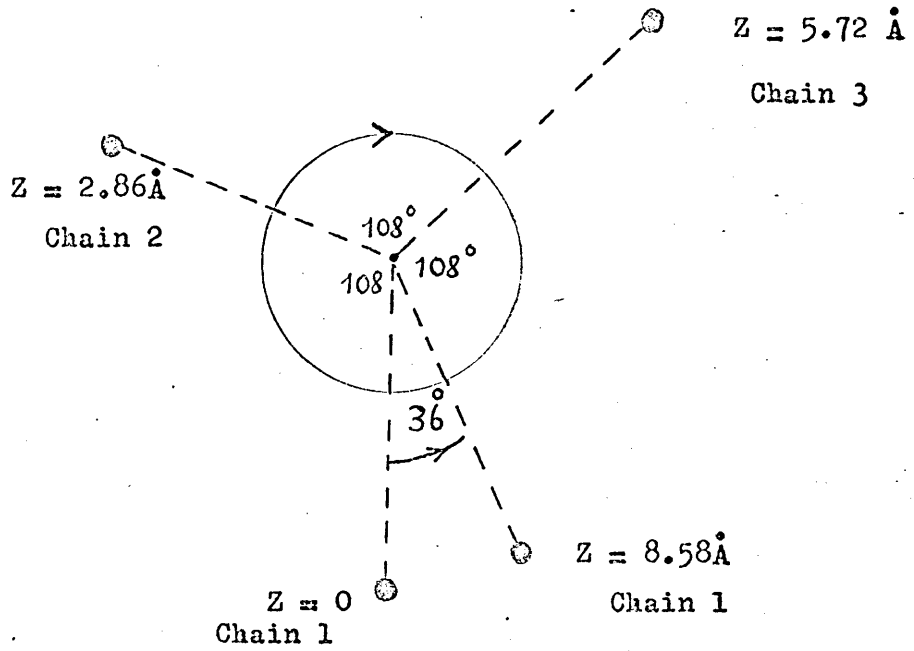

b) Axial Projection of Four Equivalent Positions along the Molecule

into the structure.The basic structural unit is therefore a three residue sequence.The diagram shows this sequential positioning as 1= glycine , 2= proline, and 3= hydroxyproline. It should be remembered though that positions 2 and 3 may be occupied by other amino acids, such as lysine, arginine etc. The spatial operation that brings coincidence for one chain is a rotation of 36° and a translation of 8.58Å along the helical axis.The equivalent operation from chain to the next is a rotation of -108° and a translation of 2.86Å. The axial period of the major helix is 28.6Å. The intramolecular hydrogen bonds are formed between the NH of position 1 (glycine) and the carbonyl oxygen of position 2 of the neighbouring chain in an anticlockwise position.The carbonyl oxygens of positions 1 and 3, and the NH of 2 and 3 that are not occupied by proline and hydroxyproline are therefore available for water binding.

3.22 The Collagen Fibrillar Structure

Whereas the collagen molecular structure outlined above is determined from the wide-angle X-ray diffraction, the collagen fibrillar structure is shown by low-angle X-ray diffraction patterns and electron microscopy.The latter methods have shown that the tropocollagen macromolecules link up laterally to form fibrils.Viewed microscopically collagen appears to be

laid down in bundles that are formed from parallel fibrous elements.Under the resolution of the light microscope the fibres appear smooth and undifferentiated.However with the magnification of the electron microscope this smooth structure is no longer apparent and the fibrils are seen to contain bands which have a periodicity of 640Å for native fibrils.The early collagen workers used positive staining techniques such as chromium staining, where the stain penetrates and identifies the highly charged regions.Using this method the 640Å period consisted of a band and an inter-band, the bands being of somewhat greater diameter than the interband regions. This axial repeat was also observed in low-angle X-Ray diffraction patterns. It was suggested that the 640Å band interband repeat was due to a regular alternation of groups of amino acids, the band regions containing high concentrations of long chain polar amino acids and the inter-bands containing mostly the smaller non-polar residues. It was proposed that the interbands form the portions of the fibril that give rise to the wide-angle X-Ray diffraction pattern, the polar amino acids located in the bands being too bulky and highly charged to pack properly.Thus the bands would be the most amorphous parts and therefore more easily penetrated by stains.Subsequent work supported this interpretation. The 640Å

axial repeat observed in native collagen collagen was interpreted in terms of a hypothetical collagen molecule of 2600Å length.If four main bonding zones are ascribed to the molecule then neighbouring molecules could bind into the fibrils by 'quarter-staggering' along their axial length.

However with the advent of negative staining techniques this 'quarter-staggering' process became untenable, thus throwing into question the meaning of the banded regions.Whereas positive staining in principle identifies the chemically charged groups of a structure, negative staining directly relates to the molecular structure.Hence with positive staining the charged band region is penetrated by the stain and identified, whereas with negative staining the molecular structure is penetrated and stained, so that details of the crystalline structure are directly obtained.Contrary to positive staining, negative staining a major light and a major dark band within each 640Å period.These are labelled the A and B bands respectively, so that the A band represents the region within the 640Å repeat distance where the stain cannot penetrate .Hence the A band may be loosely equated with the more disordered charged band region seen with positive staining.

Cox et al[21] in two recent papers have proposed a new model

for the tropocollagen molecule, and a new mechanism for its assembly into native collagen fibrils.Their evidence arises from the use of negative staining techniques and high resolution electron microscopy.We only summarise their observations and conclusions.

The A band for native collagen is measured to be 280 Å and the B band 360Å.The individual tropocollagen molecules can be seen running through the A and B bands. By depositing 'segment long spacing' (SLS) collagen , (corresponding to the period of the tropocollagen) on to the recostituted native collagen,they have shown that the tropocollagen molecule spans 5A and 4B bands of the native collagen fibrils.Fig 3.23 shows the tropocollagen molecule next to a native collagen fibril, and the individual macromolecules.

By dividing the tropocollagen molecule into five main bonding zones separated by four main non-bonding zones, they have shown that the macromolecules nay be assembled into native fibrils by allowing a main bonding zone on a particular macromolecule an initial random choice in combining , in a structurally complimentary manner, with a main bonding zone on another macromolecule.Thus the a or bonding zones on the macromolecule produce the A bands of the native fibril, and the b or non-

Fig. 3.23

Schematic diagram of the tropocollagen molecule and a native collagen fibril, to show that one macromolecule covers 5A and 4B bands. The individual macromolecules are shown running through the fibrils.

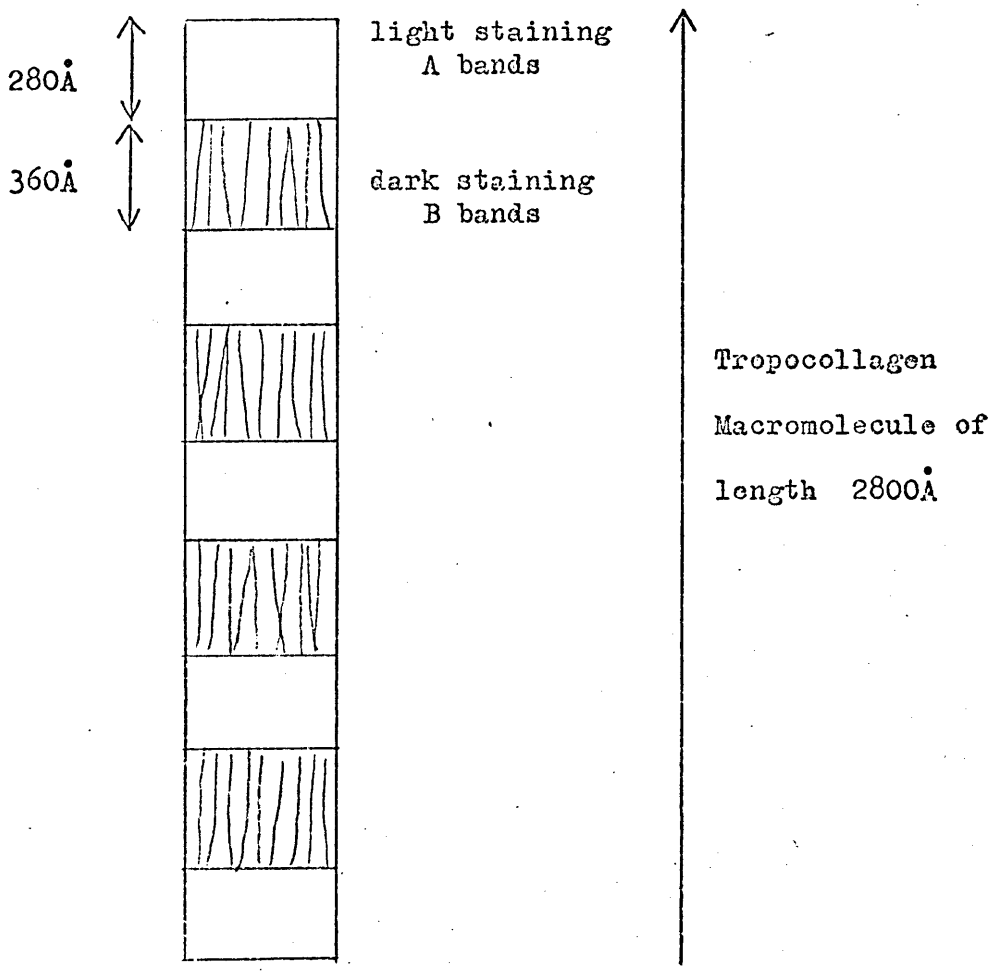

bonding zones of the macromolecule produce the B bands of the native fibril. They show on this basis that the number of tropocollagen macromolecules present in the B band to the number in the A band of a native collagen fibril is 4:5 .

They examined electron micrographs of cross-linked fibrils with several cross-linking agents.In each case examined the light-staining region was increased at the expense of the dark or B bands, compared with the native fibril.They conclude that since the introduction of intermolecular cross-links into the collagen fibrils results in an increase in the size of the light staining or A bands , that the light bands in native collagen correspond to regions where the macromolecules are bonded together; and in addition that the B bands represent areas where only a few intermolecular bonds are present and the lateral attracion is weak.They state that in the case of native collagen the intermolecular bonding 'consists of electrostatic, hydrophobic, and hydrogen bonds between the amino acid side chains arranged specifically, so that structural complementariness of groups exists in those regions of the macromolecule represented by the A bands.'They go on to state that '....Hence we may suppose that the A regions of the structure correspond to a system of receptor and determinant sites (to use

immunological terminology) distributed in different sides of the macromolecule within each A band or bonding zone'

They conclude from the results of the cross-linking experiments that the cross-linking reagents do not react uniformily with the collagen along the entire length of the fibril, but only with certain portions of the structure.'Subsequently they state that ' .....These findings are in conformity with the observations of Grassman[46] et al that the amino acid sequences are of a non-homogeneous nature, and that regions containing a preponderance of polar amino acids are separated by regions of relatively non-polar character.'

Thus we may conclude from this paper that the native collagen fibrils consist of definite repeating units of axial periodicity 640Å, and that this periodicity occurs because of the existence of specific bonding and non-bonding zones on the tropocollagen macromolecules which make up the fibril.Hence the A bands, as seen in electron micrographs using negative staining techniques, represents regions along the fibril where lateral intermolecular bonding forces occur, and the B bands where the individual macromolecules are largely free of these forces. Since the A bands contain the majority of the charged amino acids it seems reasonable to conclude that the bonding forces

between neighbouring macromolecules are predominantly electrostatic, although hydrogen bonds and hydrophobic bonds are mentioned equally.

3.3 The Structure of Wet Collagen

Many experimental results indicate that water is intimately involved in the structure and stabilization of collagen. However the molecular changes which occur in the collagen fibre have been most extensively studied using X-Ray diffraction techniques. We outline here the work of Rougvie and Bear[20], who carried out a quantitative analysis of the various features of of both the wide and small-angle diffraction patterns of tendon collagen which are affected by moisture content.

They constructed a moisture sorption isotherm, (Fig 3.31) and found that the primary sorption amounted to approximately 13gm H_2O/100 gm collagen, when interpreted through the B.E.T equation. (see Chapter Six). By relating the moisture content with the X-ray changes they observed that the hydration - sensitive equatorial spacing observed in the wide-angle X-ray pattern moved from approximately 10.6Å for dry fibres, to a maximum of 14.6Å for completely hydrated specimens; similarly that the small-angle meriodional macro period increased from

603Å to near 670Å with increasing water content.The changes in the line intensities for the small-angle pattern likewise indicated that increased ordering of the structure resulted from higher water content.We now quote Rougvie and Bear.

' Description of the total sorption range can be conveniently divided into four intervals.Under rather dry conditions water sorption involves primarily the fibrillar bands at which the axes of the kinked, roughly parallel helical chains straighten as moisture is introduced.The event characteristic of the next interval is a hydration of polar groups at interbands, where relatively well-ordered, parallel chains begin to separate laterally in orderly fashion.In the meantime by the third interval the chain straightening process has proceeded to an extent where small-angle evidence of chain kinking continously disappears.Almost simultaneously segments of adjacent chains at bands and interband margins become free of each other and swim in interposed lakes of water.Finally, as the samples come into equilibrium with pure water the interchain separations at interbands once more increase to a spacing of 14.6Å(without tension).At bands and interbands multilayer sorption follows upon introduction of bound water to chain straightening or separation processes characteristic of each

Fig. 3.31

Moisture Sorption Isotherm (25°C) for Kangaroo Tail Tendon

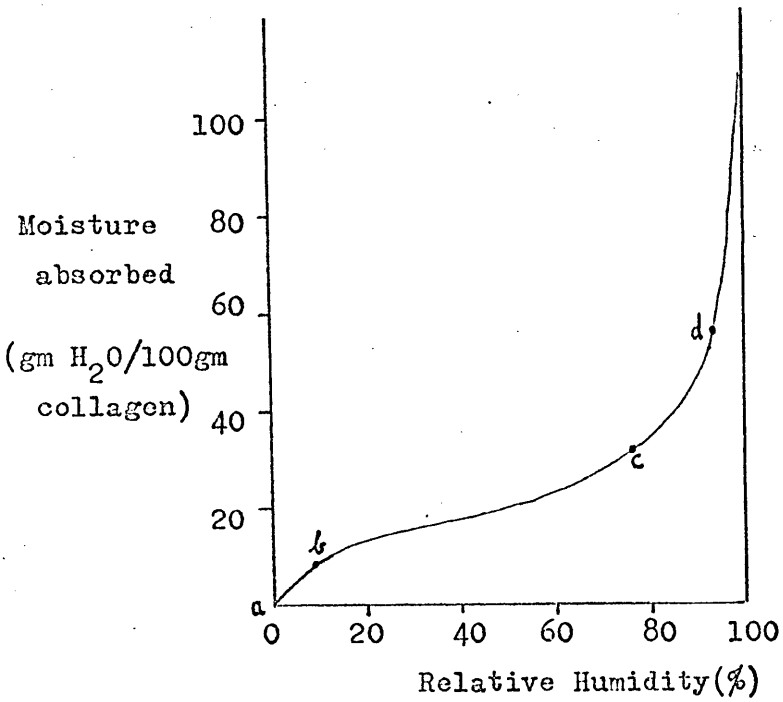

type of location.He later states:-

' All the H_2O in the interval a-b(7gms) and approximately 6 gms of that in the b-c region are assumed to be bound or 'primary layer' water.The remainder is free or multilayer water in each interval.'

Thus we have from this hydration picture that for every 100 gms of collagen approximately 7 gms is initially absorbed into the polar band regions and that a further 6 gms hydrates the polar groups in the interbands.Rougvie and Bear state that this 13gm of water constitutes the primary layer or bound water.This leaves approximately 16 gms from the interband region which is presumably strictly 'multilayer' water, in the terminology of the B.E.T equation.Hence above the approximate figure of 30 gm H_2O/100gm collagen the water would appear to be essentially free, and that above the 40gmH_2O/100gm collagen completely free.

A major contribution to the problem of collagen hydration has been made by Berendsen[22] who carried out a Nuclear Magnetic Resonance study on collagen hydration.He found that hydration of the protein can be divided into two groups.The measurements on partially dried collagen show that a large fraction of the water presents anisotropic reorientation whereas the remaining

water molecules exhibit isotropic motion.He suggests that the first type of water molecule is associated specifically with the three-fold helical structure of the collagen fibres, and that the second type occurs in regions where this helical structure is not dominant.Thus the water molecules whose motion is anisotropic are associated with the more crystalline parts of the fibril, and those whose motion is isotropic are placed in the more disordered polar band regions, as seen in electron micrographs with positive staining.

Berendsen concludes from the nature of the anisotropy of the first group that the water molecules which are linked to the collagen macromolecules form into chains in the fibre direction and are located in the channels between neighbouring fibres. A picture of a possible chain formation is shown in Fig 3.32 . He states that if each channel is filled by one continous chain of water molecules that the channels will contain 15.8gm H_2O/100gm collagen.We tentatively suggest that this corresponds to the 16gms of water remaining in the interband region, according to Rougvie and Bear, that is not primary-layer water.Berendsen states that the lifetime of a particular molecule in such a chain is short due to proton reorientation processes similar to those which occur in ice.Using the approximate energy of one hydrogen bond he calculates this time

Fig. 3.32

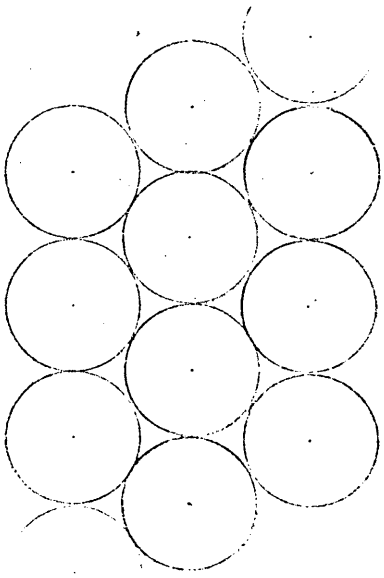

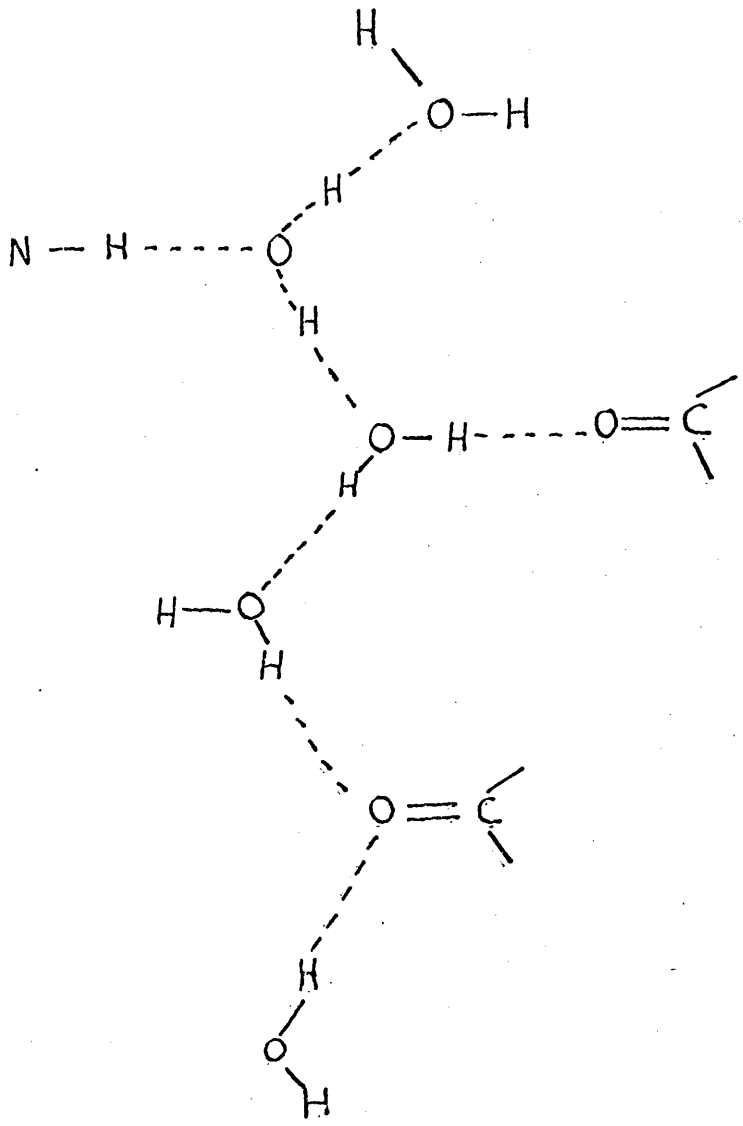

Fig. 3.32 (from Berendsen). End view of fibril collagen macromolecules with water channels in between, and proposed chain of water molecules linking neighbouring collagen molecules.

to be of the order of 10^{-6} seconds, the actual figure depending upon the state of hydration.Thus the chains are broken and rebuilt continously, allowing the molecules to jump to neighbouring chains.He states that when the water content exceeds the approximate value of 40gm H_2O/100 gm collagen there is more water present than form individual chains between the fibres, and consequently lateral separation of the fibres occurs, allowing the water to form three-dimensional structures around the fibrous macromolecules, more resembling the liquid state; and that the particular reorientation processes which lead to the observed N.M.R resonance in two-dimensional chains do not occur any longer.Thus coupling Berendsen's results with those of Rougvie and Bear, a definite molecular picture of the collagen hydration range emerges.This is important to this thesis and will be referred to in later chapters.

Chapter Four

The Electrical Properties of Wet Collagen

4.1 Introduction.

The electrical properties of wet collagen have been described by J.C.Anderson and the present author in a recent paper,[32] a copy of which is enclosed at the end of this thesis.Since both tendon and bone are bathed in ionic fluid of high conductivity when in vivo, it is clearly important to understand the electrical activity of wet collagen.

4.2 Experimental Basis.

The specimens chosen were human Achilles tendons, typically 50mms long and 5mms in diameter when wet.Before experimentation they were stored in Ringer's solution in a domestis refrigerator. The tendon consists of almost pure collagen fibres which are mostly parallel to the long axis.Because of this structure there is a large number of fine capillary channels throughout the length of the specimen through which liquid can flow.When the tendon is stretched, liquid is squeezed out and will stream back into the specimen when it is relaxed.Such a movement of ionic fluid gives rise to a streaming potential.Hence it is necessary to design an experiment in which a streaming potential can be separated from any piezoelectric potential that might be present.

The mechanism of streaming potential at its simplest depends on the adsorption of one type of ion on the surface of the molecule, with an associated diffuse layer of ions of opposite polarity extending out from the molecular surface. Thus there is a potential difference between the solid phase and the bulk of the liquid, normally referred to as the zeta-potential. When the liquid streams past the molecular surface there is a net transport of one type of ion with a resulting potential gradient which may be measured by means of electrodes placed in the liquid stream. To a first approximation the streaming potential V_S is given by the relationship[33]

$$V_S = \epsilon \zeta P / \eta \kappa$$

where ϵ = the dielectric constant, P = the applied pressure, ζ = zeta potential, η = coefficient of viscosity, and κ = specific conductance.

For a complicated molecular structure such as that of collagen ζ varies with the pH of the liquid owing to the many acidic and basic units in the macromolecule which may be ionized. At a given pH termed the iso-electric point, there is no net charge on the macromolecule and the streaming potential is zero. This evidently depends upon the relative number of acidic and basic units in the collagen macromolecule.

The piezoelectric potential is dependent upon the applied stress, and may be expected to be independent of the pH of the surrounding solution.If any charges appear on the surface of the strained fibre from the direct piezoelectric effect they will be cancelled rapidly by ions of opposite polarity absorbed from the solution.This would result in a change in the isoelectric point.Thus in order to separate the two effects experimentally, the tendon should be strained and the potential developed between two electrodes buried into it, measured, varying the pH of the surrounding solution through the isoelectric point.If potentials were observed at the normal isoelectric pH for human tendon collagen they would be attributable to piezoelectric effects.

4.3 Apparatus and Measurements.

The apparatus is shown diagrammatically in Fig 4.1 . The tendon was anchored to a brass hook H by means of a stainless steel wire suture at the lower end.The upper end of the tendon was similarly attached and connected to piano wire which passed over two pulleys, and was attached to the mass M. Freshly made Ag-AgCl electrodes were buried into the tendon a distance three cms apart, by injecting them through a fine glass capillary tube,and subsequently withdrawing the tube.

Fig. 4.1

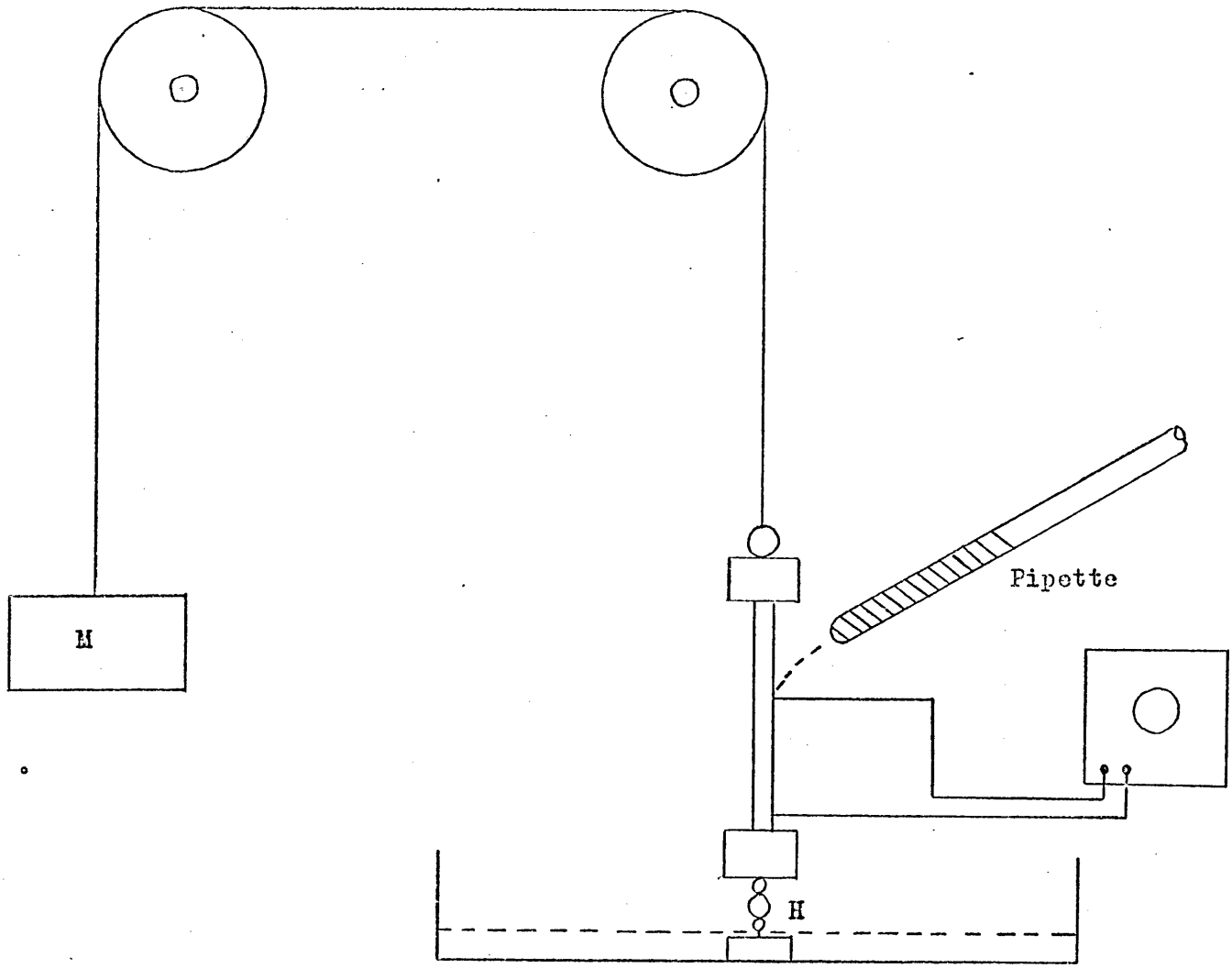

The leads from the electrodes were taken to a Tektronix oscilloscope with a storage screen, having a sensitivity of one millivolt per cm.

The tendon was prepared by allowing it to dry in a dessicator at room temperature until it was stiff, brittle, and pale brown in colour. It was then placed in a solution of known pH, prepared from standard buffer solutions (BDH and Britton and Robinsons[35]), for a period of several days until it became completely flabby. When mounted in the apparatus a slow drip of the same solution was directed over it between measurements, so that the whole length of the tendon was bathed in solution, and to prevent its drying.

To obtain quantitative readings a standard impulse was applied to the specimen by allowing the mass M, of 2-10 kg, to fall through a fixed distance of one inch. This was achieved with a hand-operated wheel. The resulting electrical impulse was displayed on the oscilloscope. The value recorded was the steady pulse amplitude obtained after repeated loadings at approximately one impulse per second for ten to fifteen seconds. In agreement with ideas of streaming potential, the signal produced was proportional to the load, and at pH 4.7 no voltage was obtained whatever the force applied. A graph of

Fig. 4.2

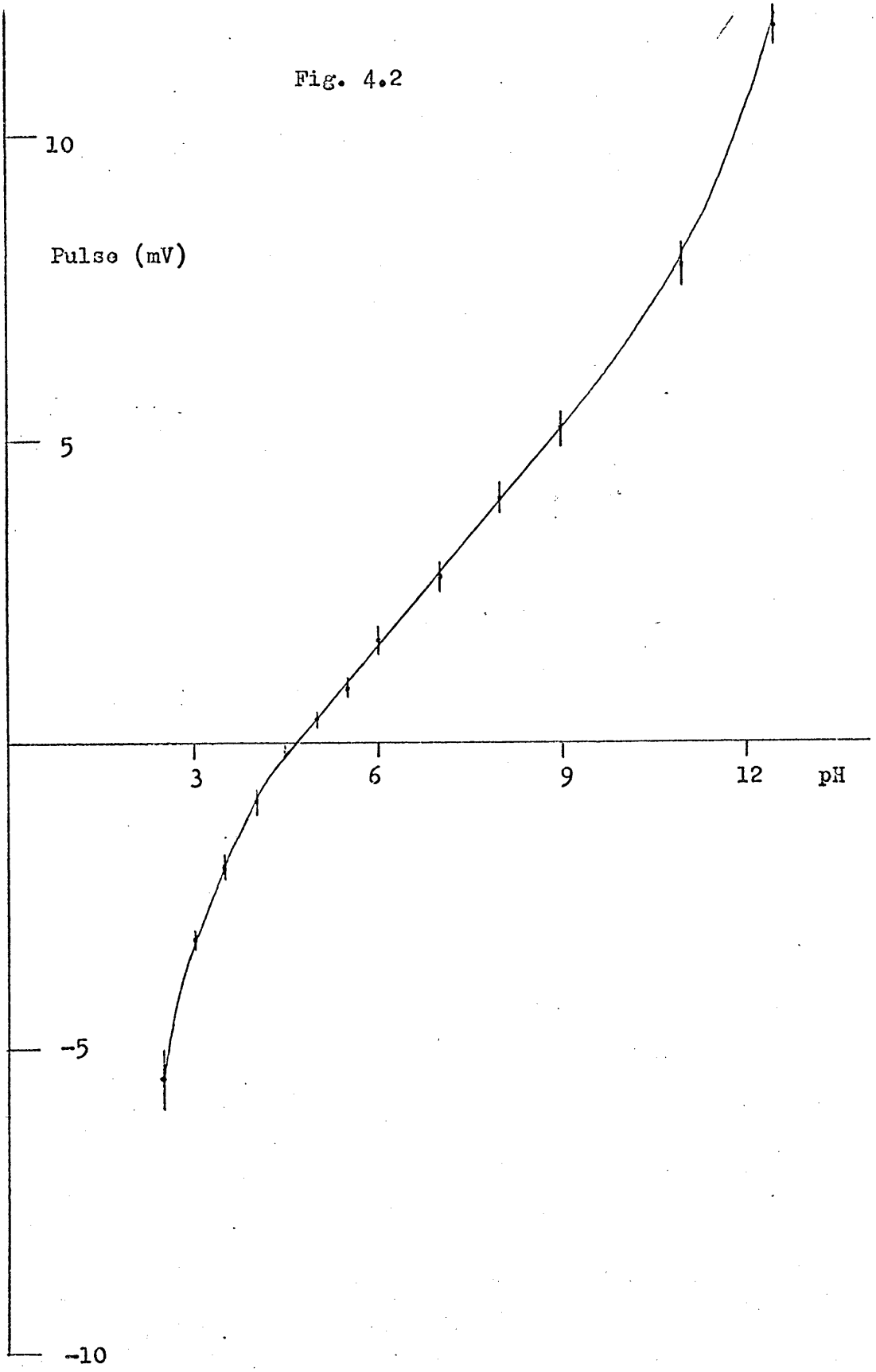

the peak voltage pulse against pH of the solution is shown in Fig 4.2 .

We remark here that if the tendon were pulled equally at both ends, no streaming potentials would be recorded between electrodes which were placed symmetrically with respect to the centre of the tendon; this assumes that no weak points exist in the structure and that the elastic modulus is nearly constant along the fibres. It is clear that when the electrodes are positioned so as to possess the same centre of symmetry as the applied stress, then the resulting streaming voltage will be zero. This condition does not occur in the experiment described here.

4.4 Electrophoretic Measurements.

Whilst isoelectric points for rat-tail and hide collagen have been reported in the literature [36,37,38,39], no information was available on human Achilles tendon collagen. Hence it was decided to build an electrophoretic micro-cell apparatus following the design of Douglas[40]. A brief outline of this form of measurement is given here.

A thin glass rectangular cell is filled with a suspension of the particles in a buffer solution of known pH. These particles are observed under the microscope, and their velocities with

depth determined upon the application of a known electric field across the cell.The particle motion resulting from the electric field derives from electroosmotic as well as electrophoretic forces. The closed rectangular cell is employed in order to separate the two effects.Electro-osmotic forces cause the liquid to move with respect to the glass, so that since the cell is closed, the liquid returns via the middle of the cell. Hence at two given depths in the cell there is no motion of the liquid with respect to the glass.Observation of the particle velocity at these depths effects a measurement of the net charge on the particle,at the given pH, with respect to the liquid.Thus the electro-phoretic particle velocity may be determined against pH. For a cell of known dimensions these depths are known accurately. Authoritative accounts of micro-cell electro-phoresis are given by Abraham and Gorin[41], and by Miller and Golder[42].

The design of Douglas uses the rectangular cell in the conventional horizontal position, but adds a thermostat which fits directly on to the microscope stage, so facilitating accurate temperature control of the solution. It also employs dark-field illumination which improves the microscopic observation.However many difficulties were found with this

'home made' apparatus, the most important of which was diffusion of the electrode solution through the porous membrane into the cell. After repeated attempts to eliminate these difficulties it was decided that reproducible results would not be obtained, and the apparatus was abandoned. Because of this we do not give details here of these experiments. Measurements were finally made on a commercial Carl Zeiss apparatus at the Chester Beatty Research Institute by Dr. Forester. This instrument uses a rectangular cell in the lateral position contrary to the design of Douglas. The effects of gravity are more easily eliminated when the cell is in this position.

The tendon was air-dried and ground up using fine glass paper. Suspensions were prepared using the buffer solutions recommended for electrophoresis by Miller and Golder[42]. An homogeniser was then used on this solution to reduce the mean particle size to approximately five microns; this allows the particles to be in view for a sufficient length of time so that their velocities may be determined. The pH range covered was from 3.5 to 10.

The cell was calibrated by plotting the particle velocity against depth for red blood cells in the bare cell and when the cell was coated with haemoglobin. The electrophoretic velocity of particles with a current of 5mA passing

through the cell solution is plotted in Fig 4.3 for an ionic strength of .05 molar solution. Since the applied electric field has no motional effect on the particles at a pH value of 4.7, we take this to be the isoelectric point for human Achilles tendon.

4.5 Discussion of the results.

The coincidence of the isoelectric point with the pH for zero electrical impulse indicates that the potentials produced are solely due to ionic streaming, there being no contribution from the piezoelectric effect. This is supported by the general similarity in the shapes of the curves of Figs 4.2 and 4.3 . We conclude therefore that the piezo-electric effect is absent from the completely wet collagen. Hence it must belong to a group of higher symmetry than the dry material. Harrington and von Hippel[43] state that the crystallinity of collagen, as revealed by X-ray studies, is destroyed by dehydration, and Bradbury et al[44] demonstrated that systematically disposed water molecules in the collagen macromolecule constitute an important part of the diffracting structure. Esipova et al[45] also found that hydration increased the crystallinity of collagen and inferred that the oxygen atoms of water, bound to the ordered part of the collagen

Fig. 4.3

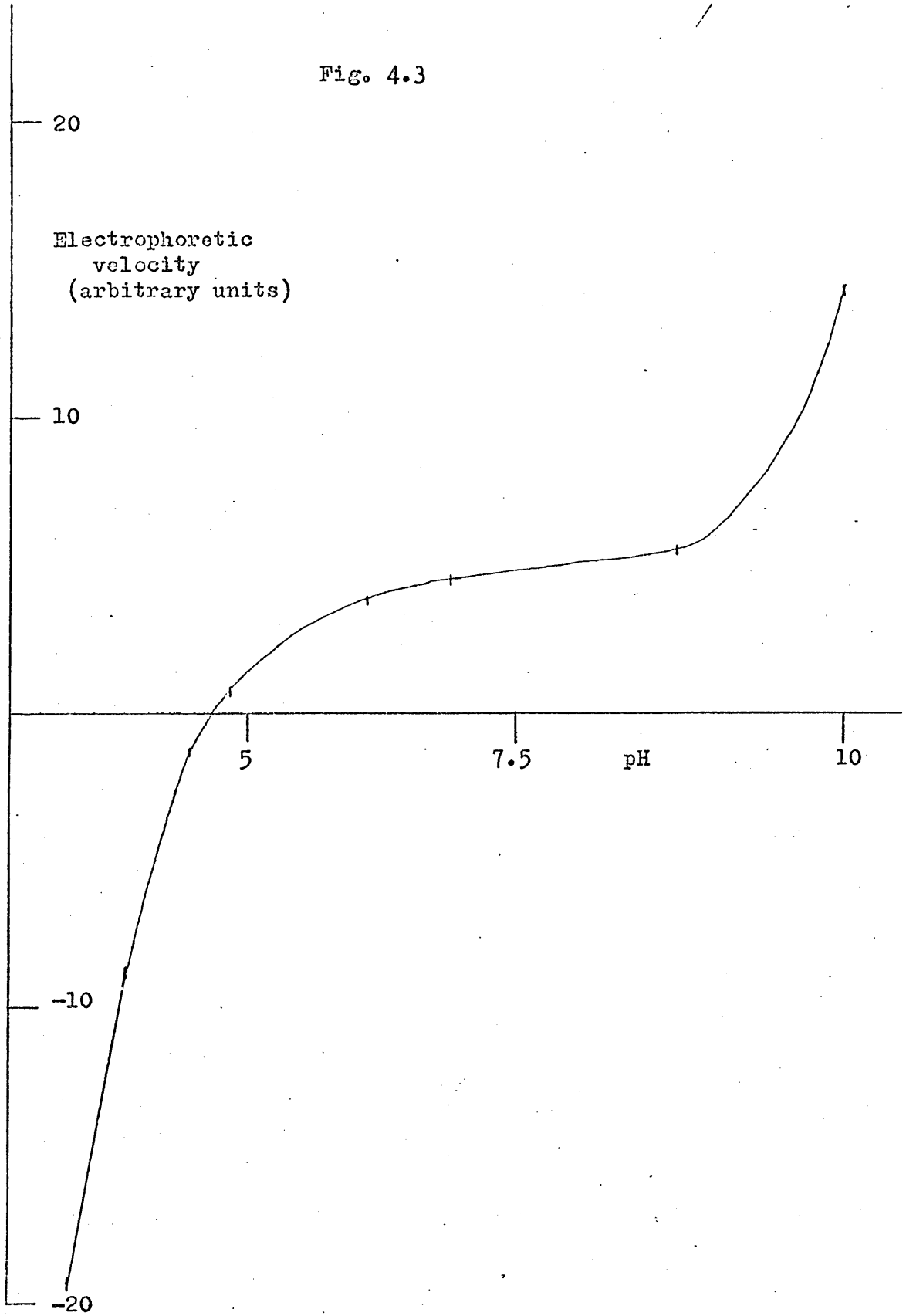
20
Electrophoretic
velocity
(arbitrary units)
10
5
7.5
pH
10
-10
-20

structure, that is the interband region, lie close to the axis of the polypeptide chains. He suggested that the collagen structure might be stabilized by doubly hydrogen-bonded water bridges of the type shown below.

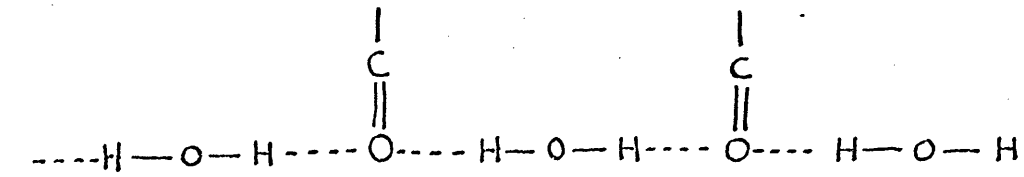

Fig. 3.32 in Chapter Three shows the chain structure proposed by Berendsen as a result of proton resonsnce work on collagen. The experimental support for this orientating chain structure places this water model on a firmer basis than that suggested by Esipova et al, especially since it involves the water molecules in reactions between neighbouring fibrils; and the continous reorientation processes account for the molecular interaction which would otherwise lead to a large broadening of the proton resonance signal. We note that both these wet collagen structures effectively possess the same symmetry, the point group which is $m.\infty:m$, and this point group is one in which piezoelectric effects cannot occur. Thus, whereas dry collagen has been shown to be piezoelectric belonging to the ∞ point group (see Chapter Two), the wet collagen is non-piezoelectric by virtue of structured water raising its molecular symmetry to the point group $m.\infty:m$.

Neutralization of the piezoelectric charge by ions from the surrounding solution does not therefore occur.

Chapter Five

The Piezoelectric Properties of Dry Bone

5.1 Methods of Measurement of Piezoelectric Constants

The physical properties of most large-size piezoelectric crystals are normally investigated by measuring the electrical impedance of the crystal over a wide frequency range. Various cuts for different crystals will suffice to measure the piezoelectric constants, the elastic constants, and the free dielectric constants. The mode of vibration that can be related most satisfactorily to the dielectric and piezoelectric constants of a crystal is the longitudinal mode. This is because the resonant frequency of a long thin bar is controlled by Young's Modulus of the bar, and the capacitance measurements can be directly related to the piezoelectric, elastic, and dielectric constants.For a detailled account the reader is referred to Mason.[49]

However for weakly piezoelectric materials and lossy ones, such as wet bone, the above methods are not the most satisfactory, and it was considered that more accurate measurements would be obtained if the bone were driven under

conditions of moderately heavy loading. Hence it was decided to follow the example of Fukada.[1] An apparatus was built which incorporated his method of measurement. Fig 5.1 shows the practical construction.

5.2 Description of Apparatus.

The specimen, a piezoelectric reference crystal and the output detector crystal are mechanically clamped together, and electrically insulated from each other. In Fukada's apparatus the detecting crystal was of Rochelle Salt, and the signal resulting on this when the input was applied to the specimen was compared to that obtained when the input was applied across a quartz crystal. Considering the temperature variations of Rochelle Salt's physical properties, its hygroscopic nature, and its brittleness, it was decided that a ceramic such as lead zirconate titanate (PZT5) would be more suitable for this apparatus. Consequently both the Rochelle Salt and quartz crystals were replaced by the piezoelectric ceramics. The clamping pressure which enables the piezoelectric vibrations to be transmitted throughout is applied by a lever mechanism on to an insulated plunger which presses on to the specimen. A known set of weights is then hung from the arm of the lever so that a

Fig. 5.1

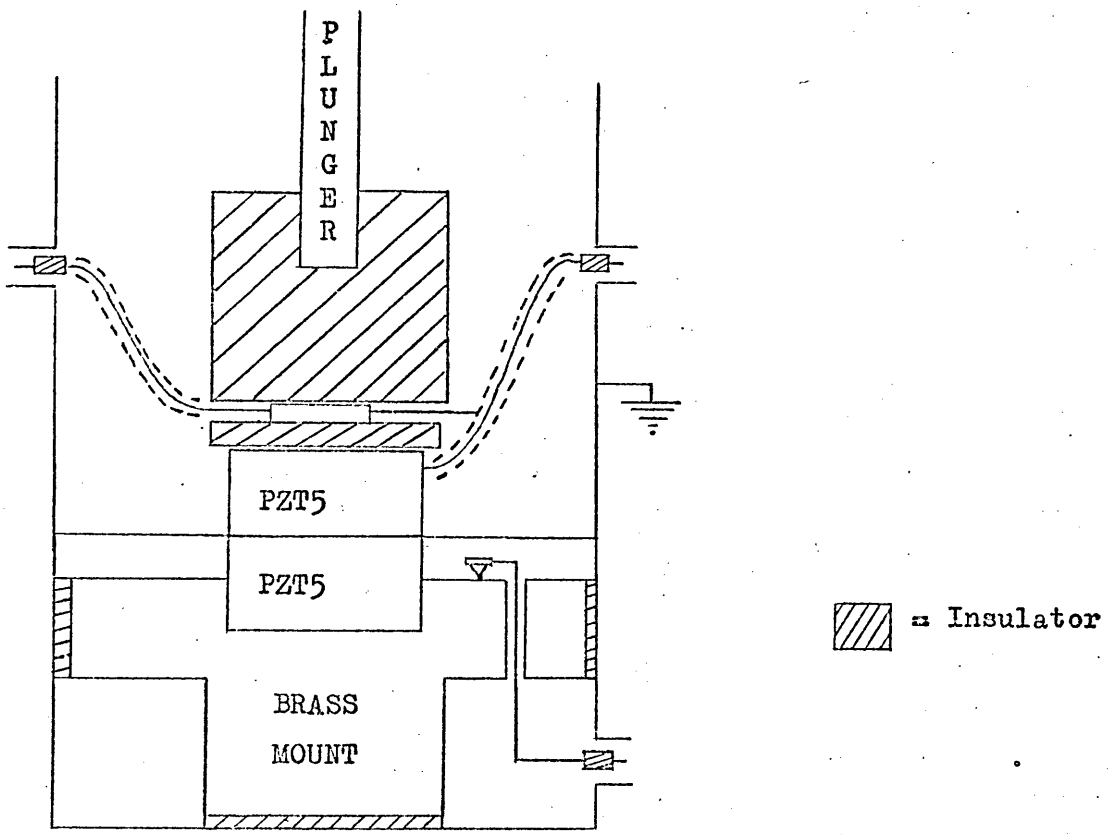

constant clamping force is applied to the system.This provides a uniform transmission coefficient.Electrical connection to the specimen is made via a coaxial plug screwed into the outside brass cylinder, which is at earth potential.The upper PZT5 ceramic lies between the insulator above and a thin circular brass disc below.The two conducting faces of the ceramic are electrically connected to a second coaxial plug on the opposite side of the brass cylinder. The lower ceramic sits in a brass mount which renders it immobile in the horizontal direction.At the level of the lower ceramic there exists a thread on the outer brass cylinder. A threaded brass annulus, into which the upper cylinder fits, screws down on to this, and if the thin brass disc is placed on the lower ceramic, screwing down causes it to be firmly held against the upper face of the ceramic.The brass cylinder, thin disc, and the upper face of the lower ceramic are therefore at earth potential.Hence the output detector crystal is electrically shielded.Electrical connection to the detector crystal is made via a screw which is embedded into the top of the brass mount. A wire is taken through a hole in the mount to the coaxial plug near the bottom of the cylinder.An annulus of tufnel fits round the brass mount, and with a sheet of polythene glued to the bottom of the mount, the latter is completely insulated.The ancillary

apparatus consists of a signal generator, an audio amplifier and transformer which drives the specimen, a tuned audio amplifier, and an oscilloscope.The two ceramics are one inch in dianeter, half one inch in thickness.

5.3 Experimental Procedure

In measuring the converse effect,the audio voltage from the signal generator and amplifier is fed to the specimen, which if piezoelectric, will vibrate at the same frequency.Since the two ceramics and the specimen are clamped together, these vibrations will be transmitted to the detecting ceramic across which an A.C voltage will appear, owing to its own direct effect.The upper PZT5 is electrically shorted, so that it functions merely to transmit the vibrations of the specimen to the detecting ceramic. The signal appearing across the detector is selectively amplified and measured, and fed to the oscilloscope for display. The input signal is then applied across the top ceramic, by throwing a switch, and the specimen shorted out.(In practice this latter action is not necessary because of the large difference in the piezoelectric coefficients of bone and PZT5.)The signal appearing across the out-put ceramic is similarly measured and

displayed.Knowing the applied voltages and the output signals, and the specimen dimensions, the d coefficient of the specimen can be related to that of the upper ceramic.(This is evaluated in detail in the section).

When it is desired to measure the direct effect in the specimen, the detector ceramic is driven at the audio frequency, and the output signals are taken off the upper ceramic and the specimen respectively.The output signals appearing across the ceramic and the specimen depend upon their effective impedances at the operating frequency, and the loading of the amplifier and leads, as well as the dimensions of the specimen.Knowing these impedances the d coefficients of the specimen and the PZT5 ceramic, operated in the direct effect, may be related to each other. This is treated in detail in 5.5 .

The principles of measurement require that the components which form the vibrating system should operate well away from their resonant frequencies, so that all the components are essentially in phase or anti-phase.This means that they should be operated under forced vibration conditions.In a simple analysis one may imagine the multi-component system to oscillate as a single body in the thickness mode such that $\lambda \gg 2d$, where λ is the wavelength of the oscillation and d is the effective

thickness of the single component system . Consideration of the dimensions of the componentsleads to the operating frequency being in the low audio range.

5.4 Theory of Measurement of The Converse Effect.

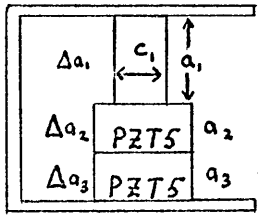

This explanation is largely that of Fukada.

The above diagram is a schematic illustration of the apparatus, and shows a specimen crystal, a reference crystal, and the detector ceramic clamped together.The fundamental thermodynamical equations for a crystal vibrating under conditions of constant entropy may be written in the matrix form

$$S_i = \sum_{j=1}^{6} s_{ij} T_j + \sum_{k=1}^{3} d_{ki} E_i$$

$$\delta_m = D_m/4 = \sum_{n=1}^{6} d_{mn} T_n + \sum_{p=1}^{3} (\epsilon^T_{mp}/4) E_p$$

This notation has been explained in Chapter Two.

The voltage V_s is applied to the electrodes of the specimen which are separated by the distance c_1 .The strain resulting from this voltage , in the vertical direction, is given by the first relation above, and for the present case may be written,

$$\Delta a_1/a_1 = 1/E_1(F/A_1) + d_s(V_s/c_1)$$

where a_1 is the vertical length of the specimen.

A_1 = the X-sectional area of the specimen.

E_1 = Young's Modulus of the specimen

F = the oscillatory force.

d_s = the operative piezoelectric coefficient of the specimen.

Hence the change in a_1 is given by

$$\Delta a_1 = a_1/E_1(F/A_1) + a_1/c_1(V_s d_s)$$

The upper ceramic will deform by the amount $\Delta a_2 - \Delta a_1$, relative to the upper clamp, and since it is shorted at this stage, we have

$$\Delta a_2 - \Delta a_1 = a_2/E_2(F/A_2)$$

where E_2 = Young's Modulus of the upper ceramic.

A_2 = X-sectional area of upper ceramic.

The deformation of the detector ceramic is given by,

$$\Delta a_3 \; \underline{\Delta} a_2 = (a_3/E_3)F/A_3 \; + d_{PZ}(a_3/a_3)V_3$$

where E_3 = Young's Modulus of lower ceramic.

A_3 = X-sectional area of lower ceramic.

d_{PZ} = Operative d coefficient of the lower ceramic.

V_3 = Voltage appearing across the lower ceramic.

If it is assumed that the clamp prevents the total system from deforming the clamping frame deforms by $-\Delta a_3$, and we have,

$$-\Delta a_3 = (a_4/E_4)F/A_4$$

where a_4, E_4, and A_4 are the effective values, as before, for the frame. If the last four equations are added, we obtain

$$0 = F \sum_{i=1}^{4} a_i/(E_i A_i) \; + d_s(a_1/c_1)V_s \; + d_{PZ}V_3$$

It is shown in the next section dealing with the theory of the direct effect measurements, that the relationship between the oscillatory force F and the output voltage V_3 appearing

across the detector ceramic is

$$V_3 = \frac{d_{PZ}\, F}{C_{PZ} + C_L} \times \left(\frac{1 + j(X'_{PZ}/R_L)}{1 + (X'_{PZ}/R_L)^2} \right)$$

The notation is explained in the next section. This equation may be written,

$$V_3 = KF$$

where K is a constant for given circuit conditions and operating frequency. Hence substituting for F in the last but one equation we obtain

$$(a_1/c_1)V_s d_s = -V_3 \left(d_{PZ} + 1/K \sum_{i=1}^{4} (1/E_i A_i) a_i \right)$$

If we now relabel V_3, V_{OS}, to indicate that it is the output voltage when the input voltage is fed to the specimen, the last equation reads

$$d_s (a_1/c_1) V_s = k\, V_{OS}$$

where k is a constant for the apparatus. When the input voltage

is applied across the reference ceramic and the specimen shorted out, a similar analysis as that followed above leads to the result,

$$d_{PZ}\, V_{PZ} = k\, V_{O.PZ}$$

Hence eliminating the constant k between these two equations we obtain

$$d_s/d_{PZ} = (c_1/a_1)(V_{PZ}/V_s)(V_{O.S}/V_{O.PZ})$$

This is therefore the required relation linking the operative 'd' coefficient of the specimen with that of the reference ceramic, when both are operated in the converse effect.

Consideration of the electromechanical relations of a free oscillating crystal below its resonant frequency shows that the electrical impedance is largely capacitive. Hence in the above case this capacitance shunts the driving amplifier, so requiring the source to drive more current through the circuit than at higher frequencies. As long as the source is capable of supplying the current needed, the piezoelectric may be satisfactorily operated at low frequencies in the converse effect.

5.5 Theory of Measurement of The Direct Effect

We have already remarked that for the direct effect measurements the lower detector ceramic is driven at the audio frequency, and that the output signal is taken off the reference ceramic and the specimen respectively. Hence comparison of the piezoelectric properties of the specimen with those of the reference ceramic is made by relating the two output signals, for the same applied voltage to the lower ceramic, to the two piezoelectric coefficients in question.

We now treat the case of a voltage appearing across a piezoelectric crystal resulting from an applied force F. The impedance of the crystal is assumed to be wholly capacitive, and much greater than the loading resistance of any measuring instruments. The definition of the piezoelectric 'd' coefficient of a crystal operated in the direct effect, is that it relates the ratio of short circuit charge per unit area of electrode , flowing between electrodes which are perpendicular to a specified axis, to the stress applied along or around a specified axis , when all other stresses are constant. This last qualification means that the crystal must be essentially free. The direct effect may thus be written, neglecting subscripts,

$$P = dT$$

where P is the polarization per unit area.

T is the applied stress.

The charge per unit area σ, is given by the relation

$$\sigma = Q/A = Ce/A = dF/A' \quad \text{and} \quad e = (A/A')dF/C$$

where Q is the total amount of charge produced.

A' is the area on which the external force acts.

A is the area of the electrodes.

C is the capacity of the crystal

e is the voltage appearing across the electrodes.

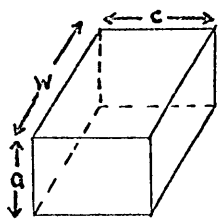

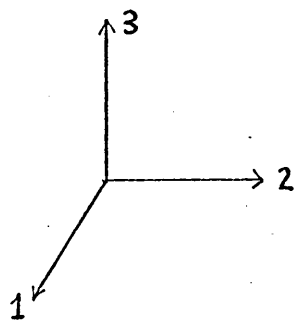

We consider the situation existing in the above piezoelectric crystal, where the force acts on the 3 faces, and the electrodes are painted on the 2 faces.

$$A' = cw, \quad \text{and } A = aw \quad \therefore A/A' = a/c$$

where in previous notation when the crystal is clamped in the apparatus, a is the vertical length of the crystal, and c is the distance between the electrodes. Therefore we have, retaining the unity of C,

$$e = (a/c)\, dF/C$$

If the capacitive loading C_L of the amplifier and leads is not negligible when compared with C, the above relation becomes,

$$e' = (a/c)\, dF/C + C_L$$

$$\therefore e'/e = C/C+C_L = C/C'$$

We may represent the above crystal and circuit loading by the equivalent circuit drawn below.

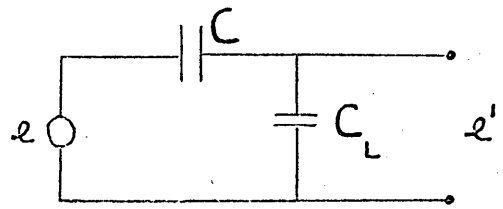

We now go to the most general situation where the crystal is lossy and has a shunt leakage resistance R_c , and the resistive loading of the amplifier and leads is R_L . The equivalent circuit is now ,

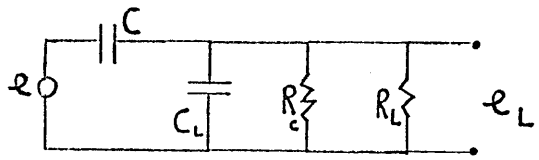

It is clear from the last potential divider circuit that we may represent the above circuit as

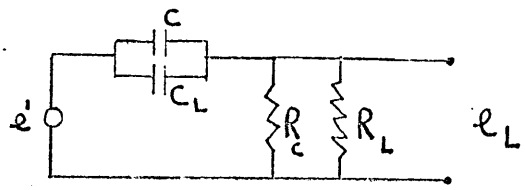

This is in fact using Thévenin's theorem. If R is the resultant parallel combination of R_c and R_L we have

$$e_L = e' \cdot \left(\frac{1 + j(X_{c'}/R)}{1 + (X_{c'}/R)^2} \right)$$

where $X_{c'}$ is the reactance of C and C_L in parallel at the operating frequency. Fig. 5.51 how e_L varies as the values of

Fig. 5.51

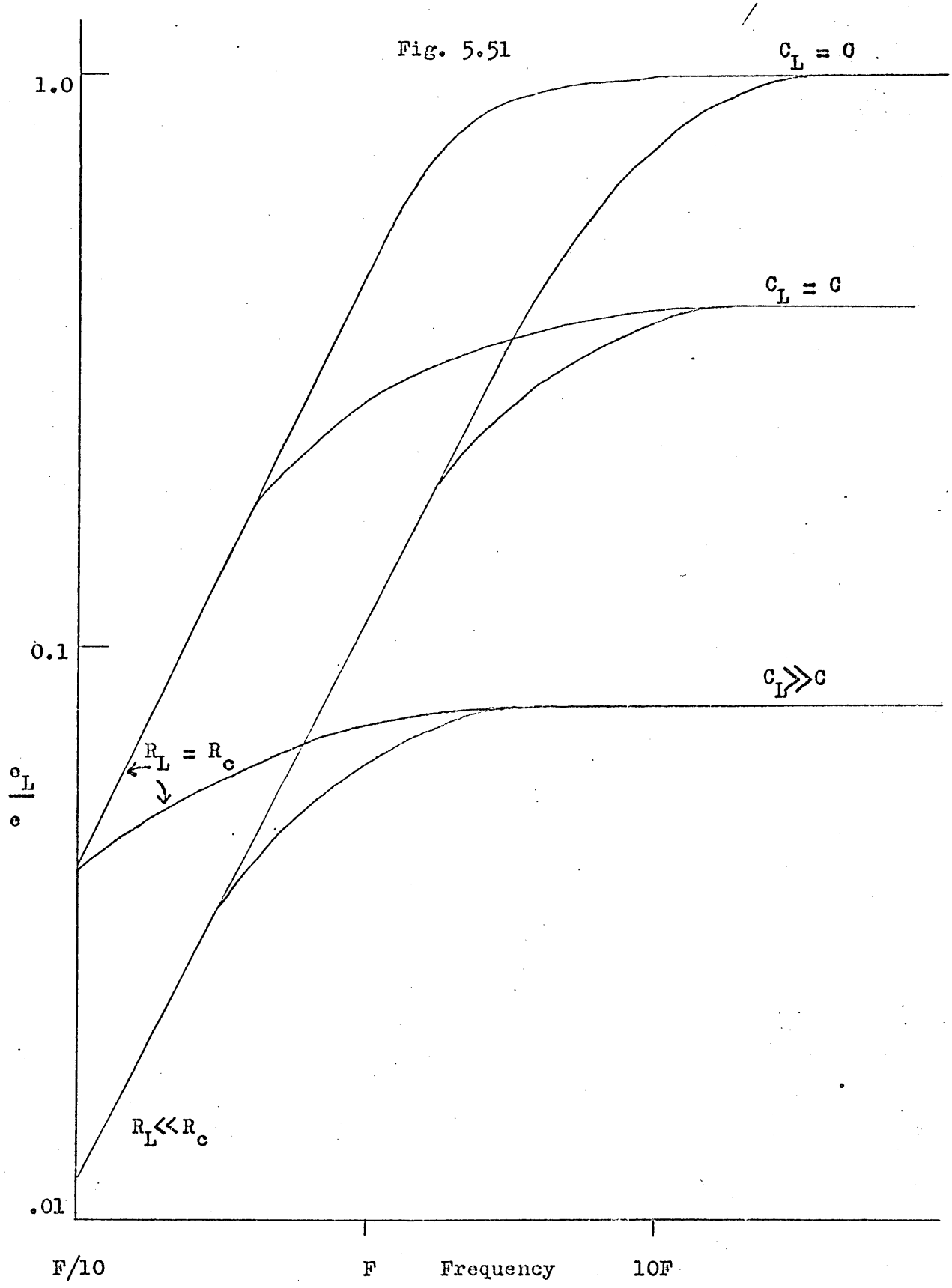
1.0
0.1
.01
$C_L = 0$
$C_L = C$
$C_L \gg C$
$R_L = R_c$
$R_L \ll R_c$
$\frac{e_L}{e}$
F/10
F
Frequency
10F

the components change. When the capacitances in the circuit are large relative to R, $X_{C'}/R \ll 1$, and we have

$$e_L = e' = (a/c)\frac{dF}{C'}$$

For very low frequencies or low R, $X_{C'}$ becomes much greater than R and so we obtain ,

$$e_L = je'R/X_{C'} = je'wC'R = jwRdF(a/c)$$

Hence for the more normal operating conditions where the voltage is capacitance controlled

$$e_L = e' = 1/C' \ (a/c)dF$$

and for very low frequencies where it is resistance controlled,

$$e_L = jwR(a/c)dF$$

In these relations w is the angular frequency. The above relations show how the voltage appearing across a piezoelectric crystal

may be expressed in terms of the stress applied, the operative piezoelectric coefficient, the crystal dimensions, and the circuit constants.It is thus apparent that by measuring the output signals when the switch is thrown, d_s may be compared to d_{PZ} .

5.6 Results for Quartz and Dry Bone, in the Converse Effect.

The apparatus was effectively calibrated using two X-cut quartz discs operated in the direct and converse effects.They were both 2.54 cms in diameter and of thickness 3mm and 1mm respectively.

5.61 Results for Quartz

The d_{33} coefficient of the PZT5A ceramics used is 374×10^{-12} coulombs/newton, $= 1122 \times 10^{-8}$ e.s.u/dyne.Cady recommends the value of 6.9×10^{-8} e.s.u/dyne for the d_{11} of quartz, so that

$$\frac{d_{11}(\text{quartz})}{d_{33}(\text{PZT5A})} = 1/162$$

The experimental values obtained for this ratio were $1/(160 \pm 20)$ for the 1mm disc, and $1/(156 \pm 15)$ for the 3mm

disc.The measurements were taken over the audio range 300 to 6000Hz.The errors are the spread of the results in this range, as no dependence upon frequency was observed.There is therefore satisfactory agreement with the theoretical value, since the magnitude quoted above for the d_{11} of quartz has a spread of approximately 10% according to Cady.

5.62 Determination of the Converse Piezoelectric Coefficients in Dry Human Bone.

These measurements were carried out on pieces of human femoral bone which had been stored in a domestic refrigerator for two weeks, fresh initially, before the present author received them.Fig. 5.62 shows the right-handed Cartesian coordinates which are ascribed to the femur, and a typical specimen which was used in the experiments.

The two specimens excised from the femur were practically cubic in shape, with a length of one centimetre.They were cut with a normal fine saw, and polished with glass paper.Drying of the specimens was accomplished by placing them in a closed box containing silica gel, for at least 48 hours.This was considered to be preferable to drying by continous heating, which was the drying method adopted by Fukada, since the bone protein

Fig. 5.62

Diagram of Bone Femur and Typical Specimen

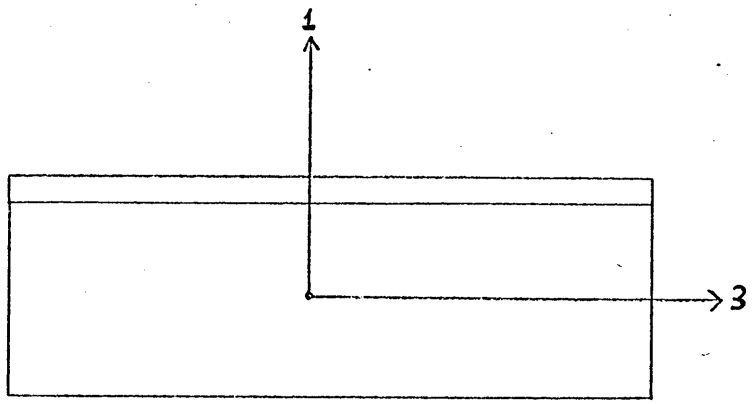

Side View

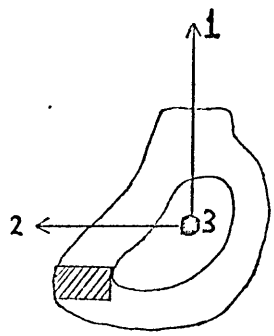

View in Cross-section

denatures when kept at 65°C or above for several hours. In our opinion this method produces suitable specimens with the least amount of damage done to them, thus facilitating their description as pieces of 'dry bone'. They appeared very white in colour. (This preparation technique was improved upon for the later measurements on the beef specimens, and will be described later.)

For these human specimens the electrodes were painted on with conducting araldite to which thin coaxial leads were attached. The araldite was partially cured by placing the pieces of bone under a 60watt bench lamp for approximately ten minutes, and then leaving the specimens for about six hours to finally dry. It is extremely unlikely that the heat supplied by the lamp denatured the protein, since it was short-lived, and indeed for some of the measurements, curing was achieved by drying at room temperature for 24 hours, so reducing the total amount of heat supplied. The quantitative results support this. It is apparent from Chapter Two that with one rectsngular specimen all the nine non-shear coefficients, relative to the bone long direction, may be measured. It is these coefficients which were determined. for all the bone specimens , whether human or bovine. We did not take several obliques cuts, as is normally the practice in piezoelectric crystal measurements, as this had already been done by Fukada.

We considered that the measurement of these non-shear coefficients, relative to the bone long direction, warranted the greatest attention for two reasons. Firstly, there appeared to be considerable doubt on the magnitude of these coefficients for the bone specimens, (which had been dried by heating), in Fukada's experiments (see 5.9). And secondly, it should be the magnitude of these coefficients which would provide the greatest information on the piezoelectric role of collagen in bone. These bone coefficients were measured over the same frequency range as for the quartz crystals, and similarly the error is the spread of the results. The magnitudes of the d_{ij} , $(i,j = 1,2,3)$ are, in units of 10^{-8} c.g.s

$$\begin{pmatrix} 0.1 \pm .10 & 2.5 \pm .18 & 1.4 \pm .17 \\ 0.2 \pm .10 & 0.8 \pm .02 & 1.4 \pm .18 \\ 0.9 \pm .08 & 1.6 \pm .04 & 0.5 \pm .05 \end{pmatrix}$$

When these measurements were made the signs of the coefficients were not determined.

5.63 Determination of the Converse Piezoelectric Coefficients in Dry Beef Bone.

Both the direct and converse measurements made on fresh beef femoral bone were carried out on the same two specimens which had been previously been used for the wet piezoelectric measurements.These are labelled 'Large Specimen No.1' , and 'Large Specimen No.2' , and their dimensions in mm in the 3,2, and 1 directions are 14.0x10.0x6.0 , and 13.5x7.0x6.5 respectively, so that both their longest dimensions coincide with the long direction.Pertinent to this section, the wet history of the larger specimen is that its pH was always kept between 6.88 and 7.40, whereas the smaller piece served to determine any possible variation of the electrical signal with the effects of pH on bone, and was subjected to buffer solution pHs down to 4.5 for several days at atime.

At no time was heat applied to the beef specimens. Conducting araldite was dispensed with, and the electrodes were painted on with 'Silver Dag', a suspension of predominantly silver and graphite in amyl acetate.The leads were found to be satisfactorily connected by the dag to the bone, if the former were left to dry completely for an hour or more.The specimens wre cut on a wet circular diamond saw so that they remained cool throughout the cutting period.They were finally polished on wet glass paper and placed in salt solutions buffered to pH 7.0 .These fresh pieces of bone were observed to be

brilliantly white in colour, similar to polished ivory. We consider this preparation procedure to be an improvement on that used on the human bone. The orientation of the beef specimens was better, and there was no possibility of denaturation of the bone protein having occurred in the preparation. After the wet piezoelectric measurements had been completed the two specimens were completely dried with silica gel and P_2O_5.

It was decided to take all the measurements on beef bone at 1kHz, since an examination of the previous results on human bone taken in the range 300 to 6000 Hz revealed no dependence upon frequency. The error indicated for these beef results represents the scatter of approximately ten observations for each coefficient taken over a period of three months. The values are, in units of 10^{-8} c.g.s

L. Sp. No.1

$$\begin{pmatrix} +.11 \pm .05 & 11 \pm .04 & -.25 \pm .1 \\ -1.38 \pm .2 & .04 & +.65 \pm .15 \\ -.21 \pm .07 & -.48 \pm .1 & -.40 \pm .1 \end{pmatrix}$$

L.Sp. No.2

$$\begin{pmatrix} +.55 \pm .1 & .11 \pm .1 & -.25 \pm .1 \\ -1.60 \pm .2 & .04 & +.70 \pm .1 \\ -.20 \pm .1 & -.32 \pm .1 & -.45 \pm .1 \end{pmatrix}$$

No sign has been allocated to the d_{12} coefficient and the d_{22} coefficent as both signs were obtained for these two coefficients during the course of the measurements.

5.7 Determination of the Direct effect Coefficients in Quartz and Dry Beef Bone.

5.71 Quartz.

It has been remarked in 5.5 that if the voltage across a piezoelectric crystal is to give the magnitude of the operative piezoelectric coefficient, the value of $(X_{c'}/R)$ must be known. For the reference ceramic, C' = its own static capacitance C plus that of the amplifier and leads C_L.

$C = (\epsilon^T/\epsilon_o)\epsilon_o\ (A/t)$ farads, where

ϵ_o = dielectric constant of free space, = 8.85×10^{-12} farads/metre.

ϵ_T/ϵ_o = relative dielectric constant, free.

A = area of the electrodes, = 5.0×10^{-4} m^2.

t = thickness of ceramic = 1.27×10^{-2}.

Inserting these values into the expression above we obtain C = 605pF. This value was obtained when the capacitance of the ceramic was measured on the Wayne Kerr Bridge. When the reference

ceramic was placed in the apparatus , its capacitance and that of the shunting leads was measured to be 796.2pF $\pm$ .1pF.Hence $C' = 796.2pF$ and $X_{C'} = 200Kohms$ at 1 kHz.

For all dry measurements R derives from the input resistance of the tuned amplifier, which varies from 10^6 ohms to 250K as the gain is increased to a maximum.When the signal was taken off the PZT5 the gain was very low so that we may effectively ignore $X_{C'}/R_L$ compared to 1.We thus obtain the relationship,

$$(e_L)_{PZ} = d_{PZ} F/ C'_{PZ}$$

For the quartz 3mm crystal $C_{Q'}$ was measured to be 163pF, so that $X_{C'} = 10^6 ohms$, and $X_{C'}/R = 1.25$. We therefore obtain

$$(e_L)_Q = 1/1.60 \cdot (d_Q F)/C_{Q'}$$

From these two relations we obtain the result that

$$\frac{d_{PZ}}{d_Q} = (3.0)\ (e_L)_{PZ} /(e_L)_Q$$

The ratio of the two output voltages taken over readings at 1 kHz is 45 $\pm$ 10.(The error here represents the maximum

scatter. We therefore obtain ,

$$d_{PZ}/d_Q = 138 \pm 30 .$$

This is not such a good result as for the converse effect, but this is to be expected since the errors are greater here.

5.72 Results for Dry Beef Bone.

As for the quartz crystal the capacitance is nearly all due to the cables. For a typical bone specimen C_B, was measured to be 188 ± 2pF. Using a similar analysis as for quartz the result is obtained,

$$\frac{d_B}{d_{PZ}} = (c/a)\ (1/3)\ \frac{(e_L)_B}{(e_L)_{PZ}}$$

where d_B is the piezoelectric coefficient of dry bone. The results for the two specimen are , in units of 10^{-8} c.g.s

L.Sp. No.1

$$\begin{pmatrix} +.073 \pm .003 & .145 \pm .007 & -.20 \pm .02 \\ -1.4 \pm .07 & .03 & +.54 \pm .05 \\ +0.3 \pm .1 & -.50 \pm .02 & -0.4 \pm .1 \end{pmatrix}$$

L.Sp. No.2
$$\begin{pmatrix} +.56 \pm .05 & .14 \pm .01 & -.20 \pm .02 \\ -1.68 \pm .08 & .03 & +.60 \pm .05 \\ -0.25 \pm .02 & -.55 \pm .06 & -.42 \pm .05 \end{pmatrix}$$

Summary of the dry results,(excluding errors) in c.g.s units

Human Bone
2 Specimens
$$\begin{pmatrix} 0.1 & 2.5 & 1.4 \\ 0.2 & 0.8 & 1.4 \\ 0.9 & 1.6 & 0.5 \end{pmatrix} \times 10^{-8}$$

Beef Bone
Converse Effect
$$\begin{pmatrix} +.11 & .11 & -.25 \\ -1.38 & .04 & +.65 \\ -.21 & -.48 & -.40 \end{pmatrix} \times 10^{-8} \quad \text{No.1}$$

$$\begin{pmatrix} +.55 & .11 & -.25 \\ -1.60 & .04 & +.70 \\ -.20 & -.32 & -.45 \end{pmatrix} \times 10^{-8} \quad \text{No.2}$$

Beef Bone
Direct Effect

$$\begin{pmatrix} +.07 & .15 & -.20 \\ -1.4 & .03 & +.54 \\ +0.3 & -.50 & -.04 \end{pmatrix} \times 10^{-8} \qquad \text{No.1}$$

$$\begin{pmatrix} +.56 & .14 & -.20 \\ -1.7 & .03 & +.60 \\ -0.3 & -.55 & -.40 \end{pmatrix} \times 10^{-8} \qquad \text{No.2}$$

5.8 Interpretation of The Dry Results

It is immediately apparent from the above figures that this piezoelectric effect is highly directional. Because of this, and the fact there is no doubt that dry tendon collagen is piezoelectric, it was decided that an effort should be made to determine if the dry bone results could be explained as deriving from the bone collagen. It is desirable to relate the coefficients found by Fukada for tendon collagen to the bone collagen fibres, and the structure of these fibres relative to the bone long direction. In doing this, consideration should be given to the relative permittivities of tendon collagen and bone, both in the dry state. It is clear from the piezoelectric properties of parallel collagen fibres (see 5.9 and Chapter Two), that if the protein

fibres in bone were all accurately parallel to the bone long direction, and in the same sense, then relative to this direction the piezoelectric matrix would be identical in symmetry with that found for Achilles tendon, that is

$$\begin{matrix} 0 & 0 & 0 & d_{14} & d_{15} & 0 \\ 0 & 0 & 0 & d_{15} & -d_{14} & 0 \\ d_{31} & d_{31} & d_{33} & 0 & 0 & 0 \end{matrix}$$

Hence if this were the case for the specimens investigated here, one would only measure d_{31}, d_{32}, and d_{33} as non-zero coefficients. This is not the case for these results, so that it must be concluded that the collagen fibres are not all in the long direction for the specimens used. Reference to Chapter Three indicates that in a relatively small specimen that has been excised from a femur, the collagen fibres will statistically speaking make an oblique angle with the long direction of the femur. Hence as a first step in attempting to relate the properties of tendon collagen to bone collagen it is necessary to account for a possible non-alignment of the protein fibres with the bone long direction. We use the two right-handed coordinate systems shown below. The bone long direction

coincides with the 3' axis, and the net fibre long axis with the 3 direction. The two coordinate systems are linked by rotation of ϕ° about the 1 axis. The angle of rotation θ about the bone long direction denotes the orientation of the fibres about their own fibre axis. The transformation matrix $\vec{a}$, changing the description of the piezoelectric effect from the undashed to the dashed system of coordinates is

$$\vec{a} = \vec{R}_{\phi}\vec{R}_{\theta}$$

where R_{θ} is the rotation through θ° about the 3' axis

R_{ϕ} is the rotation through ϕ° about the 1' axis.

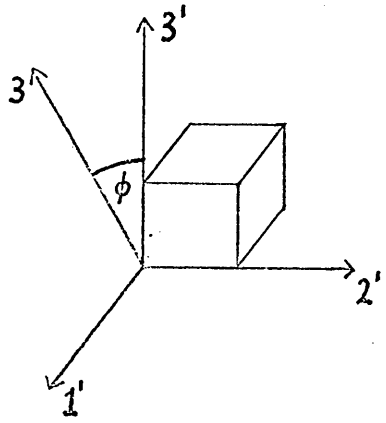

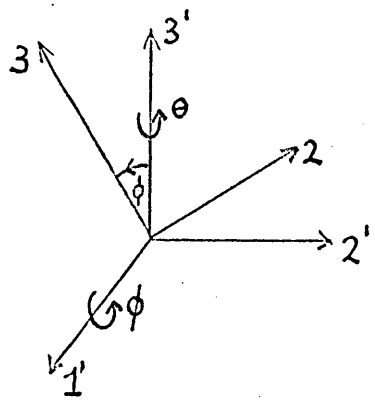

If the piezoelectric coefficients of the irreducible (∞)T group are transformed to the above oblique set of coordinates, the following non-shear terms are obtained.

$d'_{11} = 0$; $d'_{12} = -\frac{1}{2}\sin 2\phi\, d_{14}$; $d'_{13} = \frac{1}{2}\sin 2\phi\, d_{14}$;

$d'_{21} = -\sin\phi\, d_{31}$; $d'_{22} = -\sin\phi\cos^2\phi\, d_{31} - \sin^3\phi\, d_{33} - \sin\phi\cos^2\phi\, d_{15}$;

$d'_{23} = -\sin^3\phi\, d_{31} - \sin\phi\cos^2\phi\, d_{33} + \sin\phi\cos^2\phi\, d_{15}$;

$d'_{31} = \cos\phi\, d_{31}$;

$d'_{32} = \cos^3\phi\, d_{31} + \sin^2\phi\cos\phi\, d_{33} - \cos\phi\sin^2\phi\, d_{15}$;

$d'_{33} = \sin^2\phi\cos\phi\, d_{31} + \cos^3\phi\, d_{33} + \sin^2\phi\cos\phi\, d_{15}$;

Thus with the above values, the matrix of the non-shear terms is ,

$$\begin{matrix} d'_{11} & d'_{12} & d'_{13} \\ d'_{21} & d'_{22} & d'_{23} \\ d'_{31} & d'_{32} & d'_{33} \end{matrix}$$

It is apparent that the angle θ is absent from the above coefficients. This is to be expected since the collagen fibres are symmetrical in their own 1 and 2 directions. Had we started

with the coefficients of the $(\infty.m)T$ group, the above matrix would be modified so that polarization would not occur in the 1' direction. Likewise if the coefficients of the $(\infty:2)T$ group had been used, the only resulting polarization would be in the 1' direction, for simple stresses in the other two directions. Hence using a simple rotation transformation about the 1' axis the oblique coefficients are obtained, and they are the most general coefficients for a rotation about one axis. However, they do not represent the most general oblique texture coefficients, since the taking of the rotation about the 1' axis confines the fibres to the 2'3' plane(as seen in the last diagram), and there is no reason a priori, why for the arbitrary way in which the specimens were cut out, the resultant statistical fibre orientation should be in the plane 2'3', or any other labelled plane. Hence the given transformed matrix represents the bone collagen piezoelectric coefficients relative to the bone long direction, only if the net fibre orientation is in the 2'3' plane. Had a rotation R about the 2' axis been taken we would have obtained the following matrix, (the values of the coefficients are as before)

$$\begin{matrix} d'_{22} & -d'_{21} & -d'_{23} \\ d'_{12} & d'_{11} & d'_{13} \\ d'_{32} & d'_{31} & d'_{33} \end{matrix}$$

and this would represent the bone collagen piezoelectric coefficients relative to the bone long direction, only if the net fibre orientation were in the 1'3' plane.Hence the most general oblique non-shear coefficients which represent the piezoelectric properties of the bone collagen lies somewhere between these two matrices, the actual values depending upon the resultant fibre orientation in the particular bone samples under consideration.However, since these two matrices represent the extreme cases, we shall keep them separate and evaluate them using the figures measured for parallel tendon collagen fibres by Fukada.It is not certain that the bone collagen is identical in structure with tendon collagen. Both Glimcher et al[50], and Ascenzi[51], have found differences between pure collagen and that found in mineralized tissue. However the tendon collagen values are expected to give a good indication of whether the oblique coefficients are capable of explaining the experimental results.Fukada's values are

$$d_{14} = -8.0\times10^{-8}\ \text{c.g.s} \quad ; \quad d_{15} = 4.2\times10^{-8}\ \text{c.g.s}$$

$$d_{31} = 0.2\times10^{-8}\ \text{c.g.s} \quad ; \quad d_{33} = 0.26\times10^{-8}\ \text{c.g.s}$$

If these values are used and a value of 10° is taken for ϕ,

the two matrices corresponding to the two extreme cases are , in units of 10^{-8} c.g.s

$$\begin{pmatrix} 0 & +1.368 & -1.368 \\ -.035 & +.740 & +.662 \\ +.197 & +.079 & +.380 \end{pmatrix}$$

and

$$\begin{pmatrix} +.740 & +.035 & -.662 \\ -1.368 & 0 & +1.368 \\ +.079 & +.197 & +.380 \end{pmatrix}$$

Although there are discrepancies it is apparent that the first matrix approaches the results for human bone, and the second matrix those for beef bone.The conclusion from this is therefore that for the human bone specimens the fibres are primarily in the labelled 2'3' plane, whereas for the beef bone specimens orientation is largely in the labelled 1'3' plane.

If the angle of orientation is increased to approximately 15° the agreement between some of the coefficients is better, especially for the beef bone specimens.However definite discrepancies exist, especially for the human bone specimens. These can be largely rectified, for human bone, if the value

of d_{31} is increased to $.9 \times 10^{-8}$ c.g.s .

It is pertinent to remark at this point that the transformed matrices only accurately represent pieces of obliquely-cut tendon collagen. Since the bone collagen fibres are not all parallel to each other, and hydroxyapatite crystals are bound to definite regions of the fibril , it seems reasonable that the bone coefficients might differ from those of tendon collagen.

Considering the structure of bone, and the approximate agreement of the relative permittivities of dry bone and dry collagen, it is concluded that the electrical signals obtained from the stressing of dry bone derive from the bone collagen, and are largely accounted for by the measured piezoelectric properties of Achilles tendon collagen fibres.

5.9 Review of Previous Work on the Piezoelectric Properties of Dry Bone and Collagen.

Fukada[2] measured the piezoelectric properties of vacuum-dried cow and horse Achilles tendon specimens in the converse effect, using his own apparatus where the specimens are electrically driven at an audio frequency. He observed that his results were consistent with those derived for an uni-directionally oriented system of collagen 'crystallites'

with 'hexagonal' symmetry, such that the piezoelectric matrix for tendon collagen is as shown below, (if the long fibre direction is along the 3 axis.)

$$\begin{matrix} 0 & 0 & 0 & d_{14} & d_{15} & 0 \\ 0 & 0 & 0 & d_{15} & -d_{14} & 0 \\ d_{31} & d_{31} & d_{33} & 0 & 0 & 0 \end{matrix}$$

He measured the d_{14} coefficient to be -8.0×10^{-8} c.g.s, so that when the tendon is operated in this shear mode the effective coefficient is of the same order as the d_{11} of quartz. He reported that a gramophone pick-up can be made using the thin sheet of tendon as an electromechanical transducer. In the same paper he gives the variation of the d_{14} coefficient with water content. This shows that the value of the coefficient decreases with increasing hydration, and that near to 38% water content(presumably by dry weight), the magnitude of d_{14} reaches zero. We mention here that Rougvie and Bear concluded that the interband region of the collagen fibril should be fully hydrated at approximately 30gm H_2O /100gm collagen , and that Berendsen effectively gives this figure nearer to 40gm H_2O / 100gm collagen. Fukada remarks on this d_{14} -H_2O content curve

that :-

' At about 40% of water content the measurement became impracticable. The leakage due to the water prevents the observation.' However, in the range 0 to 30% water content (by weight), it can be stated with certainty that the water is not free. Each water molecule in this hydration range is specifically bound to sites on the collagen molecule, and in the fibril A band, so that the wet fibres are entirely different from the dry ones. One is thus not justified in equating wet collagen to free water plus dry collagen.Rather, this experiment tends to indicate , as was shown in Chapter Four, that fully wet collagen is not piezoelectric.

In an earlier paper Fukada[1] relates his experiments on the piezoelectric properties of dry human and bovine femoral bone specimens.He states that the human bone had been 'air-dried for years', so that it is reasonable to assume that these bone specimens were not fresh.The specimens obtained from the femur of an ox were dried by heating up to 120°C.Considering that the protein in bone denatures , when subjected to several hours at temperatures greater than 65°C, it seems probable that the bovine bone specimens used in these experiments were completely denatured.The dynamic direct and converse effects were measured at 2kHz.The static direct effect was measured by a lever

mechanism which applied the desired stress on to the specimen producing an electrical charge that was measured by a vacuum tube and galvanometer.He states that his results are concordant with the piezoelectric matrix shown (A), if the z axis is inclined $10^{\circ}$to the right of the bone long axis.

$$A \qquad \begin{matrix} 0 & 0 & 0 & d_{14} & 0 & 0 \\ 0 & 0 & 0 & 0 & -d_{14} & 0 \\ 0 & 0 & 0 & 0 & 0 & 0 \end{matrix}$$

It has been shown in 5.8 that if this 10° obliqueness for this matrix is taken into account, then the matrix of the non-shear terms, relative to the bone long direction is

$$\begin{matrix} 0 & -d_{14}\sin 10^{\circ}\cos 10^{\circ} & d_{14}\sin 10^{\circ}\cos 10^{\circ} \\ 0 & 0 & 0 \\ 0 & 0 & 0 \end{matrix}$$

so that if the 3 axis is along the long direction, there should be a d_{12} term and an approximately equal and opposite d_{13} term. He comments that Yasuda has observed has observed a piezoelectric effect in bone specimens which have suffered immersion in acid for three weeks, so that the effect does not depend upon the

presence of hydroxyapatite.

In a later paper[3] on the piezoelectric effect in fibrous proteins he reports the results of his experiments on completely dried specimens of horse and cow tendon, horse and cow bone, baleen(whale bone), wool(which is the protein keratin), and bundles of silk fibres.He gives the piezoelectric matrix for all these materials as that originally found for collagen, matrix B.

$$B \quad \begin{matrix} 0 & 0 & 0 & d_{14} & d_{15} & 0 \\ 0 & 0 & 0 & d_{15} & -d_{14} & 0 \\ d_{31} & d_{31} & d_{33} & 0 & 0 & 0 \end{matrix}$$

For horse femur he determines $d_{14} = 0.65 \times 10^{-8}$ c.g.s , $d_{15} = 0.13 \times 10^{-8}$ c.g.s , and $d_{31} = d_{33} = .01 \times 10^{-8}$ c.g.s .He states that the specimens were completely dried, and that the effects were observed by the methods previously used.We infer from this that the specimens were heated to 120°C as before, so that the figures more than likely represent denatured specimens,This is supported by the fact that this value of d_{14} is the same as was found before.It is not specifically stated whether the 3 axis in the above matrix is along the bone long direction or not,but given in the context of the other unidirectional materials we conclude that this is intended,The above matrix for bone therefore

deviates sharply from that previously put forward. There is here no mention of the d_{12} and d_{13} terms, and he reports in addition the finding of d_{31} , d_{32} , and d_{33} as non-zero. The logical conclusion would be that for these new bone specimens the collagen fibres were all accurately parallel to the bone long direction. Our own results do not support this, and it has already been remarked that one would only expect to obtain coefficients belonging to the matrix B for very large bone specimens where the 'oblique' effects might cancel each other.

In a recent paper entitled 'Piezoelectricity in Polymers and Biological Materials' [4], (unpublished) Fukada describes the piezoelectric effect in wood, cellulose, bone, tendon, and the polymer poly- -methyl L-glutamate. In commenting upon the present author's work(then in the very initial stage), he states that :-

'The polarization corresponding to the piezoelectric moduli which are zero in the matrix B are sometimes observed and arises a question for the applicability of the matrix. One reason for this contradiction would be the non-uniformity of the structure in bone and tendon.' It is subsequently stated that an allowance made by the present author for the obliqueness of the collagen fibres to the long direction is unable to explain the results, and consequently he proposes a new term in the piezo-

electric equation, proportional to the spatial stress gradient. We can only surmise that Fukada considers the agreement between the transformed tendon collagen coefficients and the experimental results not sufficiently good for one to conclude that the piezoelectric properties of the bone collagen produce those of bone. We have already commented on this in 5.8, indicating that it is not definite whether the coefficients for tendon collagen apply to bone collagen. We consider that the proposed stress gradient term in the normal piezoelectric equation will be negligible at the frequency of 1kHz, which is the operating frequency from which the present results derive.

We commented in the introductory chapter, on Dainora's work and results for bone specimens that been heated in an oven at 105°C. He states that:-

'When the piezoelectric specimen was loaded parallel to the long direction of the bone, a negative charge appeared on the outer surface of the compacta. This is in agreement with what was found by Fukada.' Subsequently he gives the values found for this piezoelectric modulus and states that these are the values of the d_{14} coefficient. Reference to 5.8 shows that to determine such a coefficient a value must be assumed for the angle of obliqueness. This is not given.

Chapter Six

Evaporation Measurements

6.1 Experimentation and Results.

These measurements were carried out on four fully wet beef femoral specimens of different shapes and sizes.These are labelled 'Small Specimens 1,2,3.' and Large Specimen No.1 . The latter specimen had been previously used for piezoelectric measurements at neutral pHs .The dimensions of the first two small specimens were, in cms, .75x.5x.2 , and 1.0x1.0x.8 respectively.The third small specimen was wedge-shaped, and was used for only one experiment when silica gel was placed in the balance.

The initial experiments consisted of weighing the wet bone specimens as they evaporated into the laboratory atmosphere.Subsequently this was modified so that the bone pieces dried by evaporation into an atmosphere of constant humidity.Three values of relative humidity were chosen.These were 10%($ZnCl_2$), 20%(CH_3COOK), and 32%($CaCl_2$).The saturated salt solutions were placed within the balance and the doors closed.The mirror balance used was capable of weighing up to 500mg to the nearest $\frac{1}{2}$mg without the addition of pan weights.Hence continous monitoring of the mass of a piece of bone was obtained as it

dried out.The resultant 'Mass-time' curves are thus accurate representations of dynamic behaviour.The graphic results are presented in Figs. 6.1 to 6.8 .Figs. 6.1 to 6.4 relate to 'Smaller Sp. No.2' in order of experimentation, Figs 6.5 and 6.6 similarly for Large Sp. Nol , Fig. 6.7 shows the three curves obtained for Smaller Sp. No.1 , and Fig. 6.8 is the single result for the fourth specimen.On Fig. 6.2 which is the second result obtained for that specimen, is superimposed Fig. 6.1, (the first result for that specimen) so that the two main points of discontinuity coincide.All the dry weights were determined in identical ways in the presence of silica gel and P_2O_5 .

It is clear from these evaporation graphs that many of the curves show a pronounced discontinuity.For evaporation into the laboratory atmosphere this takes the form of a sudden short-lived increase in the evaporation rate followed by a return to the pre-discontinuity rate.This behaviour is shown in Figs. 6.1 , 6.2 , 6.4 , and 6.5 .For the controlled humidity experiments only evaporation into the 32% R.H atmosphere shows a discontinuity, and under these conditions this appears as a slowing up of the evaporation rate followed by a gradual return to that existing before the change.This is seen in Figs. 6.6 and 6.7 .Some of the curves also indicate the presence of an earlier discontinuity, although much less pronounced than that

Fig. 6.1

Sm. Sp. No.2 pH6.88

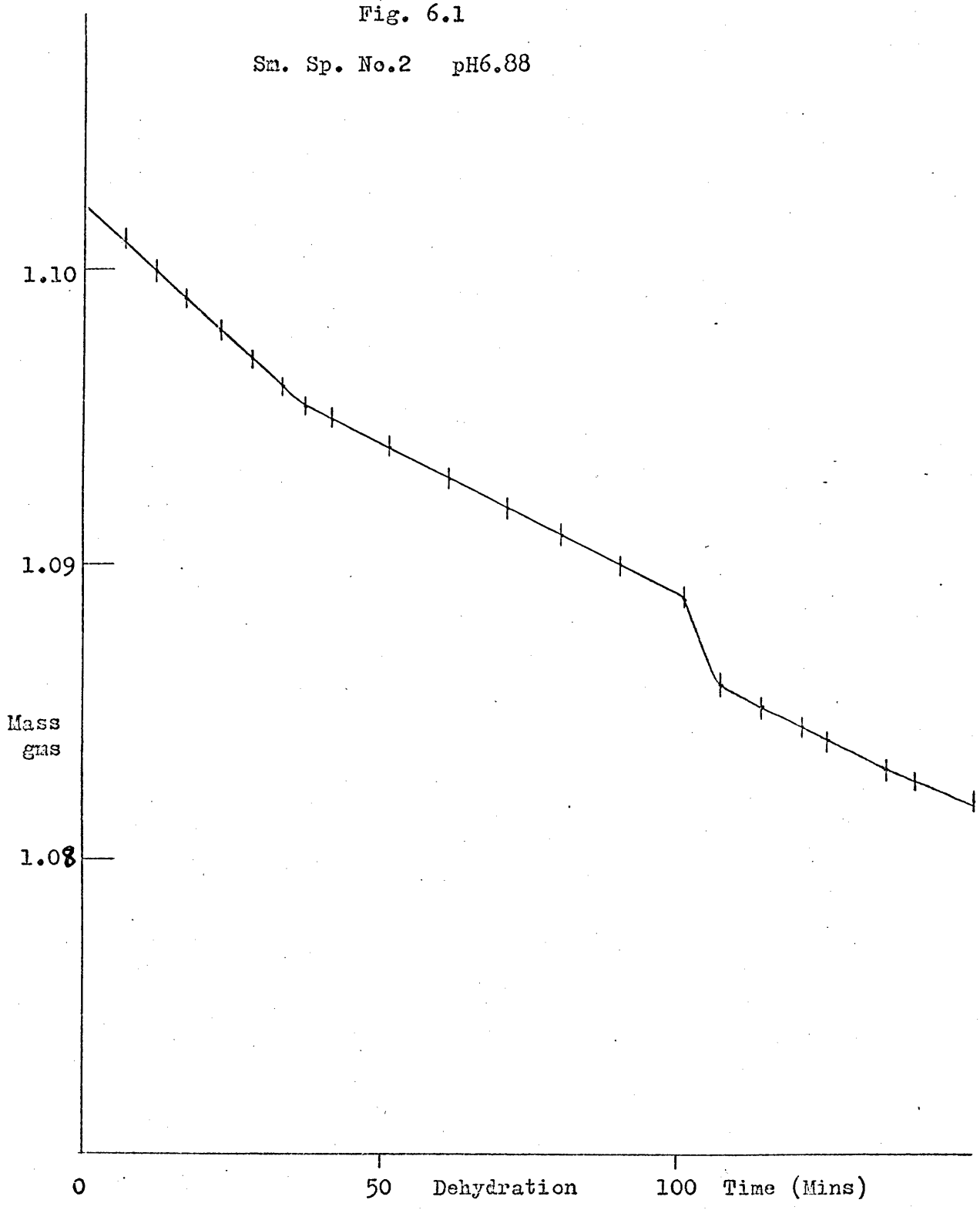

Fig. 6.2

Sm. Sp. No.2 pH6.88

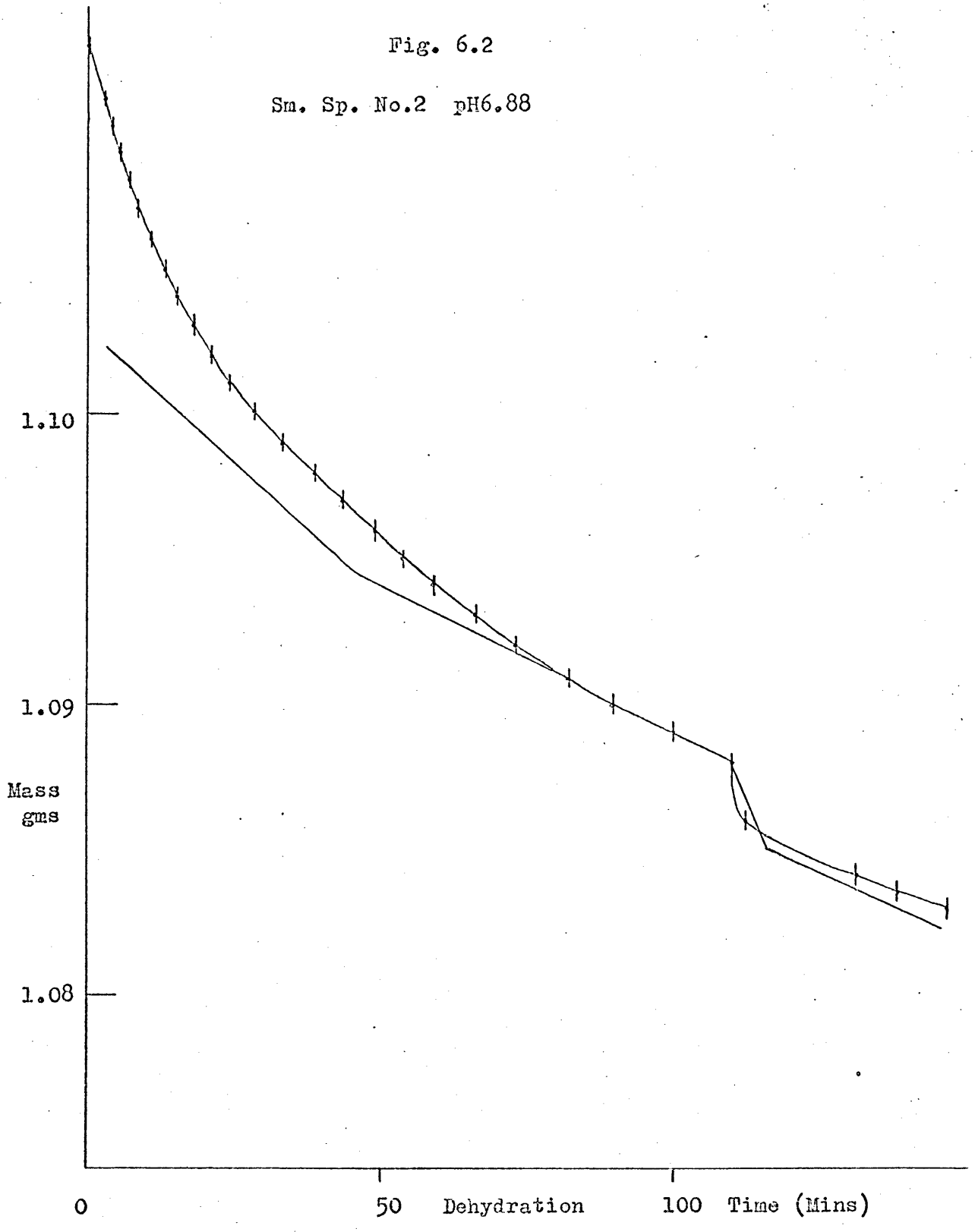

Fig. 6.3

Sm.Sp. No.2 Ethyl Alcohol

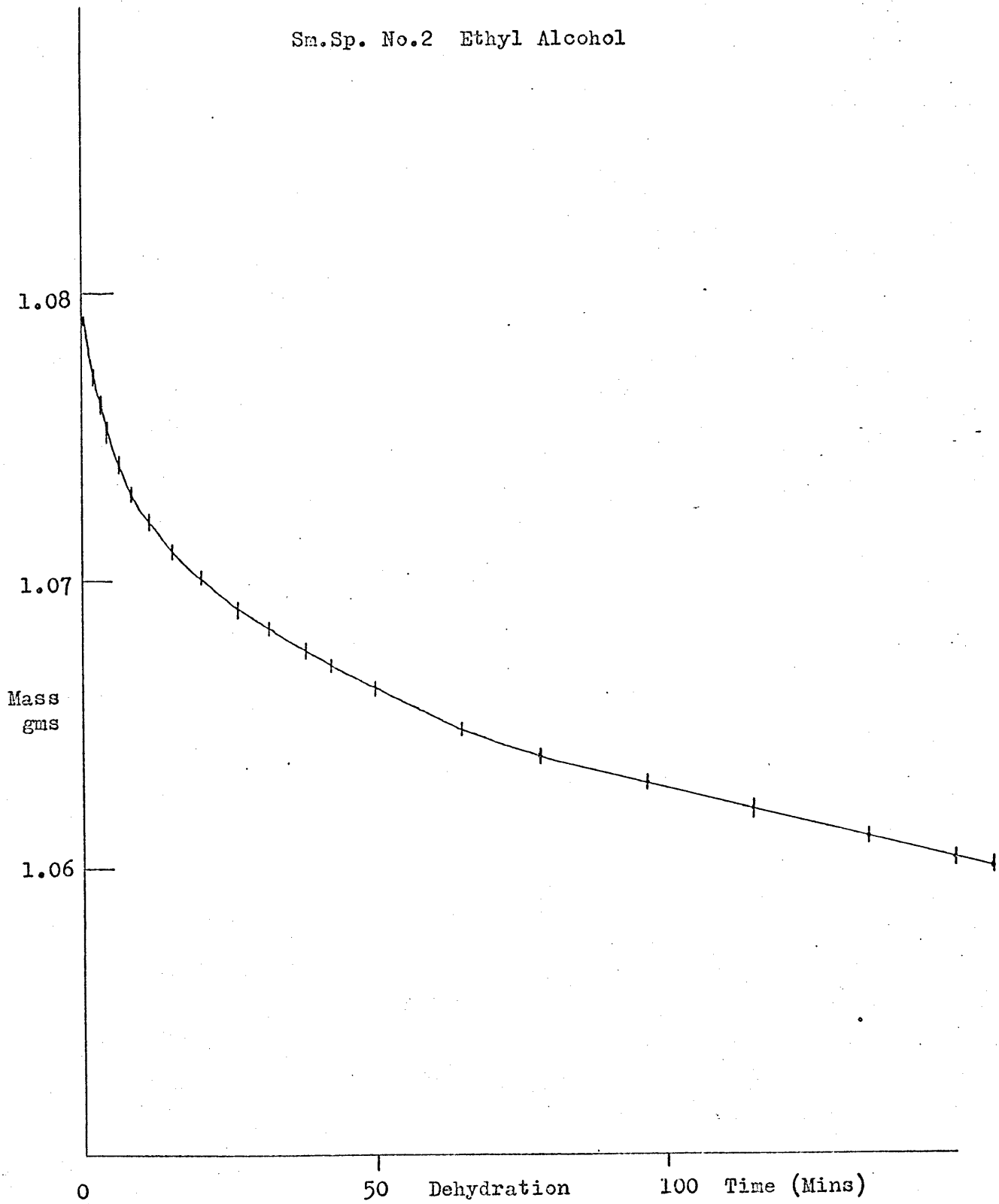

Fig. 6.4

Sm.Sp. No.2

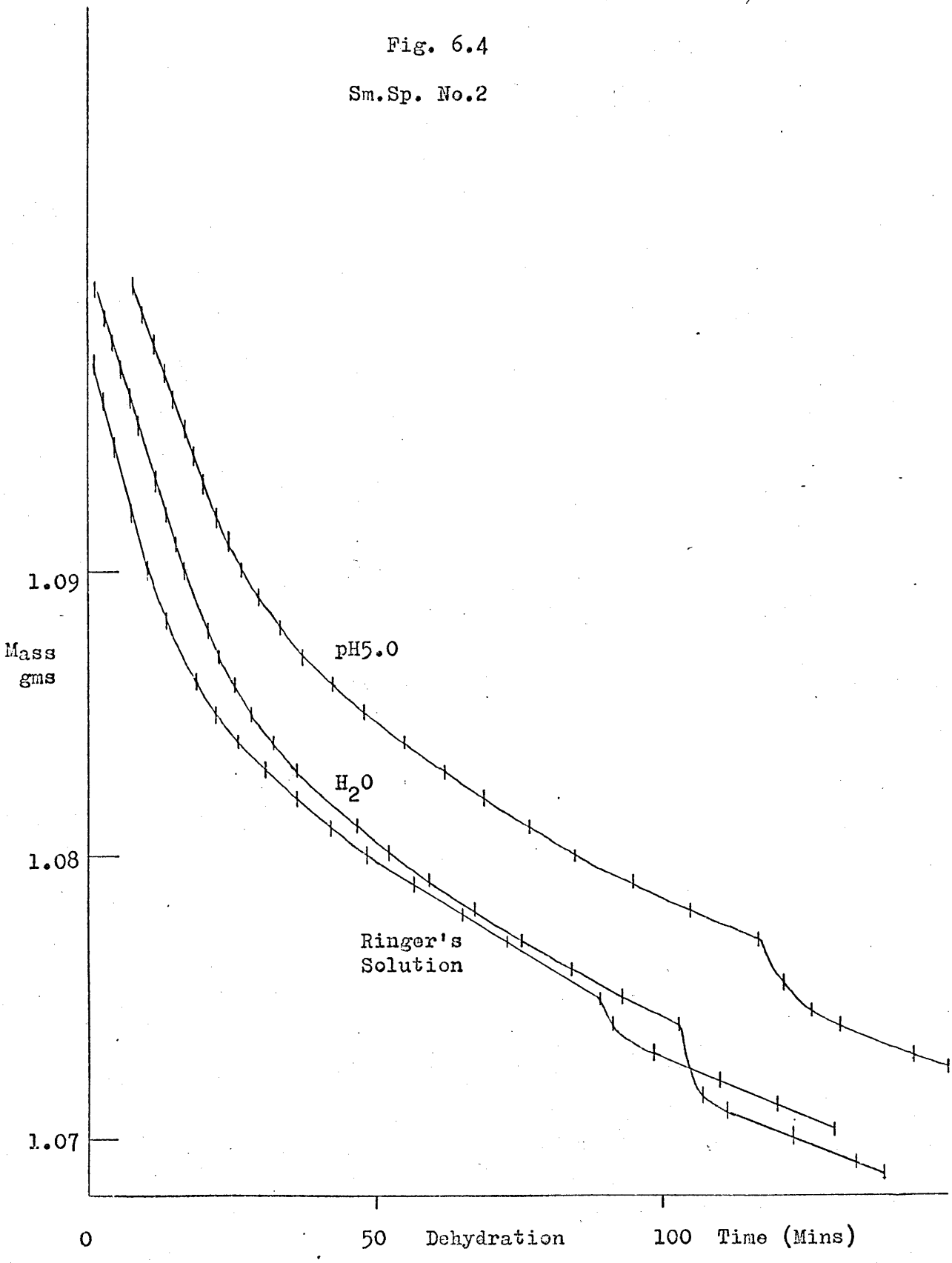

Fig 6.5

L.Sp No.1 Ringer's Solution

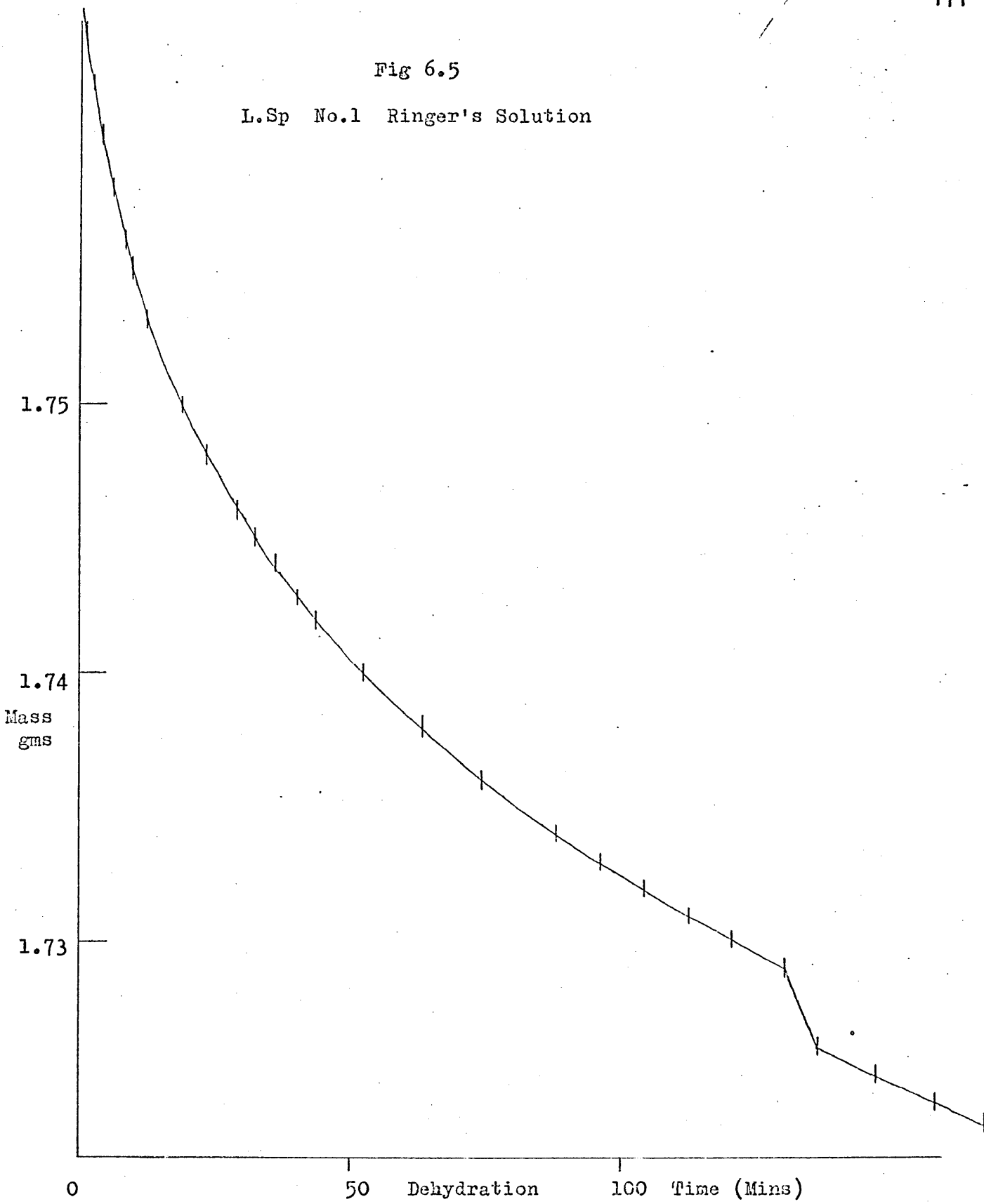

Fig. 6.6

L.Sp. No.1 H_2O

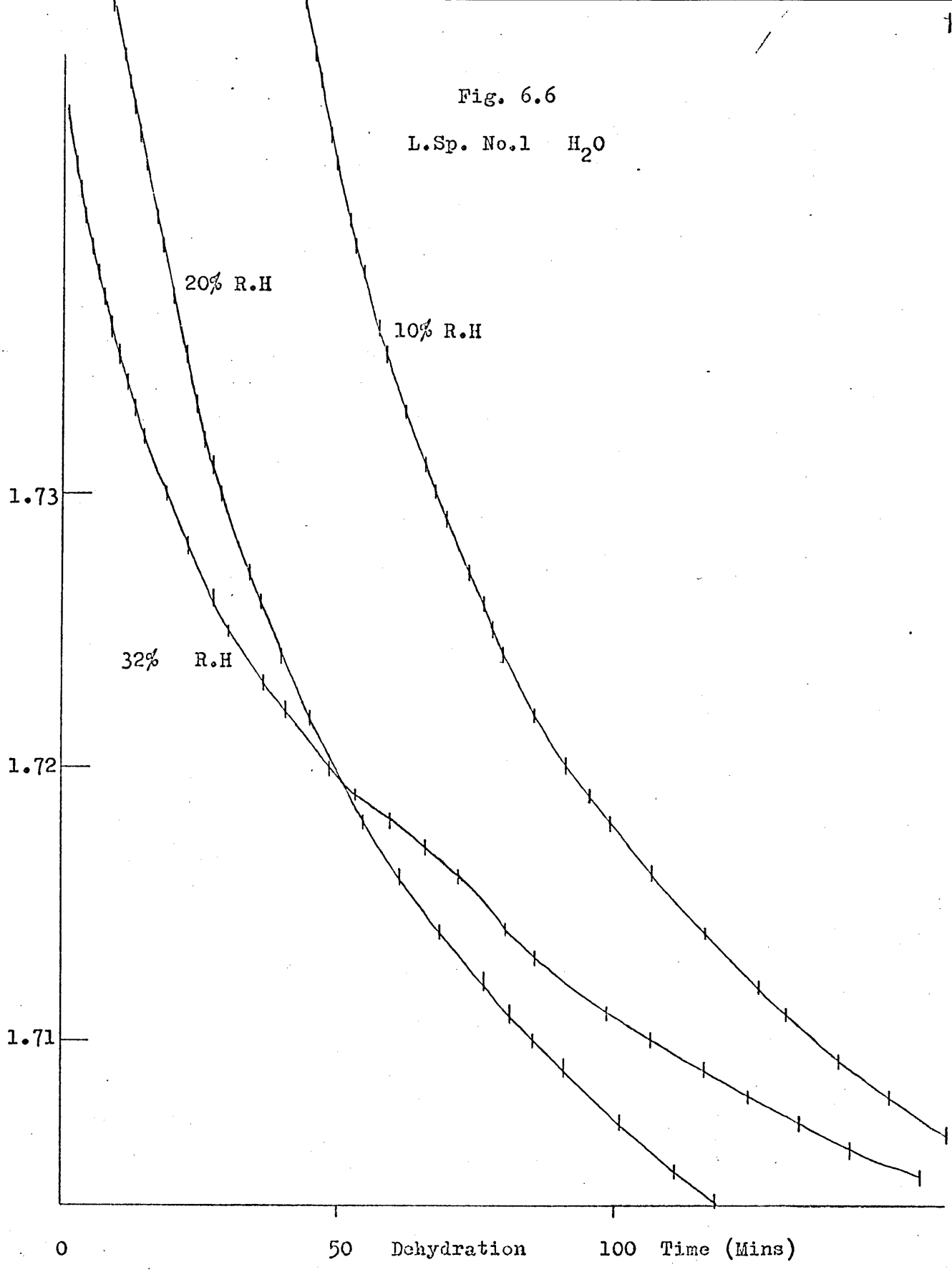

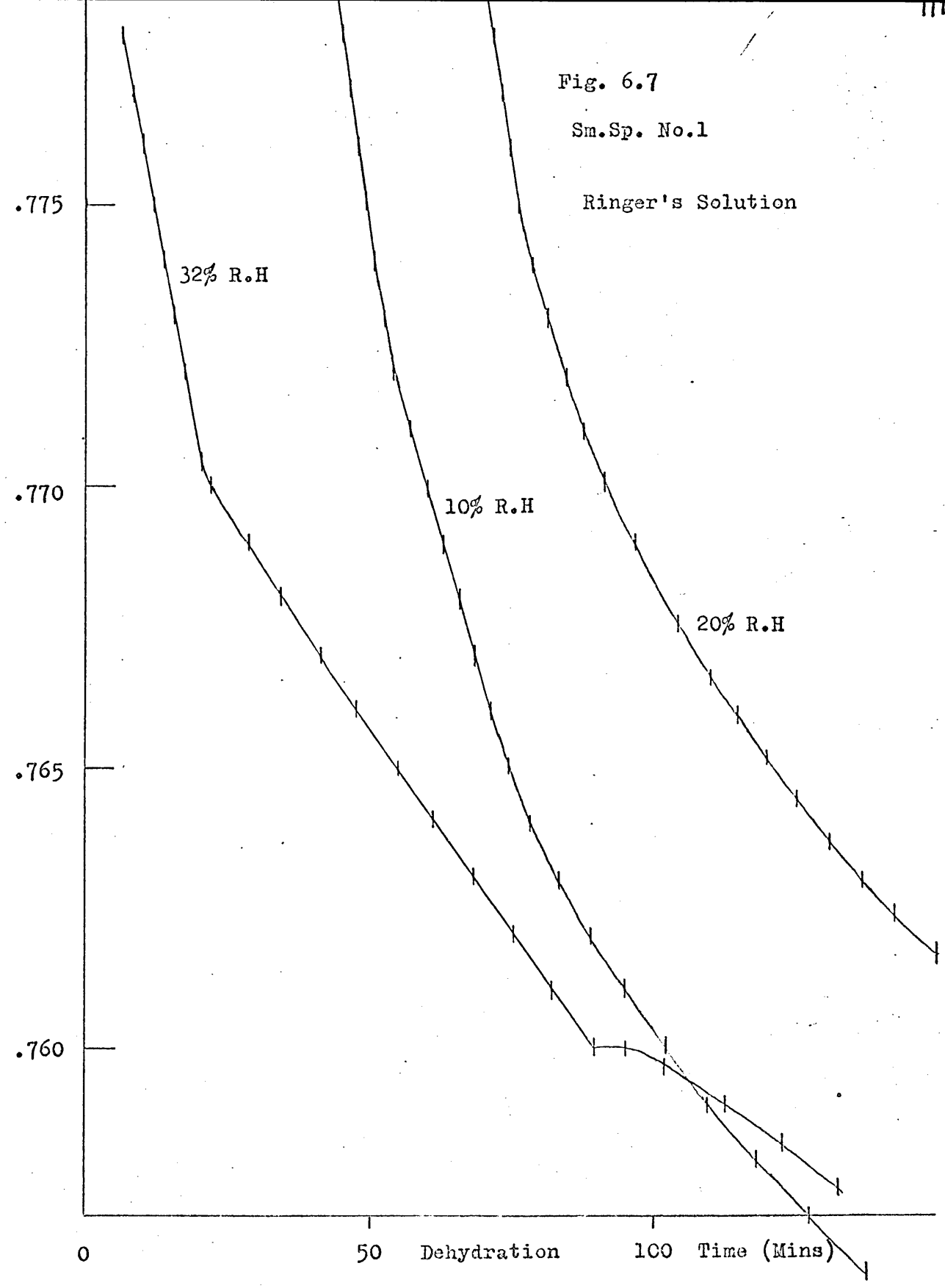
Fig. 6.7
Sm.Sp. No.1
Ringer's Solution
.775
.770
.765
.760
32% R.H
10% R.H
20% R.H
0
50
Dehydration
100
Time (Mins)

Fig. 6.8

Sm.Sp. No.3 pH6.88

Silica Gel placed in balance

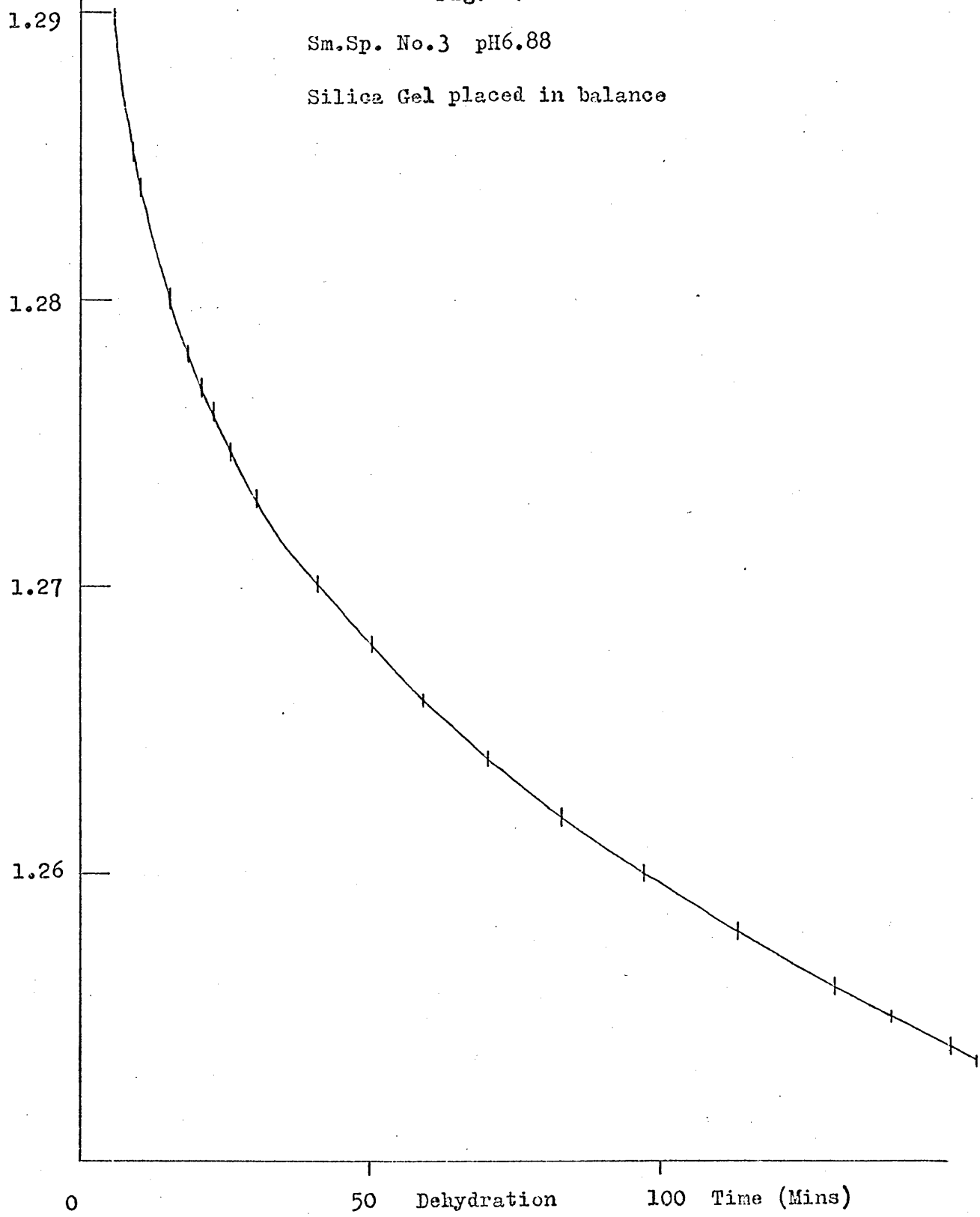

following.This is seen in Figs. 6.1, 6.2, 6.4, and 6.7. We label this change 1st Discontinuity , and the later more definite one, 2nd Discontinuity. It can be seen from the graphs that hydration of the bone specimens was not confined to distilled water, but that buffer solutions of pH 5.0 and pH 6.88 were used as well as Ethyl Alcohol and Ringer's Solution. (The buffer solutions were of .1 ionic concentration).The alcohol was employed in order to show that the second discontinuity is specifically dependent upon the presence of water in the wetting solution, rather than any polar liquid.

The results are now given for the three quantities, Max H_2O absorbed , 1st Disc. ,(where observable), and the 2nd or Main Disc. , in units of mgH_2O /gm bone .

Fig. 6.1 (First Result for Smaller Sp. No. 2)

Max. H_2O absorbed = 50.5

First Disc. = 44.0

Second Disc. = 37.2

Fig. 6.2(Second Result for Smaller Sp. No.2)

Max. H_2O absorbed = 60.0

First Disc. = 48.0

Second Disc. = 36.2

For these results the dry weight of Smaller Sp. No2 = 1.050 gm.

Fig. 6.4 (in order of experimentation, Sm. Sp. No.2)

pH 5.0 acetate buffer . Max. H_2O absorbed = 117

Second Disc. = 93.5

Ringer's Solution ($\frac{1}{4}$ strength) Max. H_2O absorbed = 115

Second Disc. = 91.5

For Fig. 6.4 Dry Wt = .985 gm

Distilled Water Max. H_2O absorbed = 117

Second Disc. = 90.5

Fig. 6.5 (First result for L.Sp. No.1)

Ringer's Sol'n Max. H_2O absorbed = 61

Second Disc. = 37.4

Dry Wt = 1.666 gm

Fig. 6.6 (Distilled Water)

Max. H_2O absorbed = 69

Second Disc. = 50.5

Dry Wt = 1.635 gm

For Fig.6.4 the mass of Sm. Sp. No.2 has fallen by 6.2% due

to the acetate buffer. For Fig. 6.6 the mass of L.Sp. No.1 has decreased by 1.87% due its immersion in distilled water, approximately pH5.0 .

Fig. 6.7 (Smaller Sp. No.1)

Max. H_2O absorbed = 61

First Disc. (32% R.H) =49

Second Disc. (32% R.H) = 35.5

The dry weight of this specimen = 0.734 gm

Considering that the balance was capable of measurements to the nearest $\frac{1}{2}$ mg, and that the above figures depend upon two independent readings, the maximum possible error associated with the above figures is 1 mg.We note that Berendsen remarks that tendon dried above P_2O_5 at room temperature still contains a few per cent water.It is thus possible that this is so for bone as well.However all the above specimens were dried by the same procedure so that this correction would apply equally to all of them.If the figures of 6.1, 6.2, 6.5 and 6.7 are linked together, because they represent specimens which have been kept at neutral pHs before the measurements were taken, we have the following results.

Maximum H_2O absorbed = $60.7 \pm .7$ mg H_2O/gm bone

First Disc. = 47.0 ± 1.5 mg H_2O/gm bone

Second Disc. = 36.5 ± 0.5 mg H_2O/gm bone

(The value of 50.5 mg H_2O/gm bone of Fig. 6.1 has been discarded because this measurement was the first to be carried out, when the surface of the bone piece was dried with absorbing paper, rather than with a non-absorbing cloth as for later results.) The above figures therefore relate to fresh bone.

Figs. 6.4 and 6.6 are for pieces of bone which have decreased in mass from their initial values at excision owing to the chemical action of the solutions in which they have been placed. For Fig. 6.4 the effect derives from a pH 5.0 acetate buffer solution, whereas the mass decrease of Fig. 6.6 is due to distilled water. As expected the % mass decrease resulting from the once-used acetate solution is much greater than that from the distilled water. If the results of Fig. 6.4 are averaged and linked with those of Fig. 6.6, we may present all the results as, in the same units as before.

A) Fresh Bone

Max. H_2O absorbed = $60.7 \pm .7$

First Disc. = 47.0 ± 1.5

Second Disc. = $36.5 \pm .5$

B) 'Treated Bone' (1.87% mass loss)

Max. H_2O absorbed = 69.0 ± 1.0

Second Disc. = 50.5 ± 1.0

C) 'Treated Bone' (6.2% mass loss)

Max. H_2O absorbed = $116.3 \pm .7$

Second Disc. = $91.8 \pm .8$

Hydroxyapatite[31] has been reported to have a primary sorption of 17.6 mg H_2O/gm apatite. If we assume that bone is 65% apatite and 35% collagen by weight, and that the evaporation occurring in the observed dehydration range is a protein reaction, then the above figures may be converted to mg H_2O per gm collagen. For fresh bone these are

Max. H_2O absorbed = $14.0 \pm .2$ gm H_2O/100gm collagen.

First Disc. = $10.2 \pm .4$ gm H_2O/100gm collagen

Second Disc. = $7.2 \pm .1$ gm H_2O/ 100gm collagen

It has been remarked in Chapter Three that Rougvie and Bear concluded that hydration of collagen first of all occurs in the band or A band region. He quotes the figure of approximately 7gm H_2O /100gm collagen as the amount necessary to hydrate this fibril region. We therefore conclude that

the main or second discontinuity observed in the evaporation experiments corresponds to the simultaneous emptying of all B bands of water, and the initiation of bulk evaporation from the A bands. This is consistent with the A band water being the more strongly bound.Since bone is slightly porous, and a amall amount of surface water is inevitable at the start of the evaporation, we consider that the first discontinuity marks the end of free water evaporation and the commencement of evaporation from the B bands.Therefore the maximum hydration of the bone collagen fibres amounts to approximately 10gm H_2O/100gm collagen. Thus, if as Rougvie and Bear suggest,the initial,polar, hydration of the B bands of the bone collagen fibrils amounts to near 6gm H_2O /100gm collagen,(this figure being necessary to complete the 'primary layer' water,) the bone collagen B bands contain half their normal 'primary layer' water(using the B.E.T equation terminology).Therefore, since the water chains proposed by Berendsen can only begin to exist after the hydration point of near 13gm H_2O /100gm collagen has been passed, there is no question of their occurence in hydrated bone.This is to be expected since their existence demands considerable swelling of the collagen fibres, which the resultant higher elasticity of the bone tends to prevent. If the results for pure collagen accurately apply for the

bone collagen, then it would appear from the maximum bone collagen hydration figure that even sorption of the last 3gm H_2O per 100gm collagen of the bound B band water is accompanied by some lateral swelling.

It is evident from the results of the 'treated' bone specimens that compared to fresh bone more water per gm bone is absorbed. If the results of Fig. 6.4, representing a 6.2% mass loss, are compared to the equivalent figures for fresh bone, it is observed that the total amount of water absorbed per gram of bone has increased by $55.6 \pm .5$ mgms, (an increase of nearly 100%), and that the mass of absorbed water per gram of bone corresponding to the second or main discontinuity has similarly increased by the amount $55.3 \pm .3$ mgms. These figures are identical within the experimental error, so that for the acetate-treated specimens increased water absorption per gram of bone is exactly accounted for by increased absorption into the A bands, the amount of free and B band water per gram of bone remaining constant. Similar examination of the results of Fig. 6.6, representing a 1.87% mass loss due to immersion in distilled water, shows that whereas the second discontinuity has increased by 14 mgm H_2O/gm bone , the total amount of absorbed water/gm bone has only increased by 8.3 mgms. These figures indicate

that increased absorption into the A band is partially at the expense of B band and free water.It would therefore appear that the chemical actions of the acetate buffer and the distilled water on bone are different; unless the above results are obtained for an acetate-produced 1.87% mass loss.

These results for the treated bone specimens cannot be explained by simply varying the relative amounts of protein and mineral in the bone, and considering the remaining bone constituents to possess the same absorbing properties as those of fresh bone, since this leads to the treated bone containing more than 100% collagen by weight! There was visual evidence of protein fibres being dissolved out in solution, so that the protein content is likely to be lowered relative to the apatite content, especially as hydroxyapatite is generally insoluble in mild acids.It therefore seems likely that the greater part of the mass loss derives from the loss of protein.

It is difficult theoretically to decide exactly where the acetic acid attacks the collagen.However, since the increased bone hydration per gram of bone equals the increased A band hydration per gram of bone and the weights of the wet treated specimens are about 1.1% less than the original weights, it would appear that the net effect is to increase the relative

amount of collagen in the A bands.Whether this is achieved by directly dissolving out A or B bands appears as yet to be unknown.With positive staining liquids the observed interband region was referred to as the crystalline region where the stain could not penetrate; so that one might expect the acetic acid to penetrate the polar band region first.However, with the advent of negative staining techniques, the A band is interpreted as the region where the macromolecules bind together with strong, primarily electrostatic, lateral forces; and the B band is the area in which the macromolecules are essentially laterally free.On this basis it seems reasonable to conclude that the B band molecules would be chemically attacked first, so that in the 640Å period of native fibrils the A band would be increased at the expense of the B band.We therefore tentatively conclude that the acetic acid and the distilled water primarily dissolve out the B band protein fibrils, and those remaining in these regions consequently adjust themselves in position,with the effect that considerable lateral bonding occurs.

6.2 A Mathematical Approach to Bone Evaporation

The flow of fluid under pressure from a given enclosure depends upon the orifice size r ,and the mean free path length $\bar{\lambda}$ of the particles inside.The term 'rarefied' refers to conditions

where $\bar{\lambda} \gg r$, and is explained by kinetic theory. For $r \gg \bar{\lambda}$, the fluid flow is described by hydrodynamical equations. When the orifice size is of the same order as the mean free path length both kinetic and hydrodynamical theories are needed to explain the dependence of the flow rate upon the pressure difference across the orifice. At S.T.P $\bar{\lambda} \simeq 10^{-5}$ cms, $= .1\mu$. The nature and size of the pores in bone that are able to act as effective evaporation sites are diverse. However the majority of the water channels are parallel to the bone long direction, so that evaporation primarily proceeds in this direction. The diameter of the approximately cylindrical pores is estimated to be in the region of $\frac{1}{2}\mu$, whereas the lengths of many pores may extend to mms or more. Hence both kinetic and hydrodynamical equations are needed to account for the escape of water vapour from the hydrated bone. In order to simplify the problem we will assume that the kinetic does not deviate too sharply from the true representation. We will define the following quantities,

J = the rate of arrival of water molecules per unit per sec, fromthe vapour above the bone surface.

n = no. of water molecules per unit area of bone surface in excess of those which would be present in a vapour at pressure p.

τ_s = Mean residence time of a molecule on the bone substrate, and is given by $\tau_s = \tau_o \exp(E_a/kT)$, where τ_o is the correlation time(10^{-12}secs) for motions that lead to the breaking of the particular protein-H_2O bond, and E_a is the binding energy , or activation energy that is necessary to break the bond.

The evaporation process is described by the following equation,

$$\frac{dn}{dt} = -n/\tau_s + J$$

For a perfect gas $J = (1/(2\pi mkT))^{\frac{1}{2}}$, where m is the mass of a water molecule. If p' average instantaneous water vapour pressure inside the bone, and p'' is that outside; and T' is the temperature of the vapour above the bone surface, we have

$$\frac{dn}{dt} = -n/\tau_s + p'/(2\pi mkT')^{\frac{1}{2}}$$

For evaporation through a simple orifice of area A

$$\frac{dn}{dt} = \frac{(\rho')^{\frac{1}{2}}}{m} \left(\frac{(p' - p'')\,A}{(2\pi)^{\frac{1}{2}}} \right)$$

where ρ' = vapour density at 1 dyne/cm^2

$W = (2\pi)^{\frac{1}{2}} / A$ is termed the resistance to flow; so that for any opening we have

$$\frac{dn}{dt} = \frac{(\rho')^{\frac{1}{2}} \quad (p' - p'')}{m\ W}$$

For cylindrical pores of average length L and radius R

$$W = \frac{3}{8} \quad (2/\pi)^{\frac{1}{2}} \quad \frac{L}{R^3}$$

Hence if the orifice is the rate limiting factor

$$\frac{dn}{dt} = - n/\tau_s + \frac{p'}{(2\pi mkT')^{\frac{1}{2}}} = - \frac{(\rho')^{\frac{1}{2}} (p' - p'')}{m\ W}$$

Eliminating p', we obtain

$$\frac{dn}{dt} = \frac{(2\pi)^{\frac{1}{2}}}{W + (2\pi)^{\frac{1}{2}}} \left(- n/\tau_s + \frac{p''}{(2\pi mkT')^{\frac{1}{2}}} \right)$$

Since W is much greater than $(2\pi)^{\frac{1}{2}}$, this becomes

$$\frac{dn}{dt} = \frac{(2\pi)^{\frac{1}{2}}}{W} \left(- n/\tau_s + \frac{p''}{(2\pi mkT')^{\frac{1}{2}}} \right)$$

The decrease of n with time is therefore given by

$$n = N_o \exp \left(\frac{-(2\pi)^{\frac{1}{2}} t}{W_s} \right)$$

Examination of the rate of evaporation of B band water in Figs. 6.2 and 6.5 , with the above equation leads to the average radius of the cylindrical pores being 3 microns.We have taken τ_s to be about 10^{-5} seconds, in accordance with Berendsen's remarks.Clearly this can only be anapproximate value since its calculation is based on one perfectly cylindrical pore of length 1cm .However this value for the average pore radius is acceptable.Although a statistical examination of the bone pore sizes has not been carried out , examination of several bone pieces with the light microscope showed many pores of this order. We therefore conclude that the above exponential relationship accounts for the bound water evaporation if a value of 10^{-5}secs is given to τ_s .

Naturally the equations derived above are not capable of interpreting the observed main discontinuity, since they describe

equilibrium processes. This equally applies if one assumes that the resultant evaporation derives from two regions of different activation energies. The nature of the discontinuity in Figs. 6.1, 6.2, 6.4, and 6.5 indicates that a definite amount of heat is suddenly given up by the bone specimen in order to overcome the increased binding force of the water molecules, whereas for evaporation into the 32% R.H atmosphere, the process of transferring the evaporation into the A bands appears more slow. It may be possible to associate these with adiabatic and isothermal reactions. That the main discontinuity does not occur when the partial vapour pressure is very low, whether due to silica gel or the 10% R.H atmosphere, indicates that A band evaporation starts before the losing of all the B band water.

6.3 A Short Account of the Brunaer, Emmett, and Teller Equation

Only a brief summary of the applications and theoretical limitations of this equation will be presented here. For a detailled account the reader is referred to the recent book by S.J. Gregg and K.S.W Sing.[34]

If a highly disperse solid is exposed to a gas or a vapour in a closed space at a given pressure the solid begins to

adsorb the gas.This results from the attractive forces that exist at the surface of the adsorbent.The nature of the forces gives rise to two types of sorption, namely physical and Van der Waals sorption, and chemisorption.Physical adsorption is used to evaluate the total surface area of a solid, which for a particular adsorbate is the total area accessible to its molecules, including accessible internal pore areas; whereas chemisorption is often used to assess that part of a surface which possesses some particular property.It is often stated that in chemisorption a transfer of electrons between the adsorbed molecule and the solid occurs, so that in effect a chemical compound is formed, although this is confined to a single layer of molecules on the surface of the solid.Thus valency forces are involved in this type of adsorption, as opposed to physical adsorption in which they are not.

The amount adsorbed per gram of solid depends upon the equilibrium pressure p, the temperature T, and on the particular gas and solid.If the gas is a vapour, that,is if it is below its critical temperature, then the adsorption in grams of adsorbate per gram of adsorbent x , may be written

$$x = f\left(p/p_o\right)_{T,gas,solid}$$

where p_o is the saturation vapour pressure of the adsorbate.

This relation describes an 'adsorption isotherm', since it relates the amount adsorbed to the pressure.For physical adsorption there are five types of adsorption isotherms according to Brunaer, Denning, Deming, and Teller.We are interested in Type 2 isotherms, the general shape of which is shown below.

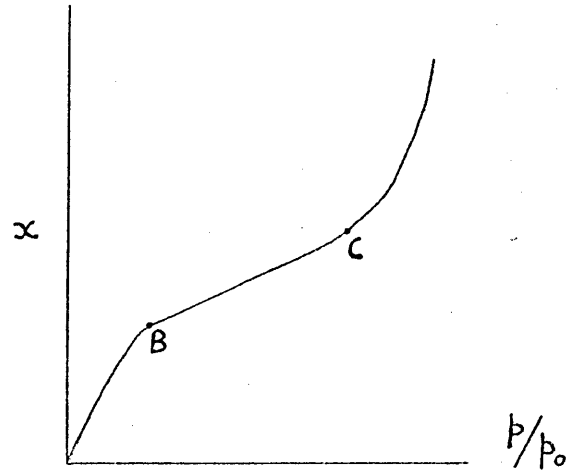

This is because the adsorption isotherm of collagen possesses this general shape which the B.E.T equation is capable of explaining.Point B is interpreted as representing as representing the completion of the monolayer of adsorbed molecules, so that subsequent adsorption is the stacking of more gas molecules on top of this primary layer.The diagram below shows the solid adsorbing surface and the various layers of adsorbed gas or vapour molecules, for a particular gas pressure, according to the B.E.T assumptions.

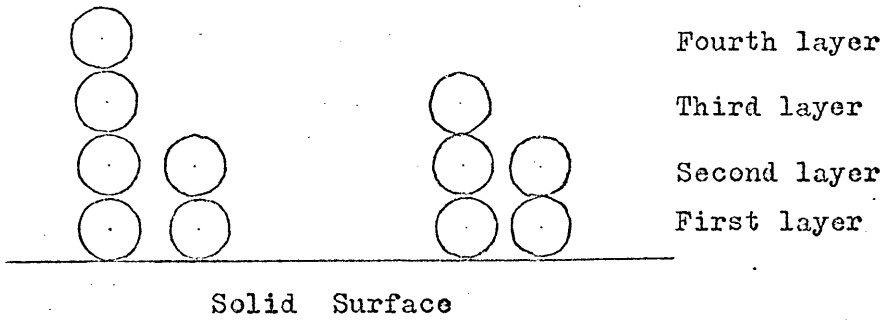

It is considered that dynamic equilibrium exists in each layer so that the number of molecules evaporating from a given layer equals the number condensing per second on the layer immediately below it.Point B in the isotherm shown exists because molecules in the first or monolayer have a much longer lifetime in this layer than those in higher layers.In other words the binding force is much greater for the monolayer molecules so that the probability of evaporation due to thermal forces is considerably lower than for higher layer molecules.

The assumptions on which the equation is derived are two-fold.Firstly, that the adsorbing surface is energetically homogeneous, so that all adsorption sites are equivalent. Secondly that 'horizontal interactions' between neighbouring molecules are negligible.It is well recognised that the second assumption must be false considering how close the adsorbed molecules will be in the higher layers.However, despite these

discrepancies, the B.E.T equation has had remarkable success in explaining various isotherms of gases adsorbed on to solids. So much so that Gregg and Sing remark:- 'It is perhaps the very breadth of its scope which has led to a somewhat uncritical application of the method as a kind of infallible yardstick, and to a lack of appreciation of the nature of its basic assumptions or of the circumstances under which it may, or may not, be expected to yield a reliable result.' This seems to have occurred, in our opinion, when describing the adsorption isotherm of collagen. To talk of adsorbed water that is primary layered on collagen, in terms of the B.E.T assumptions, seems misleading since this implies that the water which is absorbed above the 13 gm H_2O / 100gm collagen level is physically stacked above the 'monolayer' molecules, and this does not occur , in any real sense, until the 40gm H_2O/ 100gm collagen hydration point is reached. Whereas the knee in the Type 2 isotherm is interpreted by the B.E.T equation as due to a greatly increased binding force for the monolayer molecules in the 'vertical direction, the knee in the collagen isotherm indicates that the water molecules bound in the A band are more strongly bound than those which form into water chains. This concurs with the water chains being formed by the weaker hydrogen bonds, as suggested by Berendsen.

Chapter Seven

Part One : The Electrical Properties of Wet Bone.

7.11 Determination of the Piezoelectrical Properties of Wet Beef Bone.

The experiments on the electrical properties of wet Achilles tendon collagen led us to investigate the effect of pH on the electrical signal resulting from the stressing of wet bone. This was done by measuring the piezoelectric coefficients in the direct effect at 1kHz , as the specimens slowly dried out in the apparatus, for values of pH in the range 4.0 to 9.15. The same buffer solutions were used as for the electrophoretic measurements , except that dilute brine served as the basis of the pH 5.0 solution.It has already been remarked in 5.3 that these measurements were carried out on the two large specimens labelled No.1 and No.2 .The preparation of these specimens has been described in 5.63 . Since the original femur was obtained from a butcher on arrival from the abattoir, the measurements may be said to have been carried out on fresh untreated bone. In the early experiments, the larger bone specimen, No.1 was used only for pH values close to neutrality.This was in order

that the solutions should have the least chemical effect on this piece, so that a comparison could be made with the second specimen, which by this time had suffered mildly acidic and basic solutions for short intermittent periods of time (usually of the order of five days).In the early experiments the piezoelectric output voltage e_L and the wet bone D.C resistance R_{wb} were concurrently measured and plotted against time as the specimens dried out in the apparatus.For the later measurements the dehydration time was ignored, and e_L plotted against R_{wb}. This was done because as may be seen from 7.12, e_L is expected to be proportional to R_{wb} for the wet specimens, and the latter quantity could be more accurately determined as a function of water content in a single experiment using the valve voltmeter.In the initial experiments the bone specimens were dried with silica gel before immersion into the buffer solution, whereas in the later measurements they were completely dehydrated under vacuum, so that the bone pores should not retain liquid at the pH of the previous measurement.This drying procedure was avoided initially as it was thought that it might damage, unnecessarily, the bone specimens.In all experiments surface water was removed by wiping.Thus any dependence upon pHof the wet bone 'piezoelectric' signal should be best exhibited for the later measurements. In the initial

experimentation all the coefficients were measured, whereas for the later measurements attention was concentrated on the d'_{33} coefficient. Each coefficient value at a given pH, for both sets of mesurements, is typical of approximately five results. The main error in these figures derives from the measured resistance. It is remarked in the next section that the resistance values are accurate to approximately 5% , so that this is the order of the error in the values of d'. In order to avoid duplication of graphic and tabular information we have selected 13 graphs which are representative of the first set of measurements. These are shown in Figs. 7.1 to 7.13 . Tables 7.1 and 7.2 show how the d_{ij} vary with R_{wb} as the specimens dry out, for the two sets of measurements.

7.12 Expression of the Wet Bone Output Signals in terms of the Piezoelectric Coefficients.

For the majority of the measurements the lowest D.C resistance, representing the measurement made immediately upon insertion of the bone into the apparatus, was in the range 10 -30K ohms, so that the capacitative loading of the amplifier and leads (which is of the order of 10^6 ohms at 1kHz) is much greater than this, that is $X_{C',wb} \gg R_L$ (see 5.5). Hence, we have from

5.5 that if ,

d_{wb} = the piezoelectric coefficient of wet bone, in a given state of hydration.

R_{wb} = The D.C resistance of the wet specimen.

$$(e_L)_{wb} = \left(\frac{a}{c}\, d_{wb}\, F\right) jw\, R_{wb} \qquad \text{Eq. 7.1}$$

If this is compared to the PZT5 output signal

$$(e_L)_{PZ} = \frac{d_{PZ}\, F}{C'_{PZ}}$$

we obtain

$$\frac{d_{wb}}{d_{PZ}} = (c/a)\,(X'_{PZ}/R_{wb})\,\frac{(e_L)_{wb}}{(e_L)_{PZ}} \qquad \text{Eq. 7.2}$$

If the value of X'_{PZ} at 1kHz is inserted in the above equation we obtain the relationship

$$d_{wb} = \frac{c}{a} \cdot \frac{200K}{R_{wb}}\,\frac{(e_L)_{wb}}{(e_L)_{PZ}} \cdot d_{PZ}$$

This is the expression used to determine the value of d_{wb} for the wet bone specimens.The validity of this equation depends on $R_{wb} \ll X_{c'wb}$, and $R_{wb} \ll R_{TA}$ (the input resistance of the

tuned amplifier). Since both $X_{C'wb}$ and R_{TA} are of the order of 10^6 ohms at 1kHz, it is evident that the above relation holds for the larger part of the observed dehydration range. Assuming that the water behaves like a pure resistance which shunts the bone signal generator, we expect the bone output signal $(e_L)_{wb}$ to be proportional to R_{wb}, thus keeping d_{wb} constant. If the ratio of the output signals for wet bone and PZT5 is termed the Voltage Ratio (V.R), then we expect d_{wb} to be constant if V.R is constant. Hence R_{wb}, V.R, and d are tabulated in Tables 1 and 2. It proved difficult to determine the signs of the wet coefficients since they appeared to change with loss of water. Consequently only the modulus appears in tabulated form.

7.13 Observations on the Wet Piezoelectric Results

Comparing the values for wet bone with the 'd' coefficients for dry bone it is immediately apparent that the wet values are all larger than their dry equivalents. The greatest difference between the wet and dry d'_{ijk} occurs for the d'_{3jk} coefficients, and especially for d'_{311}. Whereas for the dry bone specimens d'_{311} is near to 0.3×10^{-8} c.g.s, for wet bone it takes the value of $\simeq 30 \times 10^{-8}$ c.g.s, the actual value depending upon the state of hydration of the bone. Hence, since for the dry bone pieces the largest coefficient is d'_{211}, and the wet pieces d'_{311}, the

Fig. 7.1

L.Sp. No.1 pH 6.88 d'_{111}

x = R_{wb} ; . = V.R

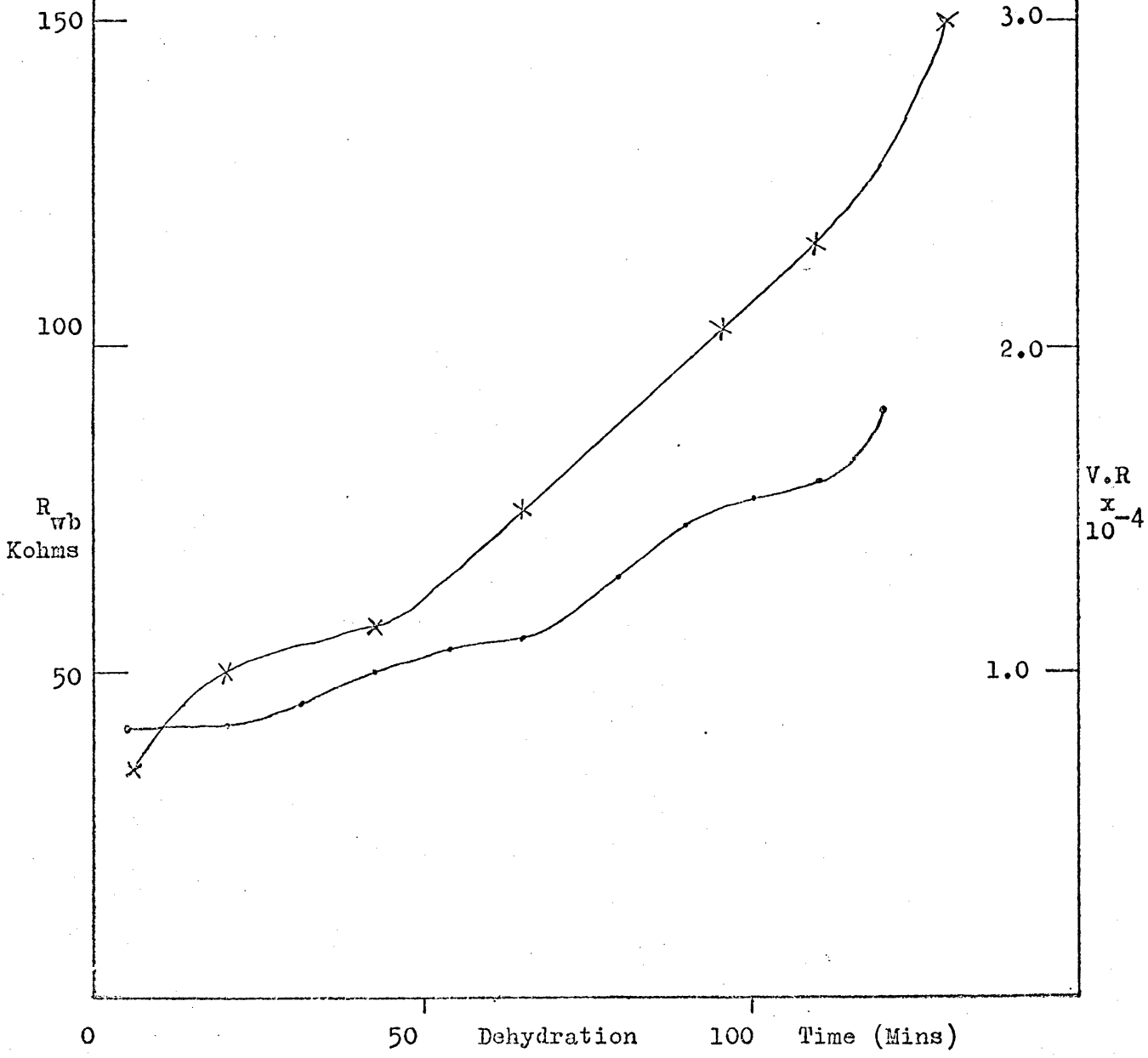

Fig. 7.2

L.Sp. No.1 pH 6.88 d'_{111}

x = R_{wb} ; • = V.R

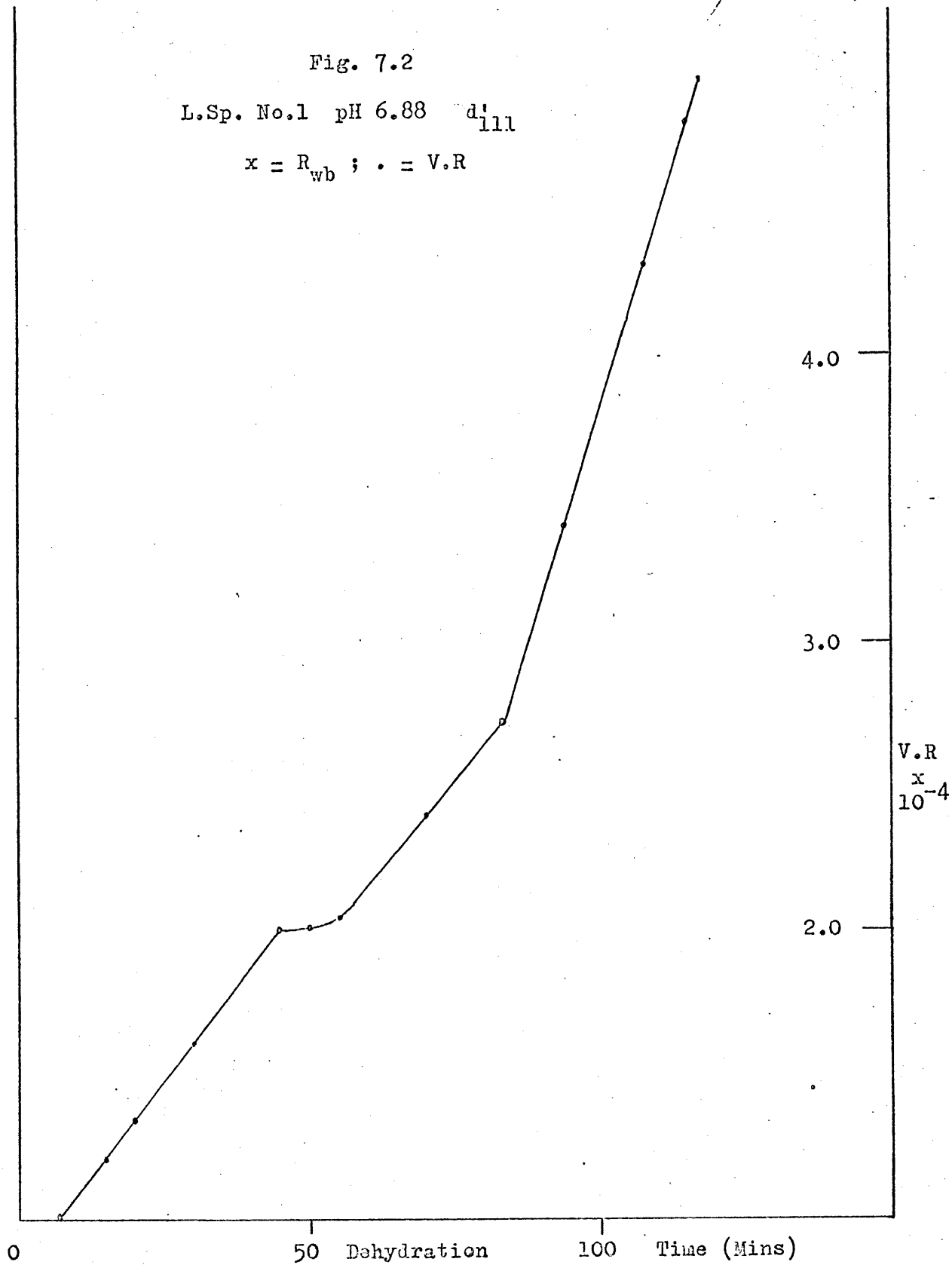

Fig. 7.3

L.Sp. No.1 pH 6.88 d'_{122}

x = R_{wb} ; • = V.R

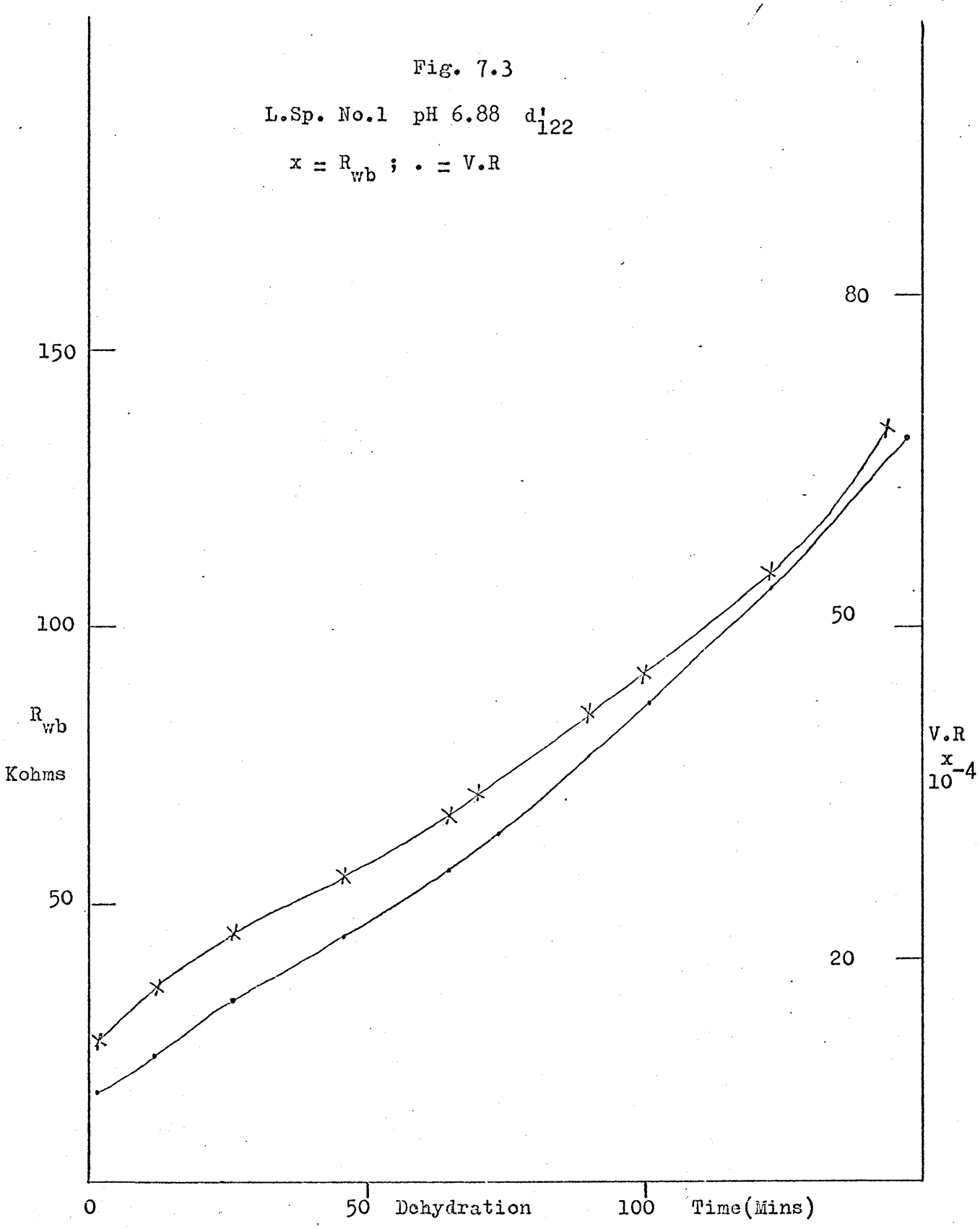

Fig. 7.4

L.Sp. No.2 pH 5.00 d'_{122}

x = R_{wb} ; • = V.R

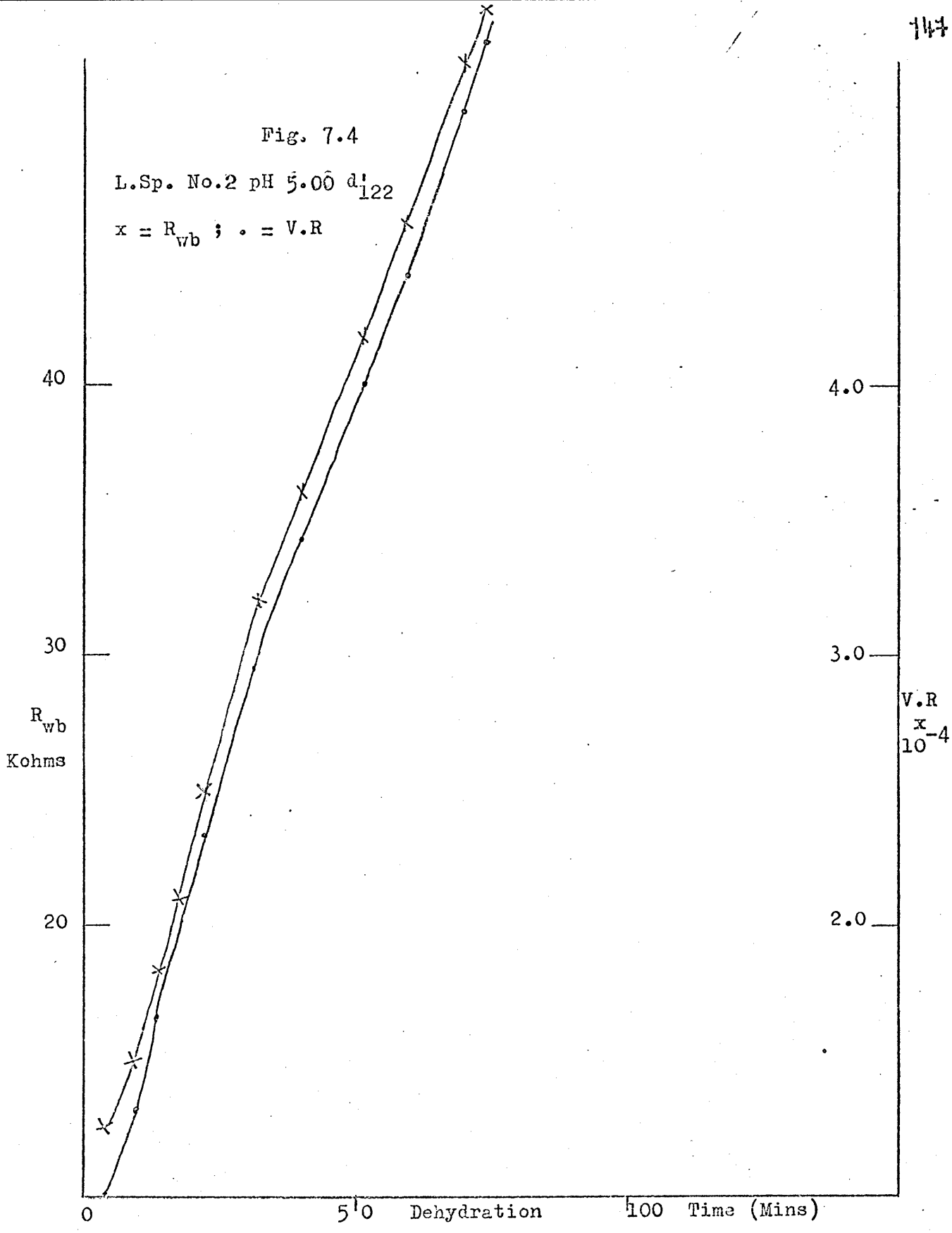

Fig. 7.5

L.Sp. No.1 pH6.88 d^{1}_{133}

x = R_{wb} ; . = V.R

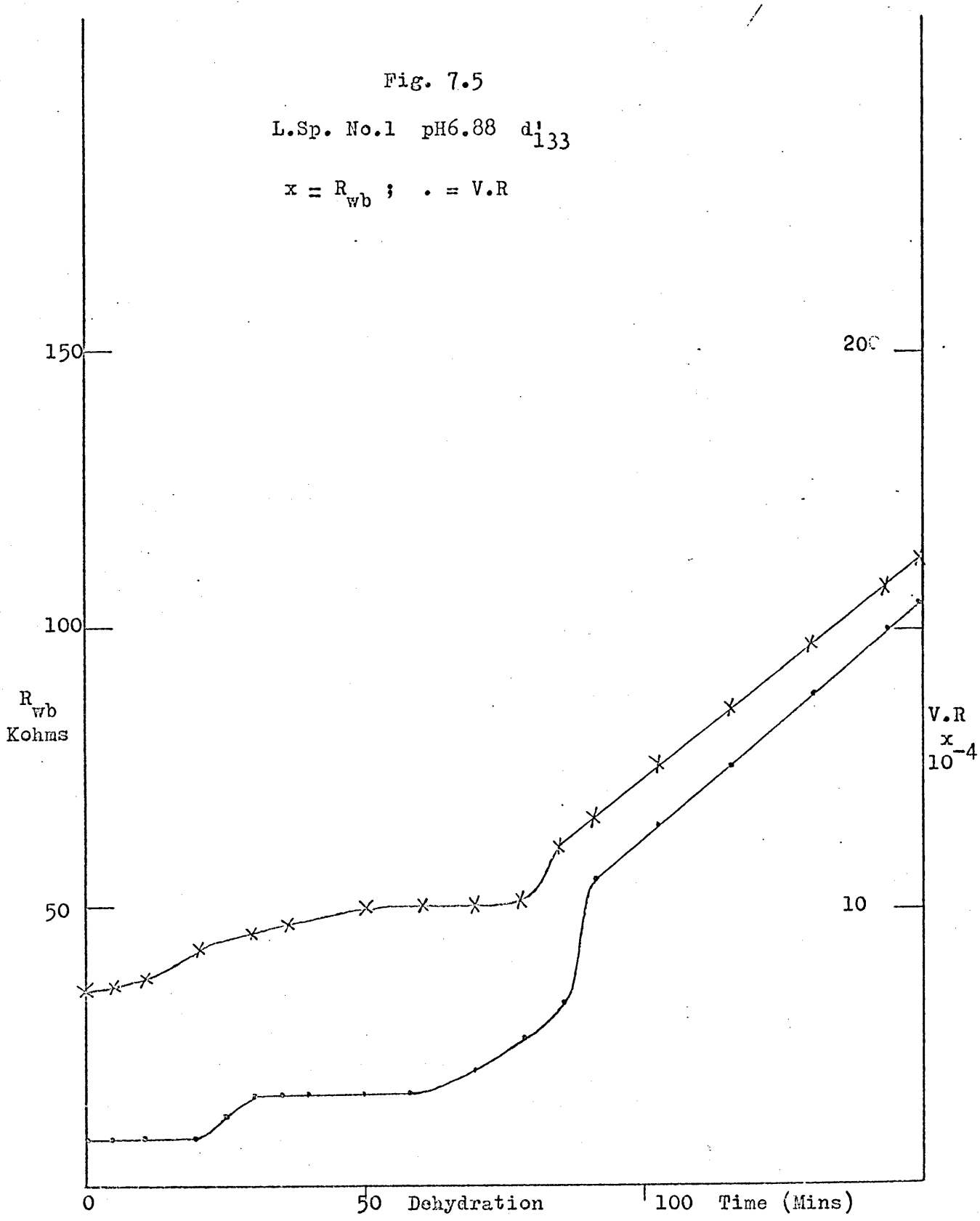

Fig. 7.6

L.Sp. No.2 pH6.88 d'_{133}

x = R_{wb} ; . = V.R

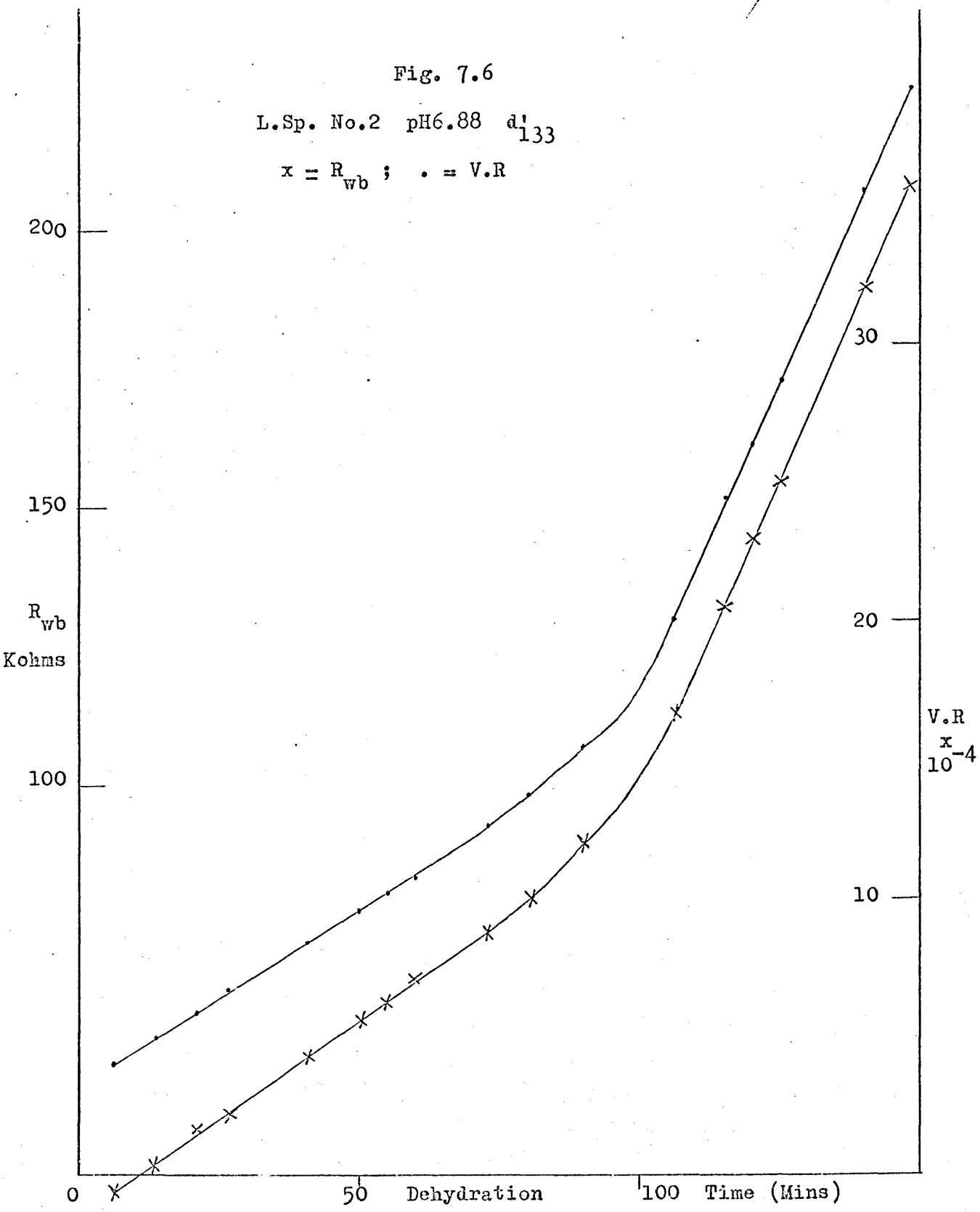

Fig. 7.7

L.Sp. No.1 pH6.88 d'_{211}

x = R_{wb} ; • = V.R

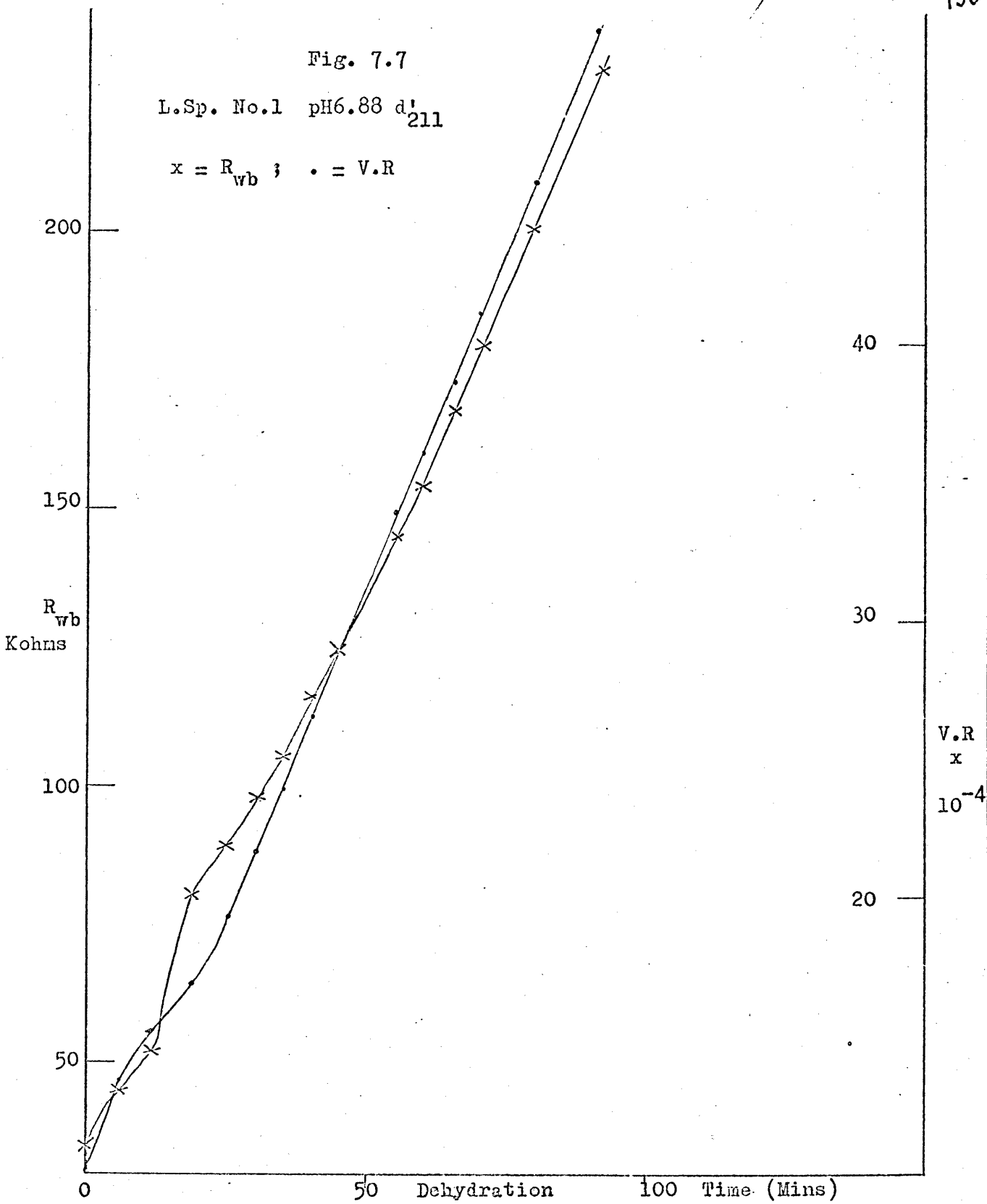

Fig. 7.8

L.Sp. No. 1 pH6.88 d'_{222}

x = R_{wb} ; . = V.R

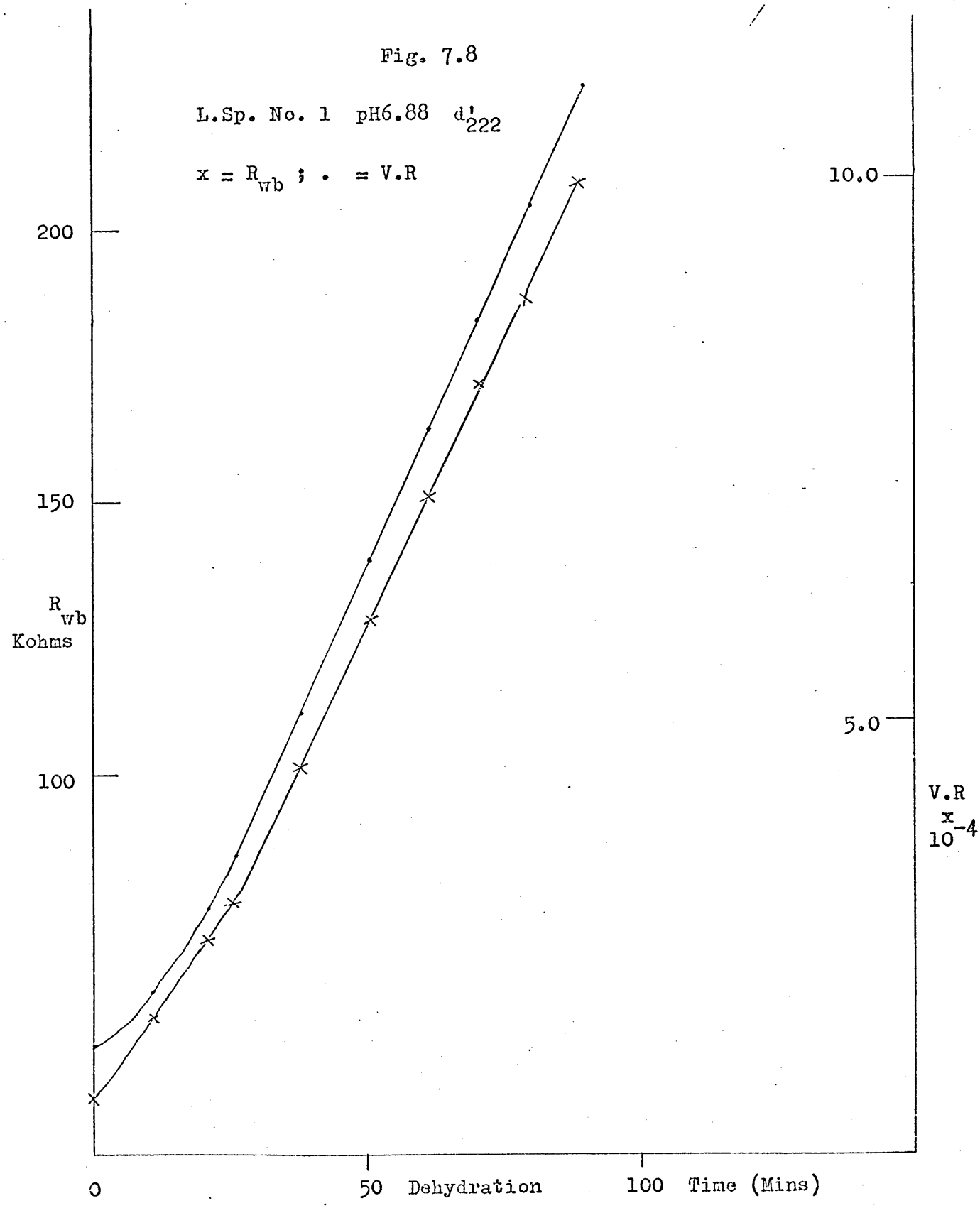

Fig. 7.9

L.Sp. No.1 pH6.88 d'_{233}

x = R_{wb} ; • = V.R

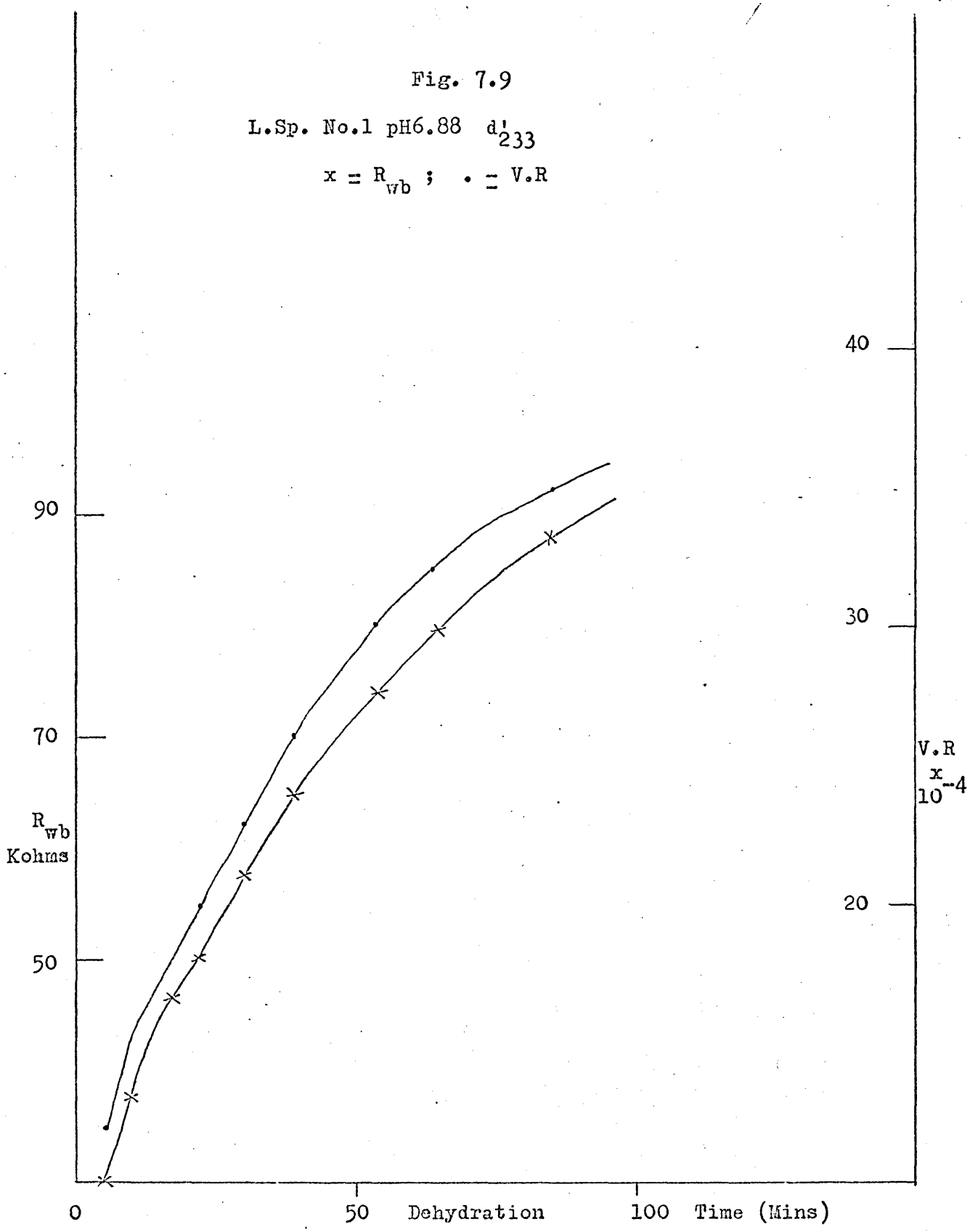

Fig. 7.10

L.Sp. No.1 pH6.88 d'_{311}

x = R_{wb} ; • = V.R

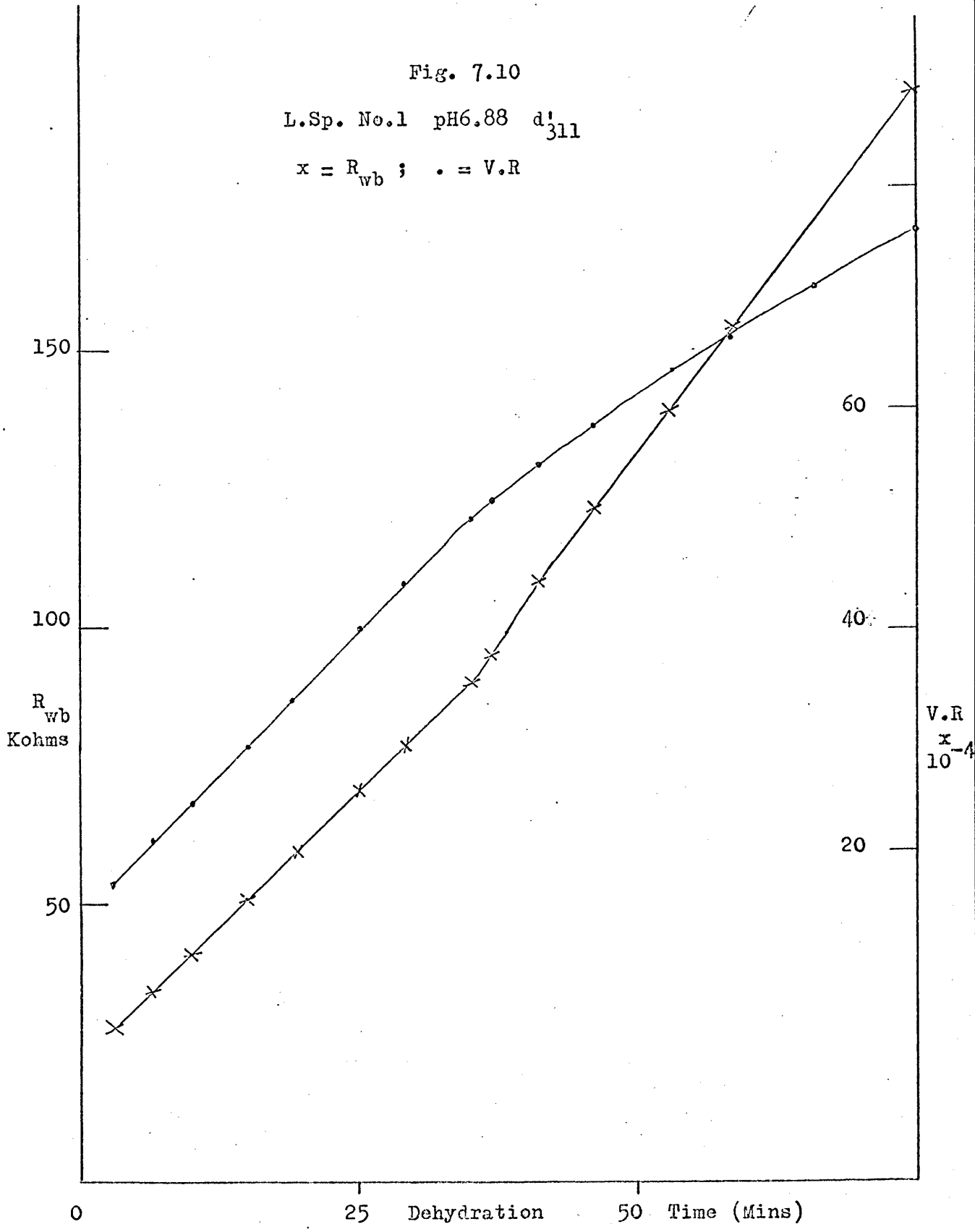

Fig. 7.11

L.Sp. No.1 pH6.88 d'_{311}

x = R_{wb} ; • = V.R

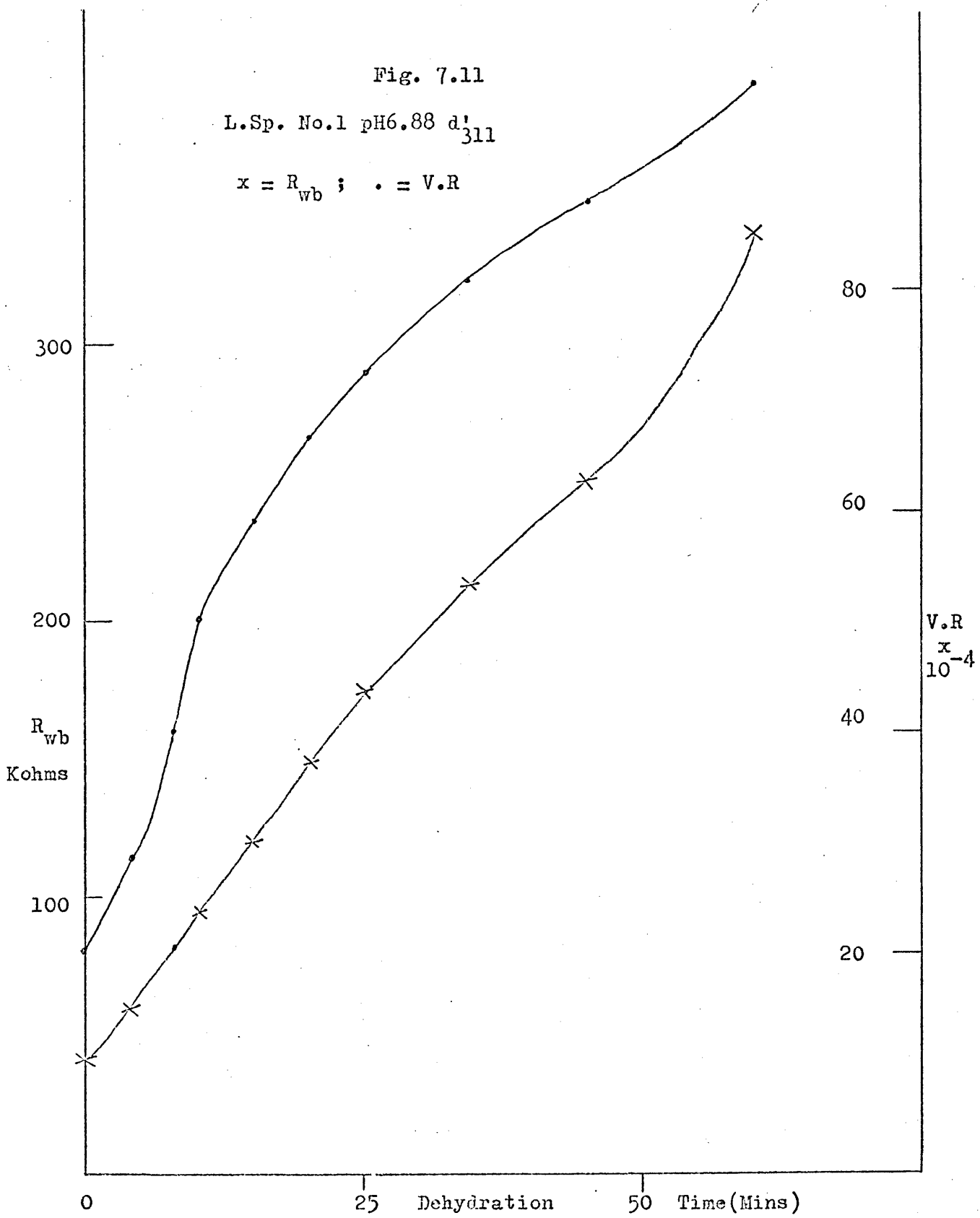

Fig. 7.12

L.Sp.No.1 pH6.88 d'_{322}

x = R_{wb} ; • = V.R

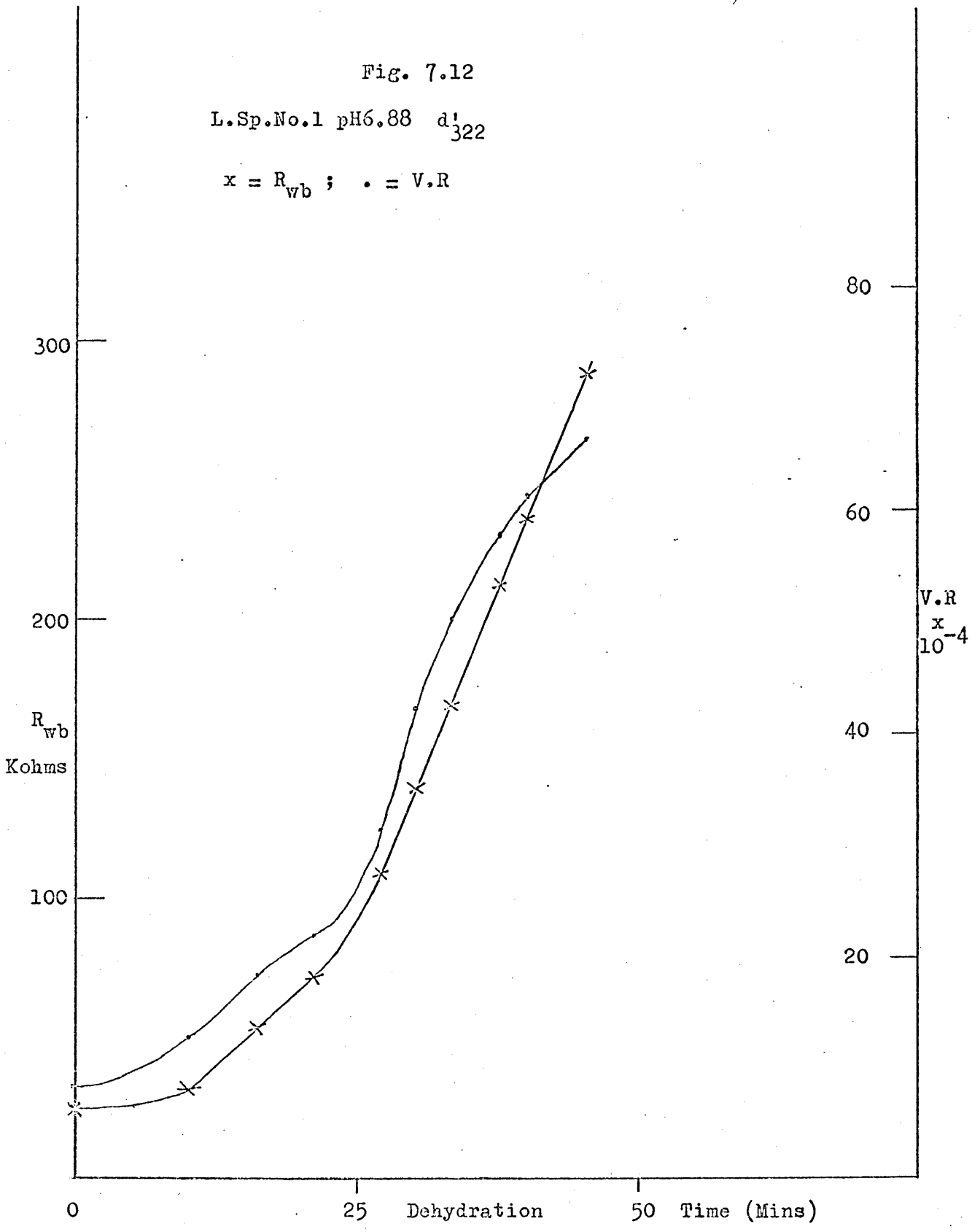

Fig. 7.13

L.Sp.No.1 pH6.88 d'_{333}

x = R_{wb} ; • = V.R

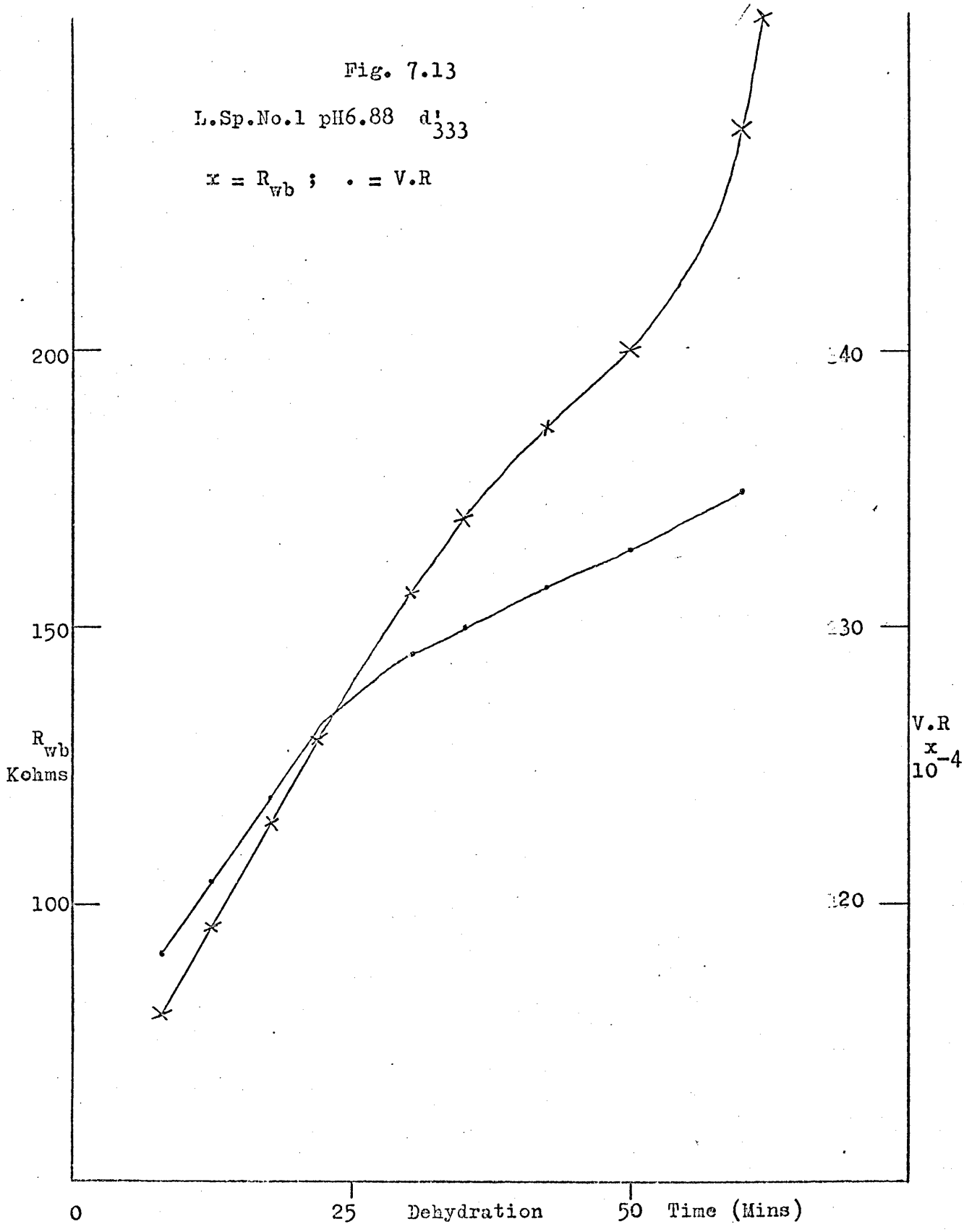

the group symmetry of wet bone would appear to be different from that of the dehydrated specimens.

Considering the figures presented in Table 1 , it is evident that the observed dehydration noticeably reduces the values of the d'_{3jk} coefficients,while to a first approximation the other coefficients appear largely independent of the observed change in water content.However for these latter coefficients it is difficult to be precise, since contrary to the d'_{3jk} coefficients the numerical changes are small compared to the quantities involved; and are of the same order as the general spread of the results.Thus, of the three results given in Table 1 for d'_{122} that at pH 5.0 appears independent of water content, that at pH 6.88 would seem to rise slightly with initial dehydration, and that at pH 4.00 appears independent of the dehydration if one ignores the first tabulated result.Likewise, of the two results for d'_{133} presented in Table 1, one appears to be independent of the water content while the other shows an initial decrease.Thus in conclusion, it is impossible to say whether the d_{1jk} and d_{2jk} coefficients show a definite dependence upon the observed change in water content.However, what may be stated is that the d_{3jk} coefficients show a definite, and by far the greatest, dependence upon the initial observed dehydration from the fully

Table One

No.1 pH6.88

R_{wb}	V.R	d'_{111}
35K	$.84 \times 10^{-4}$	$.54 \times 10^{-8}$
50K	.84	.37
57K	1.0	.39
75K	1.1	.33
102K	1.5	.34
150K	1.8	.27

No.1 pH6.88

R_{wb}	V.R	d'_{122}
25K	8.3×10^{-4}	5.4×10^{-8}
35K	11.4	5.3
40K	16.7	6.7
55K	22.2	6.52
66K	26.6	6.52
70K	32.2	7.42
110K	57.0	7.30
150K	71.5	7.50

No.2 pH5.0

R_{wb}	V.R	d'_{122}
12K	1.0×10^{-4}	1.87×10^{-8}
15K	1.3	2.00
17K	1.6	2.20
21K	2.0	2.14
25K	2.3	2.10
27K	2.7	2.25
32K	2.9	2.06

No.1 pH6.88

R_{wb}	V.R	d'_{133}
23K	6.2×10^{-4}	2.68×10^{-8}
30K	8.0	2.66
43K	5.7	1.33
50K	6.7	1.32
60K	8.3	1.37
86K	12.5	1.43
122K	16.1	1.31
150K	20.8	1.37

Table One (cont)

No.1 pH6.88

R_{wb}	V.R	d'_{133}
27K	4.6×10^{-4}	1.81×10^{-8}
50K	8.3	1.80
90K	15.0	1.80
117K	20.0	1.84
152K	28.6	2.00
190K	35.0	2.00
240K	43.5	1.95

No.1 pH9.15

R_{wb}	V.R	d'_{311}
48K	16×10^{-4}	16.8×10^{-8}
54K	19.0	17.2
66K	23.2	17.7
83K	26.4	16.1
100K	30.6	15.5
127K	35.8	14.3
162K	43.0	13.4
178K	47.0	13.2

No.1 pH6.88

R_{wb}	V.R	d'_{211}
35K	10.0×10^{-4}	8.85×10^{-8}
45K	13.3	9.15
52K	15.0	8.90
80K	16.6	6.45
88K	19.2	6.76
98K	21.8	6.88
105K	22.7	7.00
118K	26.6	7.00
125K	29.6	7.30
136K	30.8	7.00
146K	34.4	7.30
154K	36.0	7.21
170K	39.0	7.10
180K	41.0	7.10
200K	45.8	7.10
230K	51.2	6.90
270K	57.0	6.65

Table One (cont)

No.1 pH4.00

R_{wb}	V.R	d'_{122}
21K	5.0×10^{-4}	3.84×10^{-8}
28K	5.7	3.28
40K	8.6	3.50
48K	10.0	3.50
58K	12.0	3.38
65K	13.2	3.28
78K	15.7	3.25
88K	17.5	3.21
108K	20.0	3.20
120K	23.0	3.20
132K	24.8	3.18
141K	26.0	3.00
155K	27.6	2.88

No.1 pH5.0 (NaCl)

R_{wb}	V.R	d'_{311}
10.5K	7.8×10^{-4}	37.7×10^{-8}
12.5K	8.8	35.4
14.7K	9.8	33.8
18.0K	11.4	32.1
25.0K	14.3	29.0
31.0K	16.6	27.2
42.0K	20.6	24.8
54.0K	24.4	23.1
68.0K	28.6	21.2
87.0K	32.0	18.5

No.1 pH6.88

R_{wb}	V.R	d'_{311}
28K	16.6×10^{-4}	30.0×10^{-8}
60K	33.2	28.0
90K	50.0	28.0
110K	56.0	25.8
135K	59.5	22.3
155K	66.5	21.8
170K	71.5	21.2
210K	80.0	19.3

Table One (cont)

No.1 pH6.88

R_{wb}	V.R	d'_{311}
42K	20×10^{-4}	24×10^{-8}
60K	26.7	22.5
65K	35.1	27.3
95K	50.0	26.6
120K	59.0	24.8
150K	66.6	22.4
176K	71.4	20.5
215K	80.0	18.8
250K	89.3	18.1

No.1 pH6.88

R_{wb}	V.R	d'_{322}
25K	8.32×10^{-4}	11.2×10^{-8}
32K	12.5	13.1
55K	18.9	11.5
72K	21.8	10.3
112K	31.2	9.4
140K	41.6	10.0
170K	50.0	9.9
225K	60.6	9.3
290K	66.6	7.7

No.1 pH6.88

R_{wb}	V.R	d'_{222}
40K	2.1×10^{-4}	1.20×10^{-8}
50K	2.24	1.11
75K	3.62	1.12
100K	5.00	1.12
150K	7.50	1.13
200K	10.2	1.12

No.1 pH6.88

R_{wb}	V.R	d'_{233}
30K	2×10^{-4}	1×10^{-8}
38K	2.50	.98
47K	3.00	.96
50K	3.32	1.00
65K	4.32	1.01
74K	5.00	1.02

wet state.This is consistent with the result that these wet coefficients show the largest deviations in magnitude from the dry values and are therefore expected to be more dependent on water content.It may be seen that for some of the Table 1 results there is an initial rise in the value of the coefficient d'_{ijk} befor it assumes a definite variation with evaporation; whereas others indicate that the very initial values of d'_{ijk} are discontinously larger than these immediately following. If we examine this in detail in order of tabulation, we observe:- The first result of d'_{111} is greater than the rest which are largely constant.

The first two figures for one of the d'_{133} readings are approximately twice those following.

The first three values of d'_{211} are about 1.28 times greater than the rest.

The figures of d'_{311} at pH9.15 show there is an initial rise in its value before it commences to fall, so that the greatest value for these readings does not occur under the wettest state.

The next two results for pH 5.0 and pH 6.88 show d'_{311} continously falling, so that for these two sets the greatest

value of d'_{311} does coincide with the wettest conditions.

A second set of readings of d'_{311} at pH 6.88 shows the coefficient falling for the 1st two results, rising to its highest value at the third result, and subsequently falling for further evaporation. Hence for these readings the greatest value of d'_{311} does not occur for the wettest conditions recorded.

Similarly the d'_{322} results show the second reading to be the greatest in magnitude.

Hence in conclusion, it is apparent from these Table 1 observations that for the d'_{3jk} coefficients the wettest values recorded are often not the largest, and that in these cases d_{3jk} tends to change its variation with dehydration before continously falling with further evaporation.

The d'_{1jk} and d'_{2jk} coefficients do not show this dynamic behaviour, and contrary to the d_{3jk} coefficients, in many of the sets of readings, the initial values are statically larger than the rest which are predominantly stationary during evaporation. We may term these two effects transients , since they only represent initial phenomena.

Examination of the results of Table 2 shows that the value of d'_{333} which corresponds to the most hydrated recorded

Table Two

No.1 pH4.0

R_{wb}	V.R	d'_{333}
36K	24×10^{-4}	18×10^{-8}
37.5K	25.0	18.0
38.5K	24.0	16.9
40.0K	25.4	17.6
After short re-immersion		
19K	8.7	10.2
21K	8.3	8.9
25K	9.1	8.1
26K	10.1	8.5
31K	11.3	8.1
35K	14.0	8.9
40K	17.0	9.3
50K	20.0	8.9

No.2 pH5.0(NaCl)

R_{wb}	V.R	d'_{333}
85K	27×10^{-4}	7.1×10^{-8}
90K	31.0	7.3
95K	33.0	7.7
105K	37.0	7.8
110K	40.8	8.3
123K	47.0	8.6

No.1 pH6.88

R_{wb}	V.R	d'333
28K	6.7×10^{-4}	5.3×10^{-8}
32K	8.0	5.6
35K	9.3	6.0
37K	10.8	6.6
41K	13.0	7.1
50K	15.3	6.9
53K	17.0	7.3
60K	18.8	7.1
71K	22.0	7.0

Table Two (cont)

No.1 pH9.15

R_{wb}	V.R	d'_{333}
55K	$20x10^{-4}$	$8.2x10^{-8}$
61K	20.5	7.6
65K	20.7	7.2
67K	18.7	6.4
70K	18.2	5.9
80K	20.0	5.7
90K	22.0	5.6
100K	24.7	5.6
115K	28.0	5.5
129K	31.0	5.4

No.2 pH5.0		d'_{322}
32K	$6.70x10^{-4}$	$4.7x10^{-8}$
35K	8.30	5.37
40K	10.0	5.72
50K	13.7	6.15
65K	19.7	6.78
71K	23.0	7.25
80K	24.7	6.94
88K	27.7	7.12
95K	29.7	7.08

No.1 pH9.15, after 3hours re-immersion following previous results at pH9.15

R_{wb}	V.R	d'_{333}
42K	$20x10^{-4}$	$10.8x10^{-8}$
43K	20.7	10.8
43K	22.2	11.7
clamping re-checked		
44K	20.0	10.2
43K	20.7	10.6
45K	20.8	10.3
45K	21.7	10.8
Surfaces re-wiped dry		
60K	21.3	8.00
68K	23.0	7.55
75K	26.0	7.76
82K	28.3	7.80
95K	33.3	7.80

conditions appears to go through a minimum in the pH range 5.0 to 8.0 . In order to determine this more accurately it would be necessary to use many more pH solutions several times.It has already been mentioned that the sign of the coeffifient was not determined, so that the above refers to the modulus of the coefficient.Observation of Table 2 results also shows that at the pH values of 5.0 and 6.88 d'_{333} increases with the observed dehydration, whereas at pH 9.15 it decreases.At pH 4.0 it also decreases, but the fall is less pronounced than at pH 9.15. It is possible to observe pH effects from the figures in Table 1, but as has been mentioned before, the specimens were not vacuum-dried between different pH measurements, so that it is considered that the results of Table 2 are more reliable on this subject.

7.14 Interpretation of The Wet Bone Results

We remarked in 7.12 that d_{wb} is expected to be constant only if the buffer solution behaves like a pure resistance and shunts the bone signal.We have seen in 7.13 that the d'_{3jk} coefficients vary considerably with water content, and that for the Table 1 results, which represent measurements carried out on pieces immediately after their excision from the fresh femur, they all decrease considerably as the specimens dry out.Thus the very

high value of the wet d'_{3jk} coefficients over the dry equivalents depends upon the bulk presence of free water in the bone(see Chapter 6).Considering the nature of the bone, the majority of the pores in which free water may reside will be roughly cylindrical in shape, with a net statistical orientation in the bone long direction.Coupling this with the observed variation of the d'_{3jk} coefficients with pH, we conclude that considerable 1 kHz streaming is occurring in the bone long direction so producing 'streaming potentials'.

The interpretation of the other coefficients of Table 1 is not so immediately evident.What we observe is that these coefficients are all larger than the dry equivalents(as for the d'_{3jk} coefficients), but show little, if any, dependence upon the change in water content that occurs in the observed evaporation range.However, since the net orientation of the water channels is in the bone long direction, evaporation will largely proceed in this direction, and this will be aided by the liquid streaming.Thus the water which is streaming in the bone long direction will evaporate at a much faster rate than that which is streaming in the transverse channels.Hence we conclude that streaming also occurs in the transverse directions , but that the bulk of the evaporation process takes place in the bone long direction.Thus the picture emerging from the Table 1

results is that streaming occurs in all directions, but that because of its structure, the greatest potentials occur in the bone long direction.

(We note at this stage from the Table 1 graphs of d'_{133} that a sudden change appears to take place in $(e_L)_{wb}$ and R_{wb}. The tabulated form of these results shows that the signal to resistance ratio is still the same after this change of slope. We will not treat this in detail here since the separate resistance measurements on stressed and unstressed bone specimens were carried out, and these give more accurate information on this phenomenon. This is treated in the next section 7.15).

The later results of Table 2 appear only partially consistent with the presence of streaming potentials. The rise at pHs 5.0 and 6.88 of d'_{333} with the initial dehydration seems in contradiction with ideas of streaming, although with further evaporation this rise would reverse itself as the dry conditions are approached. It is interesting at this point to recall that for the earlier results of Table 1 d_{3jk} often rises in value before settling down to a continous decrease. Hence the effect of the intermittent solutions may be regarded, for these two pHs, as extending this initial region further

into the dehydration range.The results for d'_{333} at pH 9.15 show d'_{333} decreasing with evaporation, as do the results for pH 4.0.Thus it appears that the chemical effects of these solutions in is largest in affecting the middle pH range results.Considering that these ostensibly anomalous results refer to somewhat treated bone it is difficult to know what importance to attach to them .However we think that the occurrence of 'transients' in some of the fresh bone results indicates a connection between the two phenomena.It was observed during the later measurements of Table 2 that complete dehydration changed the appearance of the bone.Slight cracks became visible, primarily along the bone long direction, and the pieces were slightly narrower in the transverse directions than the original dry values.It is our opinion that the rises of d'_{333} at pHs 5.0 and 6.88 are caused by substantial transverse contraction, so that the roughly cylindrical pores or long channels which contain the free water, decrease in diameter while streaming is occurring. The effect is only apparent at these middle pHs because of the smallness of the streaming potential in this region.It will be recalled that whilst the decrease of d'_{333} at pH 9.15 was pronounced, that at pH 4.0 was less so, so that although the magnitudes of this coefficient at the various pHs indicate a

a possible isoelectric point(if one exists for bone), for bone in the general pH range 5.0 to 8.0 , the figure is likely to be nearer 5 than 8.This is consistent with the streaming being largely against collagen surfaces(see Chapter 4), although it could indicate a small streaming potential contribution from the bone mineral.

The occurrence of what we have termed transients for the d_{3jk} coefficients in the Table 1 results indicates that a small amount of contraction occurs in the very initial evaporation process even for fresh bone.This seems reasonable since a little swelling will occur as the fresh bone hydrates, so that one would expect some transverse contraction when drying.The larger initial values of the d_{1jk} and d_{2jk} coefficients indicates that a small amount of water is initially expelled from the transverse channels when the bone is loaded in the apparatus and streaming commences.

Thus we conclude that the effective 'piezoelectric' voltages generated in wet bone are predominantly streaming potentials.However we shall show in the next section that the wet bone collagen is still classically piezoelectric itself, so that even though streaming potentials are by far the greatest in magnitude, both phenomena contribute to the observed voltages in wet bone.

Chapter Seven , Part Two

Electrical Resistance Measurements on Wet Bone

7.15 Introduction.

All the resistance measurements of wet bone were carried out on the two large specimens 1. and 2. using a valve volmeter operating in its highest resistance measuring range(1 to 500 Meg ohms).Calibration of the instrument in this range was achieved with standard high stability resistors, and from these measurements all the wet bone readings are considered to be accurate to approximately 5% of their value.The electrical resistances of stressed and unstressed wet bone specimens were periodically measured as they dried out in the laboratory atmosphere.The current driven through the specimens by the valve voltmeter was approximately 10^{-8} amps.This measuring instrument was chosen as opposed to the more accurate potentiometer since a fast reading time was required owing to the continual change of the electrical resistance of the bone specimens as they dried out.It was noticed that for all the wet bone specimens and for small pieces of tendon that,irrespective of the direction in which measurements were taken, a rise time of approximately ten to fifteen seconds occurred before the meter needle reached its maximum value, and that the measured resistance was different

when the current was reversed.This effect represents the occurrence of ionic electrical polarization, which the measuring instrument sees as a large parallel capacitance.The effect is equivalent to a static dielectric constant of approximately 10^6 in the wet bone pieces used.Initially in the experiments,two values were taken for every resistance measurement.Besides the steady maximum value,corresponding to the completed polarization, an estimate was made of the initial resistance upon connection to the voltmeter. These lower values are not shown on the resistance curves presented here since they produce an identical resistance-time curve but slightly displaced in value from the maximum value. It also proved difficult to estimate these initial values accurately, since the meter needle always swung past the desired value.This charging time of approximately ten to fifteen seconds persisted even for the comparatively dry bone pieces.It is therefore concluded that the polarization is either due to induced ionic diffusion of collagen A band H^+ and possibly OH^- ions as well, or to induced diffusion of the same 'bound'ions in the apatite crystals.The results are shown in Figs. 7.14 to 7.21. Figs. 7.14 to 7.19 show in order of experimentation the results for unstressed wet bone.Figs. 7.20and 7.21 show the results when the specimens were loaded in the apparatus with a 2Kg. weight in the three bone directions, corresponding to simple tensile stresses T_{11} , T_{22} ,

T_{33} , where the latter stress represents a simple stress in the bone long direction, and the axes are the same as for the dry piezoelectric results.The corresponding resistivities are denoted by ρ_1 , ρ_2 , and ρ_3 respectively.Included with the stressed bone results should also be Figs. 7.3 to 7.6 , since they represent the earliest measurements of R_1(the resistance in the labelled 1 direction) for stresses T_{22} and T_{33} .The results for unstressed bone will be considered first.

7.16 Results for Unstressed Bone

It is apparent from the unstressed bone results that the electrical resistance in the bone long direction R_3 suddenly rises rapidly after a fixed period of evaporation.Fig. 14a which represents the earliest measurements of R_3 upon Sp. No. 1 (two months after excision at roughly neutral pHs) shows this time period to be approximately one hour.The later results of Figs. 7.17 and 7.18 upon Sp. No. 2 which had lost at least 6.2% of its weight by the time of this measurement, indicates this time to be approximately 45 minutes.Fig. 7.19 which represents the last measurements made on Sp. No. 1 (roughly 5 months after excision) shows that this time has decreased to near twenty minutes, Reference to Chapter Six indicates that as the bone specimens start to lose mass through dissolving of collagen,the main or

2nd discontinuity in the evaporation curve occurs earlier than for fresh bone.This is to be expected, since there is less total water to evaporate, and larger evaporation sites.It is therefore concluded that the sidden rise in the value of R_3 coincides with the main discontinuity in the evaporation curves, and therefore with the emptying of all collagen B band water sites.Fig. 7.14b shows the resistivity ρ_3 for Sp. No. 1 in distilled water, as a function of the loss of water in mgms. (This is obtained by combining Fig.7.14a with Fig.6.5 .) It is seen that ρ_3 rises dramatically when a sudden state of dehydration is reached. On the same axes is plotted ρ_1 for the same specimen, but immersed in Ringer's solution (one quarter strength). No sudden large change is observed.In Figs. 7.17a and 7.18a the ratio of ρ_3/ρ_2 has been plotted as a function of dehydration time in order to give an indication of the variation of these two resistivities with water content.The same information is presented in a different way in Figs. 7.17b and 7.18b , which show a plot of ρ_3 against ρ_2 . The distilled water results of Fig. 7.17 identify three regions in the resistivity - time curve.The results of Chapter Six indicate that these are associated with loss of free water, loss of collagen B band water, and loss of collagen A band water, in order of occurrence. For fully hydrated specimens it is seen that(if Δ means a variation

Fig. 7.14a

L.Sp. No.1, H_2O, Unstressed

R_3 ($\times 10^6$ ohms)

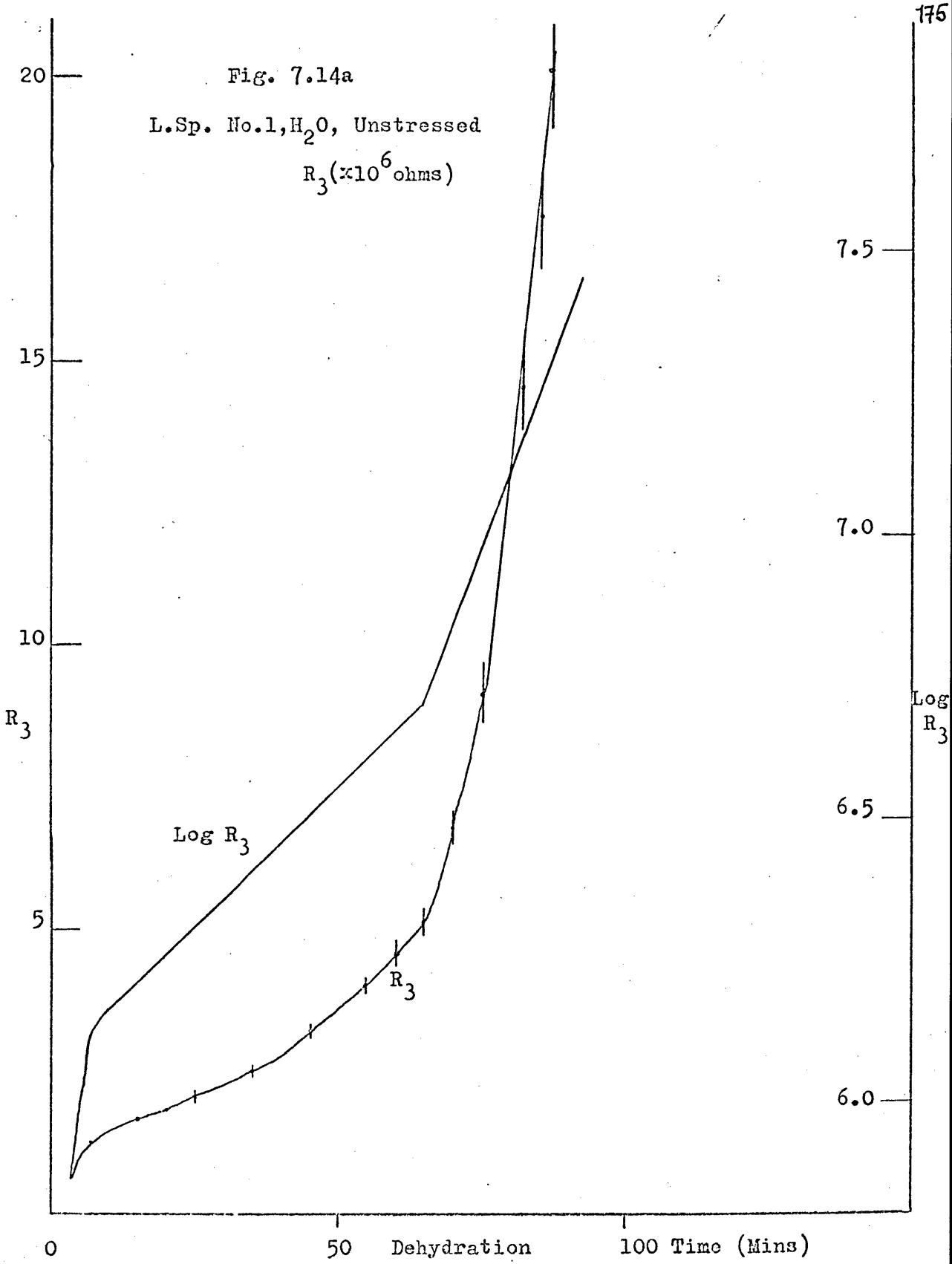

Fig. 7.14b

Resistivities ρ_3 and ρ_1 ($\times 10^6$ ohm cm)

against H_2O content. Unstressed

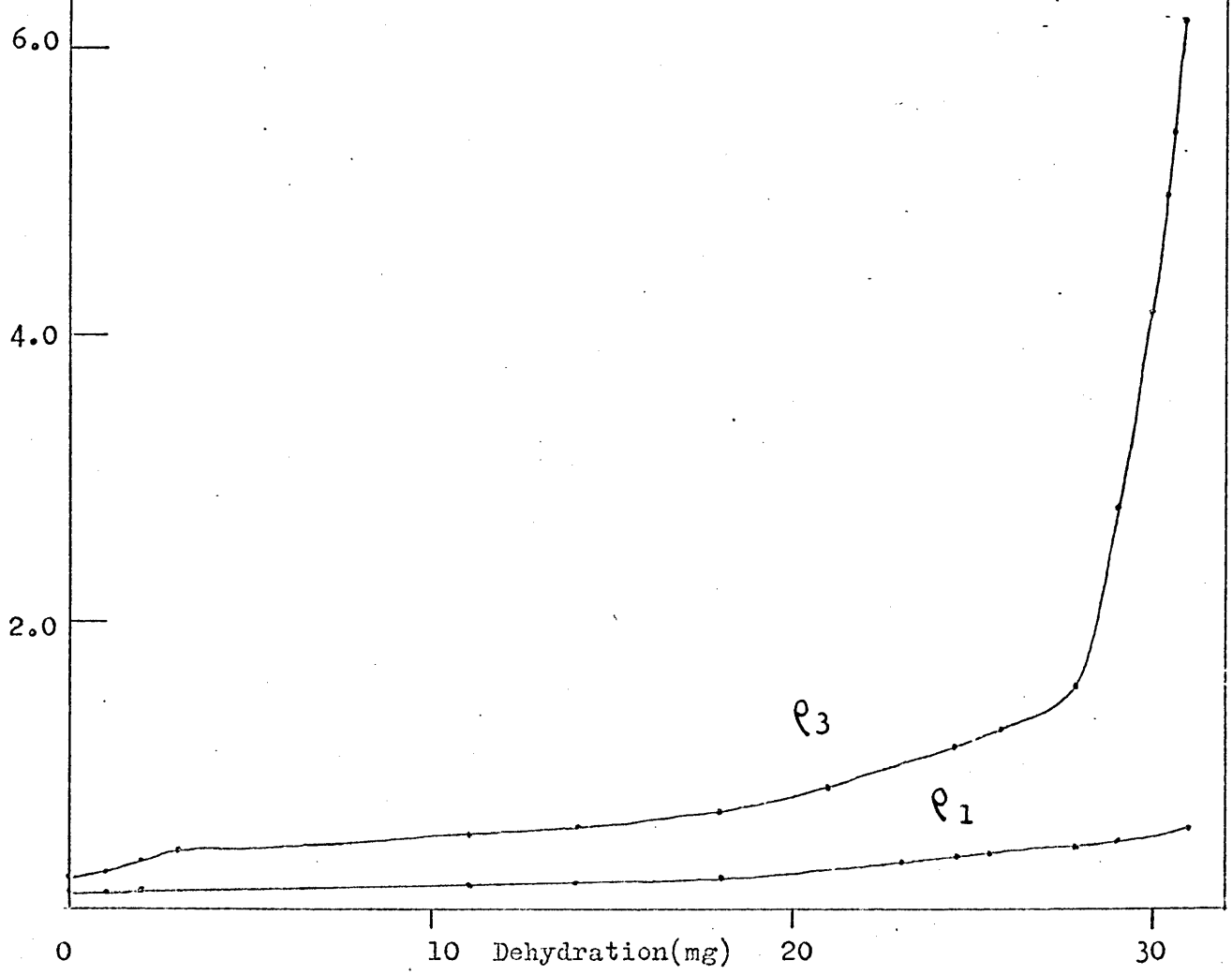

Fig. 7.15

L.Sp. No.2 Ringer's Solution.

R_1 ($\times 10^6$ ohms) Unstressed

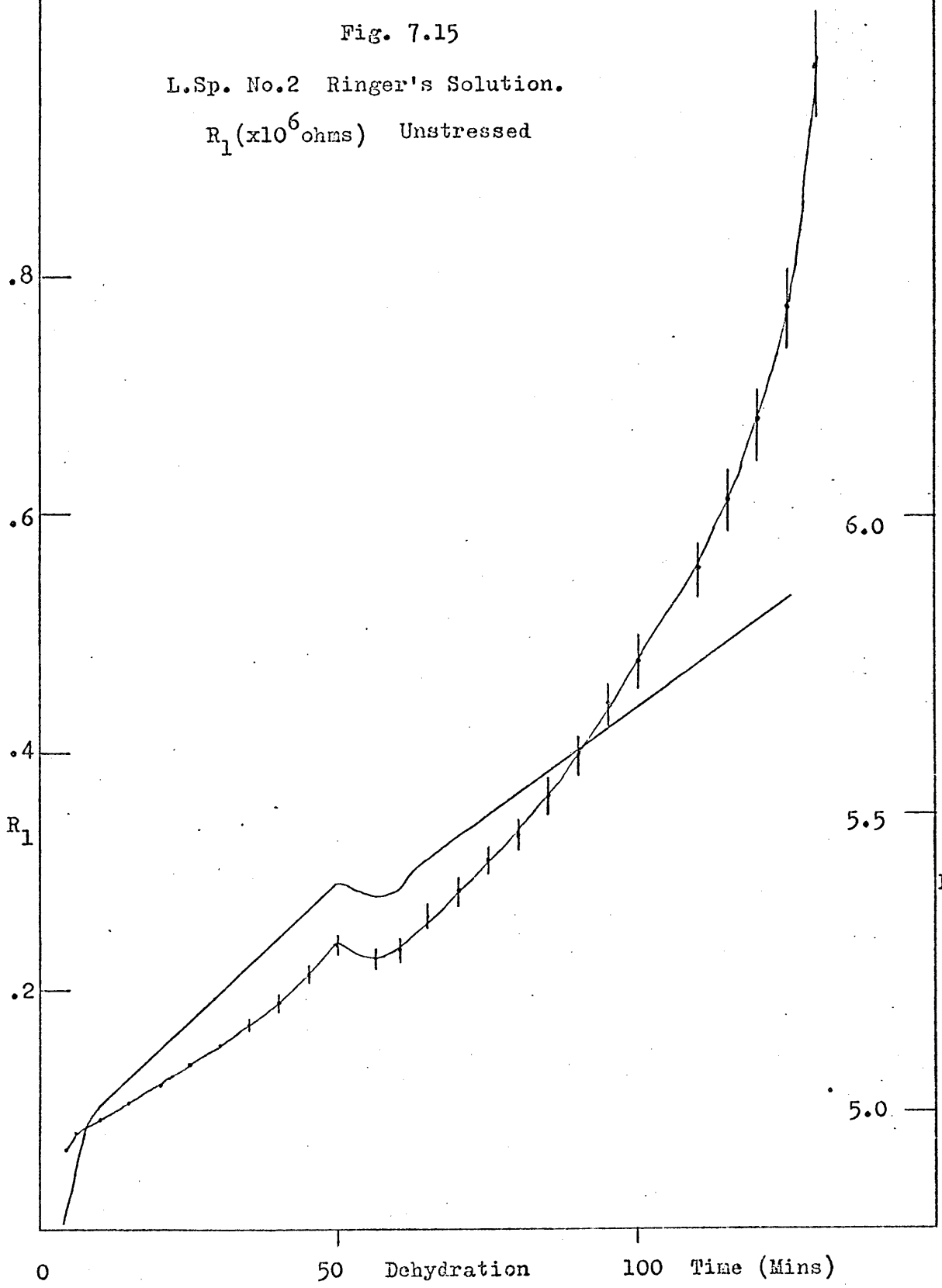

Fig. 7.16

L.Sp. No.2 H_2O Unstressed

R_2 ($x10^6$ ohms)

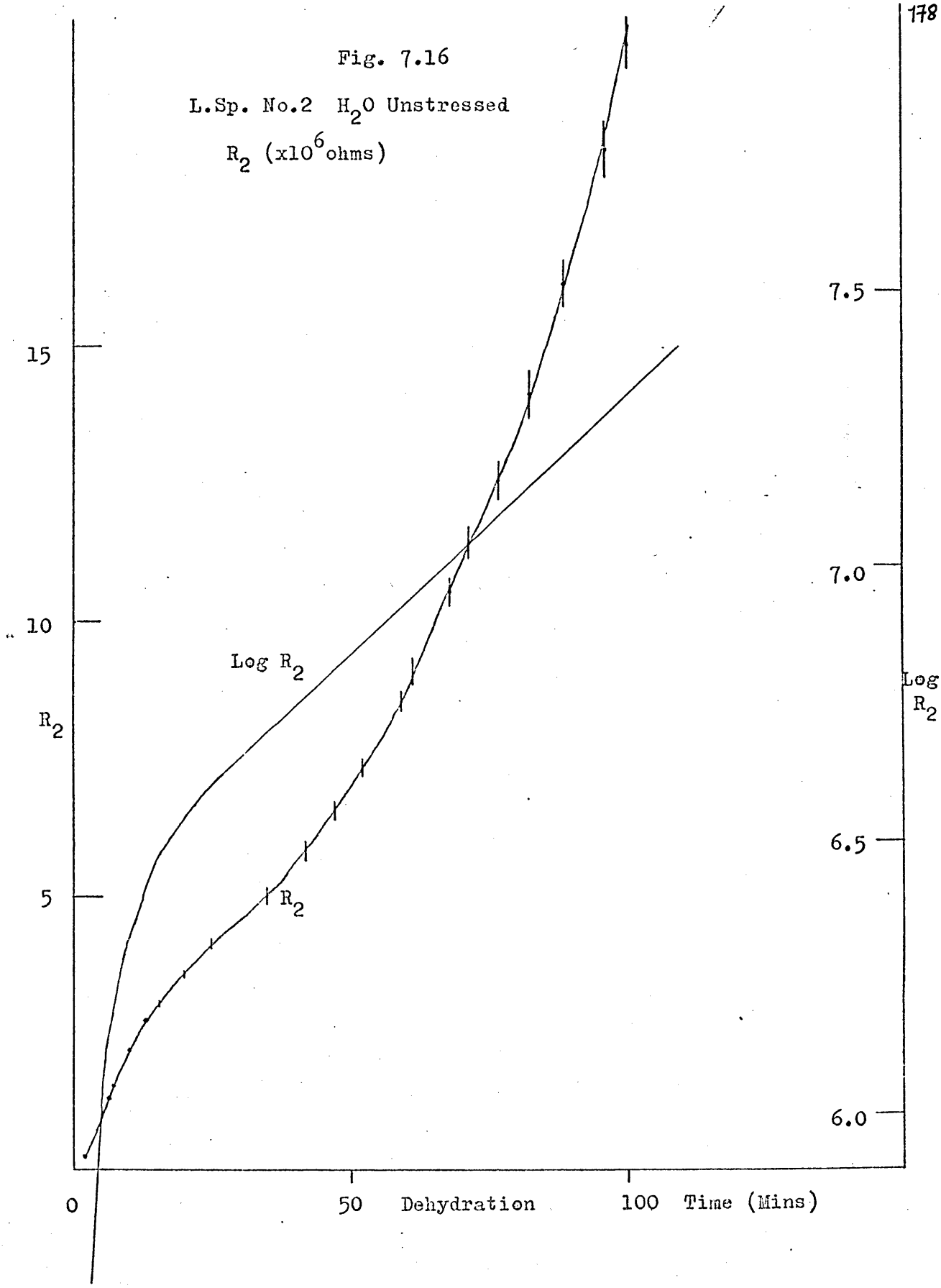

Fig. 7.17a

L.Sp. No.2 H_2O.Unstressed

R_3 and R_2 ($x10^6$ ohms)

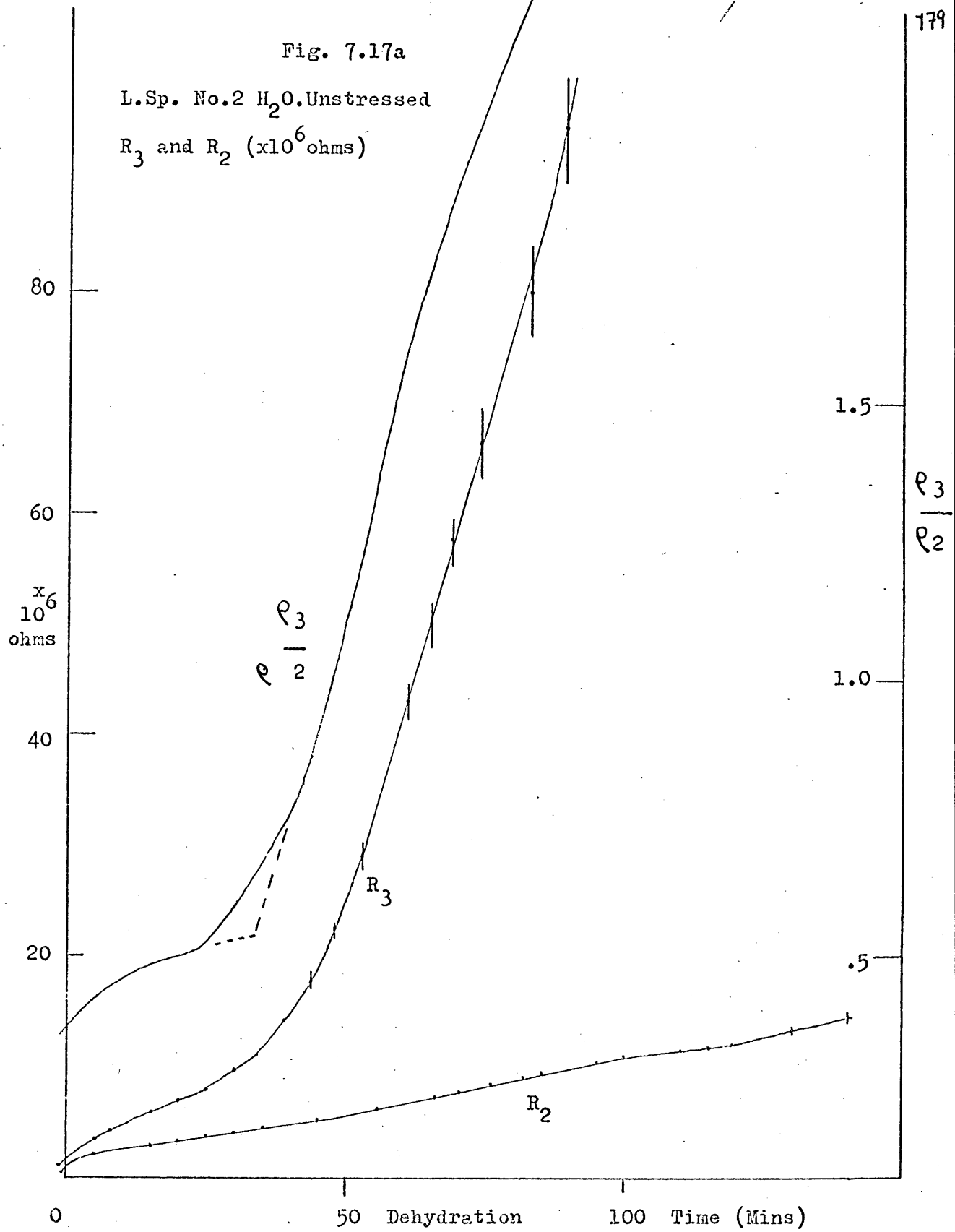

Fig. 7.17b

L.Sp. No.2 H_2O. Unstressed

ρ_3 and ρ_2 $\times 10^6$ ohm cms

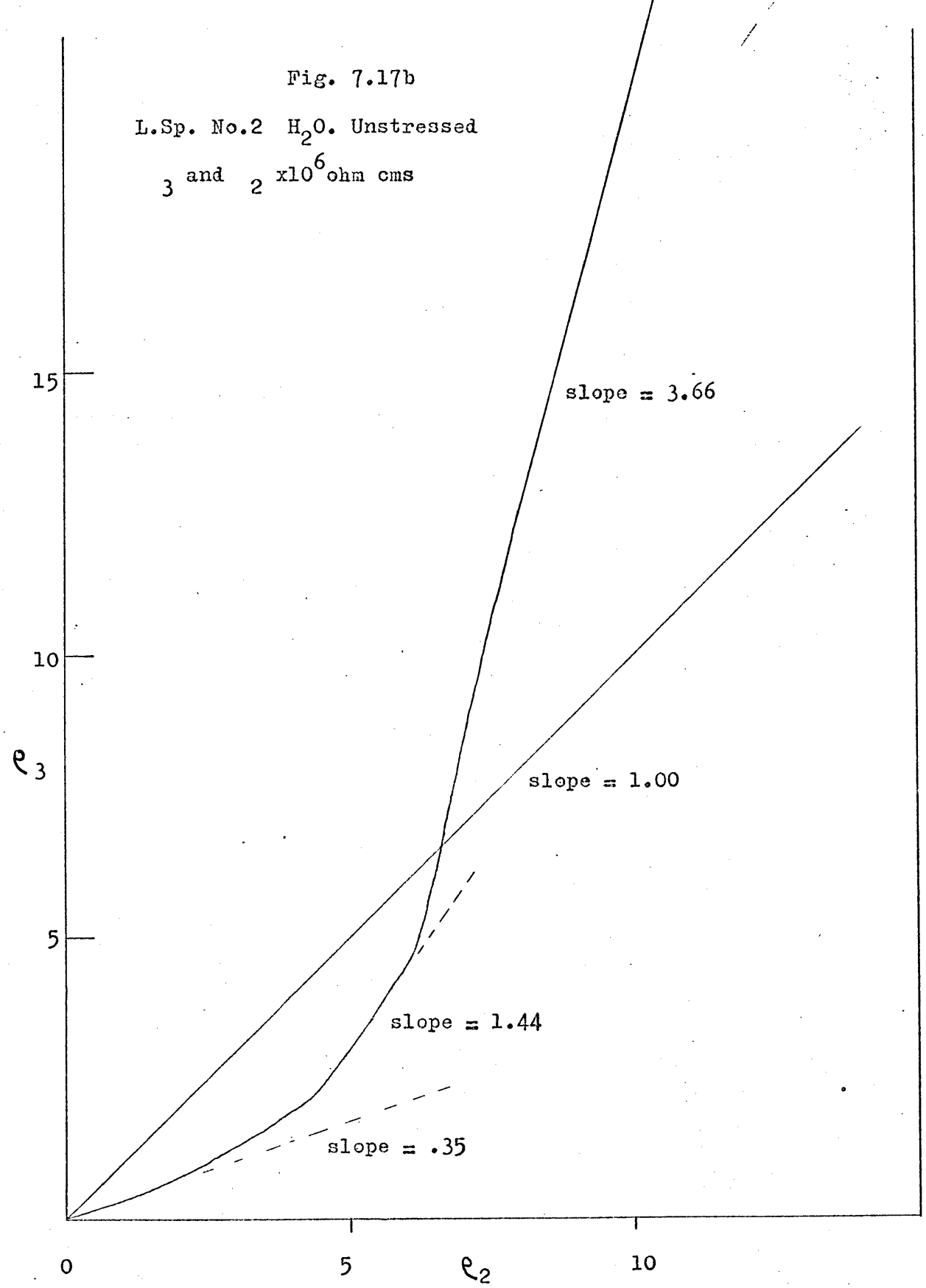

Fig. 7.18a

L.Sp. No.2 Ringer's Solution .Unstressed.

R_3 and R_2 x10^6 ohms

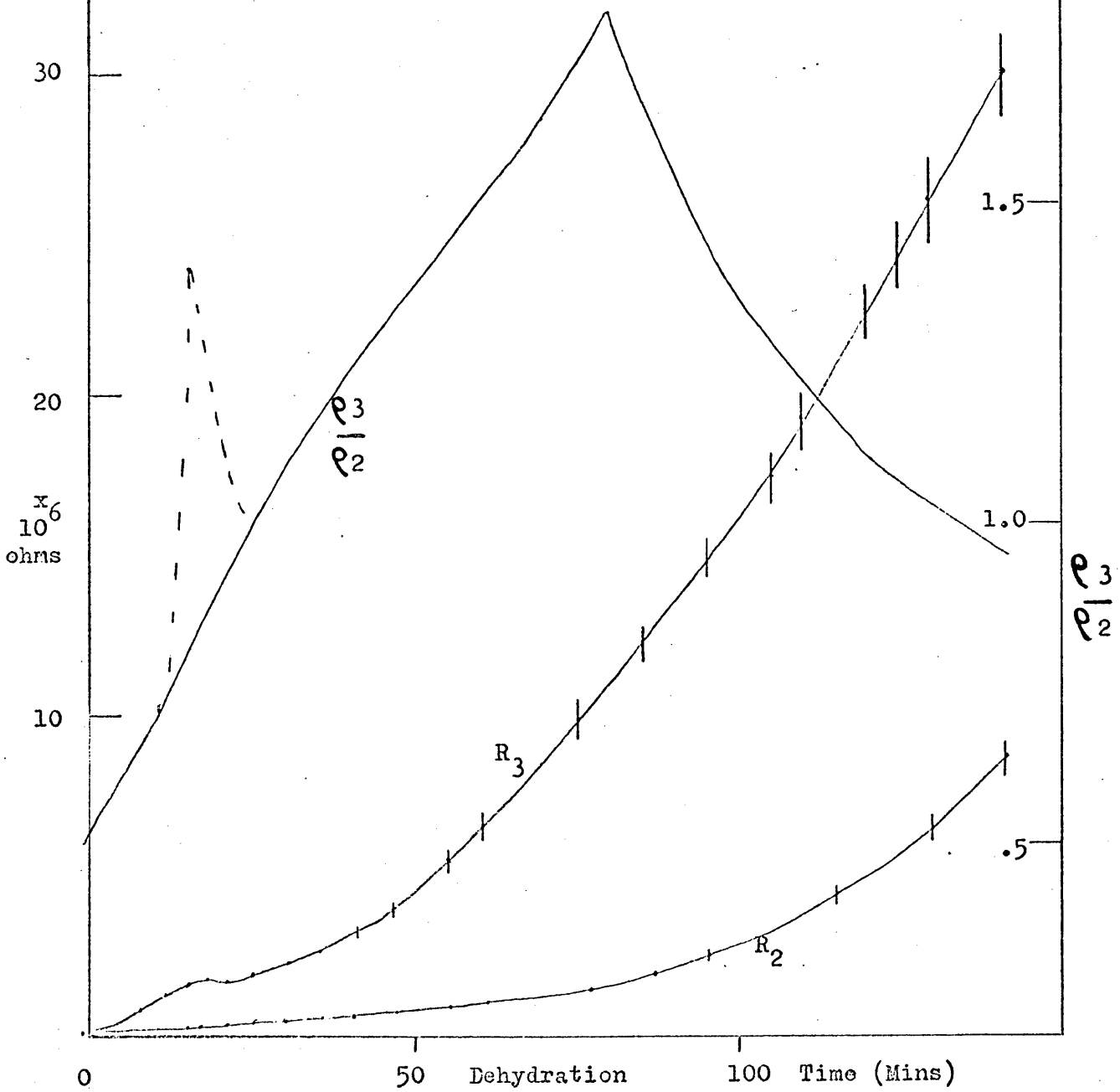

Fig. 7.18b

L.Sp. No.2 Ringer's Solution

Unstressed .

Resistivities ρ_3 and ρ_2 x10^6 ohm cm

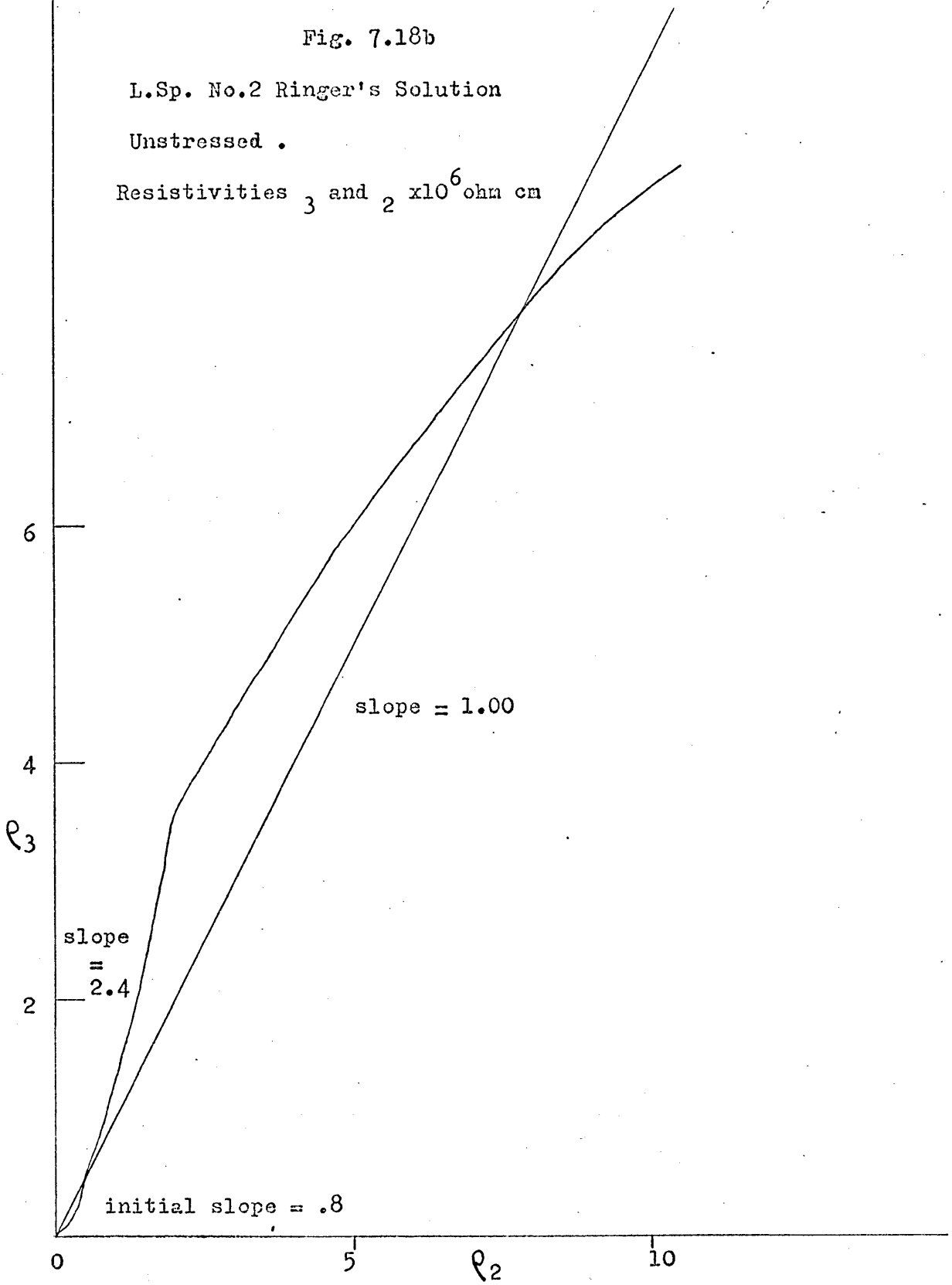

Fig. 7.19 L.Sp.No.1 H_2O. Unstressed

R_3 and R_1 x10^6 ohms

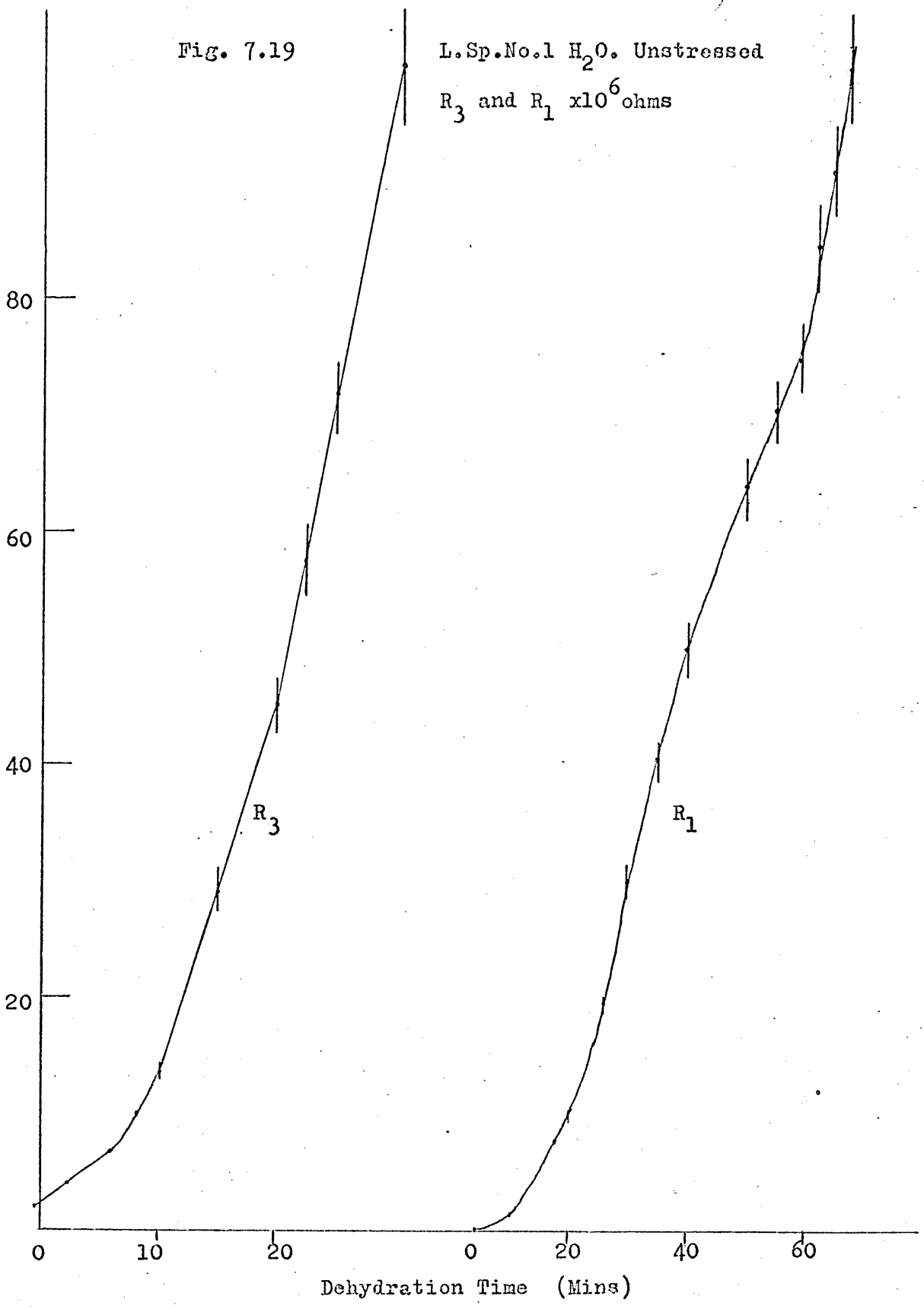

in the following variable) $\Delta\rho_3 \simeq .35\,\Delta\rho_2$, whereas for A band evaporation $\Delta\rho_3 \simeq 3.6\,\Delta\rho_2$. In the initial region, although ρ_3/ρ_2 is increasing the rate of increase with time is decreasing, as it is noted is the evaporation rate. With the evaporation from the B band ρ_3/ρ_2 starts to increase faster, and it is here that in absolute terms ρ_3 increases by approximately the same amount as ρ_2, although ρ_2 is still greater than ρ_3. When the main discontinuity is reached, corresponding to the commencement of A band evaporation, ρ_3 increases in absolute terms by roughly 3.7 times as much as ρ_2, so that ρ_3 rapidly surpasses ρ_2. The interpretation of these results falls into parts, an explanation of the variation of the ρ_1, ρ_2, ρ_3 with time, and the accounting for the relative variations of the three resistivities. We treat the former first.

Since the protein fibres and the mineral crystals are aligned largely along the bone long direction, that is our labelled 3 direction, it is perhaps not surprising that the resistivity results for this direction are different from those perpendicular to it. Interpreting the R_3 discontinuity as corresponding to the commencement of collagen A band evaporation and using Fig. 7.14b, it is apparent that the A band bound water molecules contribute far more to electrical conductivity in the bone long direction and therefore the protein fibre direction, than do

those in the B band , or the free water molecules.It is therefore suggested that the A band water molecules are primarily aligned in the fibre direction, unlike those in the B bands. The resistivity measured transverse to the bone long direction measures to a good approximation, the transverse fibre and mineral resistivity.The result that the discontinuity does not similarly appear in ρ_2 indicates that in this direction perpendicular to the bone axis,the collagen A band water molecules contribute roughly the same amount to electrical conductivity as do those in the band.(The apparent kink in the R_1 curves are however interpreted as indicative of this discontinuity, but we will leave the comment on this to the discussion of the comparative results).

The comparative results of ρ_1 ,ρ_2 ,ρ_3 are more dependent upon the resultant fibre orientation in the particular specimens than are the separate resistivities variations with water content. Although the decreasing rise rate of ρ_3/ρ_2 with free water linked with the decreasing evaporation rate indicates that the ratio ρ_3/ρ_2 rises at an approximately constant rate, in absolute terms the loss of free water affects ρ_2 by more than twice that of ρ_3. It is thefore concluded that for Sp. No.2 the free water molecules contribute more to electrical conduc tivity in the labelled 2 direction than they do to the bone long or 3 direction.

The piezoelectric results on the two dry beef bone specimens , given in Chapter Five, indicated that for both Sp. No. 1 and Sp. No.2 the protein fibres are predominantly contained in the labelled 1-3 plane. This is shown in the diagram below.

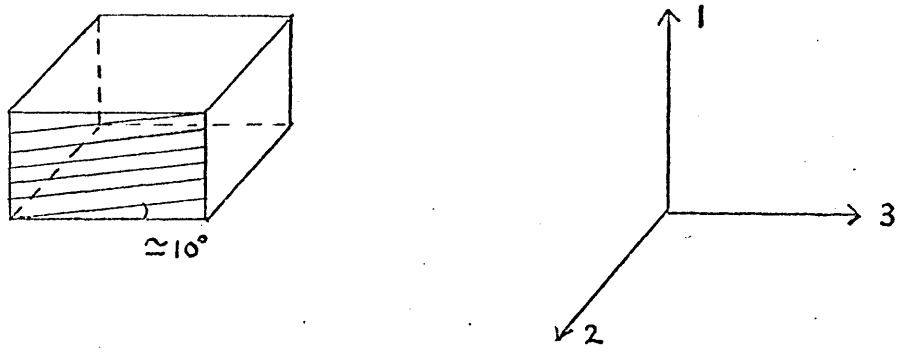

Specifically it was found that net result of all the individual specimen fibres orientations was as though they were inclined at an angle of about 10° to the bone long direction, and in the 1-3 plane. Hence for these two bone specimens all transverse directions are not equivalent.The pores which contain the free water molecules, although primarily oriented in the 3 direction, have a net component in the bone 1 direction but not in the 2 direction. If the pores are imagined to be cylindrical in shape then it may be seen from the above diagram that the free water would tend to reduce ϱ_2 more than ϱ_3 .This is what the results indicate. We now return to the comment on the R_1 - time curves.Fig. 7.15 shows what appears to be a small kink in the R_1 results correspon-

ding to the discontinuity for R_3. A similar, although less pronounced effect is shown in Fig. 7.19 which represents the last measurements that were carried out on R_1 . The evidence just given that the protein fibres have a net component of their long axes in the specimen 1 direction indicates that this kink is probably real and coincident with the main discontinuity in R_3 .

Figs.7.18 a and b show similar plots to those of Figs.7.17 , but for the specimen immersed in Ringer's solution,(B.D.H , pH roughly 7.3).It is seen that one expected effect of the ionic concentration is to lower the resistivity values compared to those for distilled water.More important though are the observed changes induced in the ϱ_3/ϱ_2 - time curve and the graph of ϱ_3 against ϱ_2 . This ratio now has a maximum value that is not coincident with the maximum state of hydration recorded.This maximum coincides with a point at which suddenly, the loss of water begins to affect ϱ_3 much less.Contrary to the results for the bone hydrated in distilled water, very little evaporation time elapses before in absolute terms, ϱ_3 increases much faster than ϱ_2 , and even in this contracted initial region the absolute increase of ϱ_2 is only just greater than that of ϱ_3 .It would therefore appear that to a first approximation the effect of the ionic concentration is to mirror the ϱ_3 -ϱ_2 points in the line of slope unity. This is

disregarding the first peak in the value of ρ_3/ρ_2 since it is probably not real. What primarily needs explaining is the point in the collagen A band evaporation where the effect on ρ_3 against ρ_2 is suddenly reduced. Comparing the results for bone hydrated in distilled water with those for Ringer' Solution it would appear that the loss of free water, and therefore associated increased ionic concentration, increases the resistivity in the bone long direction more than the transverse direction. This occurs right through the dehydration range until a certain point is reached in the evaporation when the reverse starts to happen. It seems very probable that this point corresponds to saturation being reached in the solution and therefore the deposition of ions on the pore surfaces. This would account for the increased conductivity in the bone long direction relative to that in the 2 direction, since the ions would have less effect on the conductivity in the transverse directions due to the difficulty of the charge carriers crossing the pores. One would imagine that the effective ions would be attracted to remaining polar sites on the protein fibrils and the mineral crystals. It is useful to remark here that the results of Chapter Six led us to conclude that the mineral retains its sorped water while the protein is losing its own, so explaining why variations in physical properties in the observed evaporation range are attributed to protein

reactions.Although a noticeable amount of work on the electronic properties of apatites has been done , it is considered that these are not dominant in the observed properties of bone.This is consistent with the bone matrix being the protein and not the apatite.

The quantitative resistivity results on fresh and 'treated' bone indicate that although the treated bone pieces have a higher general resistivity, the effect of treatment is much larger in the labelled 1 direction than it is in the 3 direction.This is consistent with what we have already concluded, namely that the increased pores, produced by the dissolving out of collagen are primarily oriented in the 3 direction.

7.17 Resistivity Results for Stressed Bone

These are shown in Figs. 7.3 to 7.8 and 7.20 and 7.21 . The first six curves represent the measurements made on fresh bone and the others nearly five months after excision.The maximum and minimum values for ρ_1 and ρ_3 stressed and $_1$ unstressed (treated bone) are given below in ohm cms .Except when stated to the contrary the results are bone hydrated in distilled water.All readings should be multiplied by 10^6.

Frosh Bone No.2 (Ringer's sol'n) ρ_1 .1 to 1.57 (125 mins)

Treated Bone No.1 Unstressed ρ_1 .67 to 207 (60 mins).

Treated Bone No.1 T_{11} ρ_1 .16 to 4.6 (60 mins) to 10.8(120 mins)

Treated Bone Nol T_{22} ρ_1 .4 to 12.8(62 mins) to 22(82 mins)

Treated Bone No.2 T_{33} ρ_1 .47 to 22 (67 mins) to 37(87 mins)

Treated Bone No.1 T_{33} ρ_3 .05 to 17 (100 mins)

Treated Bone No.2 T_{33} ρ_3 .2 to 7.5 (90 mins)

It is apparent from the figures on ρ_1 that the application of stress to the wet specimens lowers the resistivity, and in particular the values corresponding to partial dehydration. This is likely due to a change in the pore sizes.

The early resistivity results (Figs. 7.3 to 7.8) carried out simultaneously with the wet piezoelectric measurements, on fresh bone showed that the application of stress in the 3 direction (T_{33}) caused a sudden rise in the rate of increase of ρ_1, unlike applied stress in the two direction T_{22}. These early results indicate the possible occurrence of this sudden change for T_{11}, but it appears that the effect is most definite for stress applied in the bone long direction. This view is substantiated by the graphical results of Figs. 7.20 on 'treated' bone. From the nature and the timing of this sudden change in $\frac{d}{dt}\rho_1$ it is equivalent to the main discontinuity which occurs in the unstressed ρ_3 results. Figs. 21a and b indicate that nothing approaching the main discontinuity occurs in ρ_3 when stress is applied in the bone long direction, although the earlier results

Fig. 7.20a

L.Sp. No.1 H_2O T_{11}

R_1 x10^6 ohms

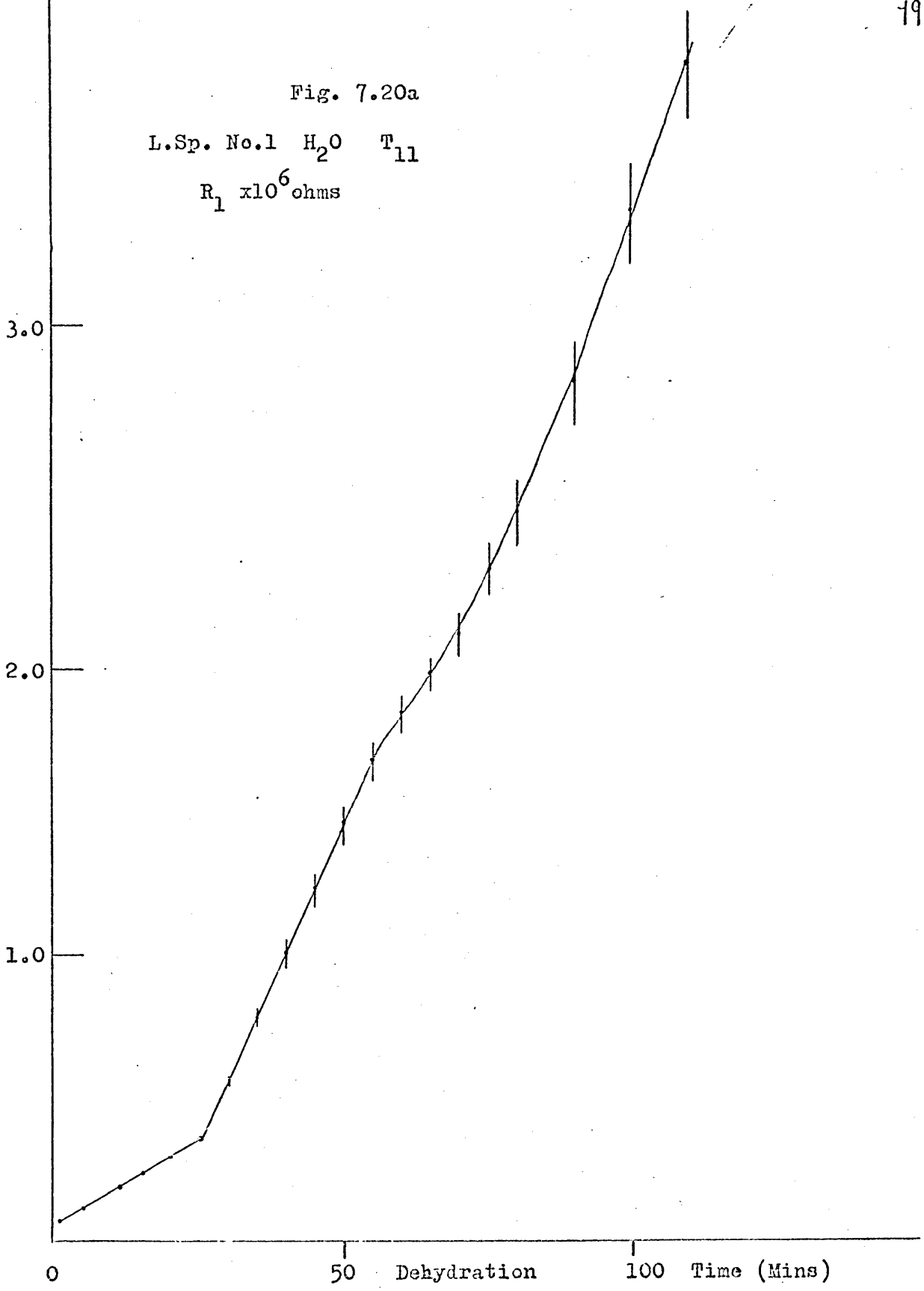

Fig. 7.20b

L.Sp. No.1 H_2O T_{22}

R_1 x10^6 ohms

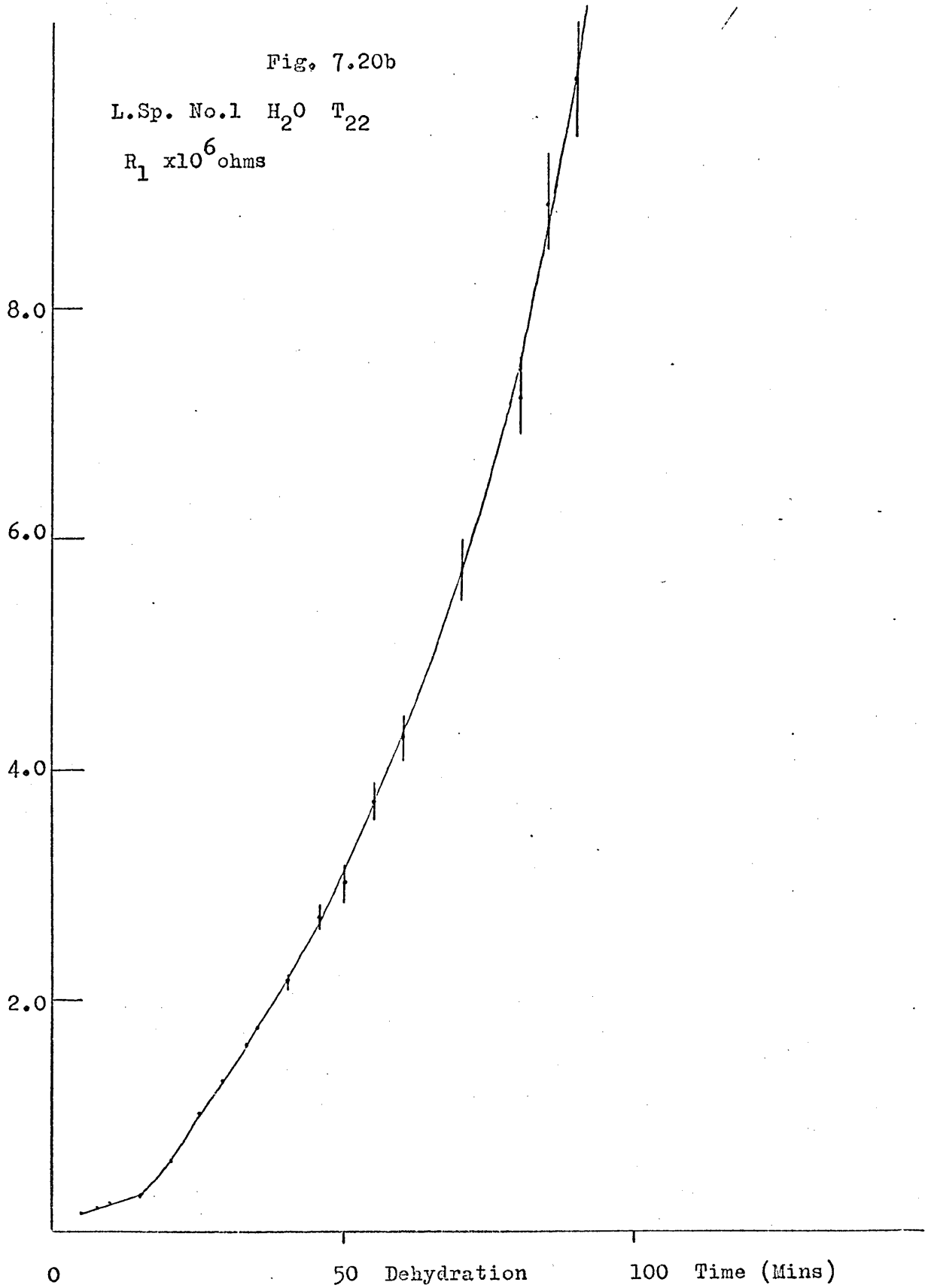

Fig. 7.20c

L.Sp. No.2 H_2O T_{33}

R_1 x10^6 ohms

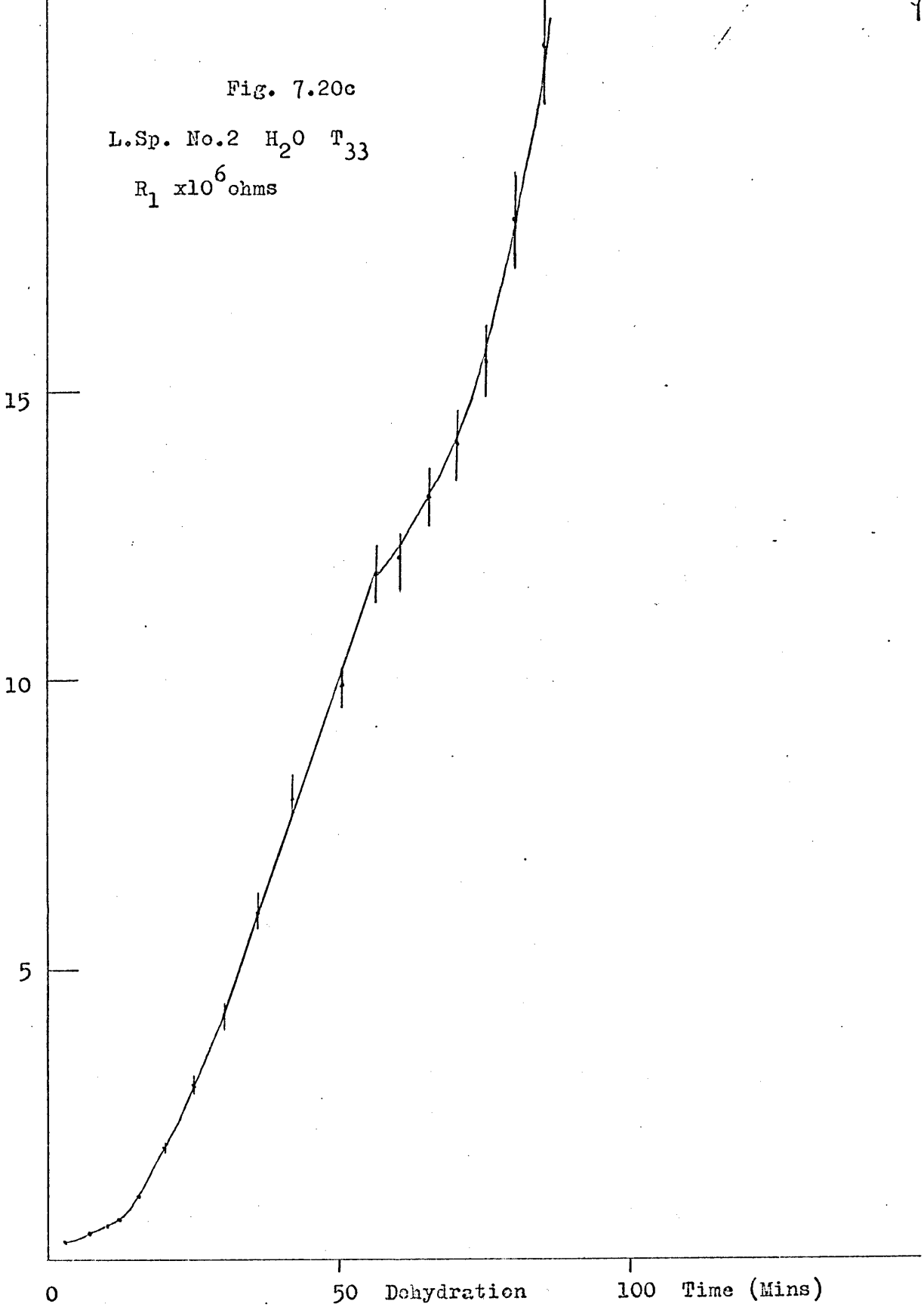

Fig. 7.21a

L.Sp. No.1 H_2O T_{33}

R_3 x10^6 ohms

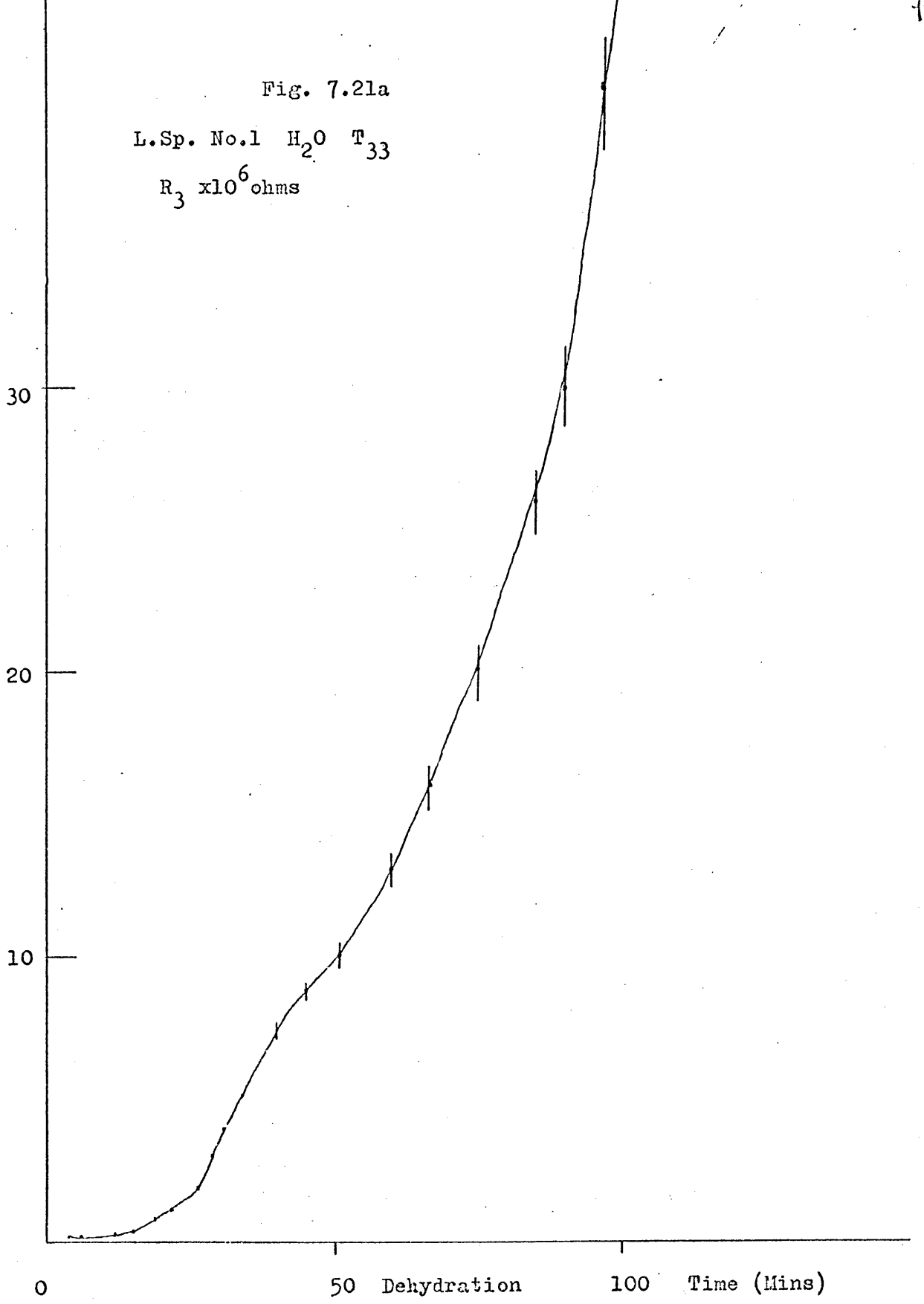

Fig. 7.21b

L.Sp. No.2 H_2O T_{33}

R_3 x10^6 ohms

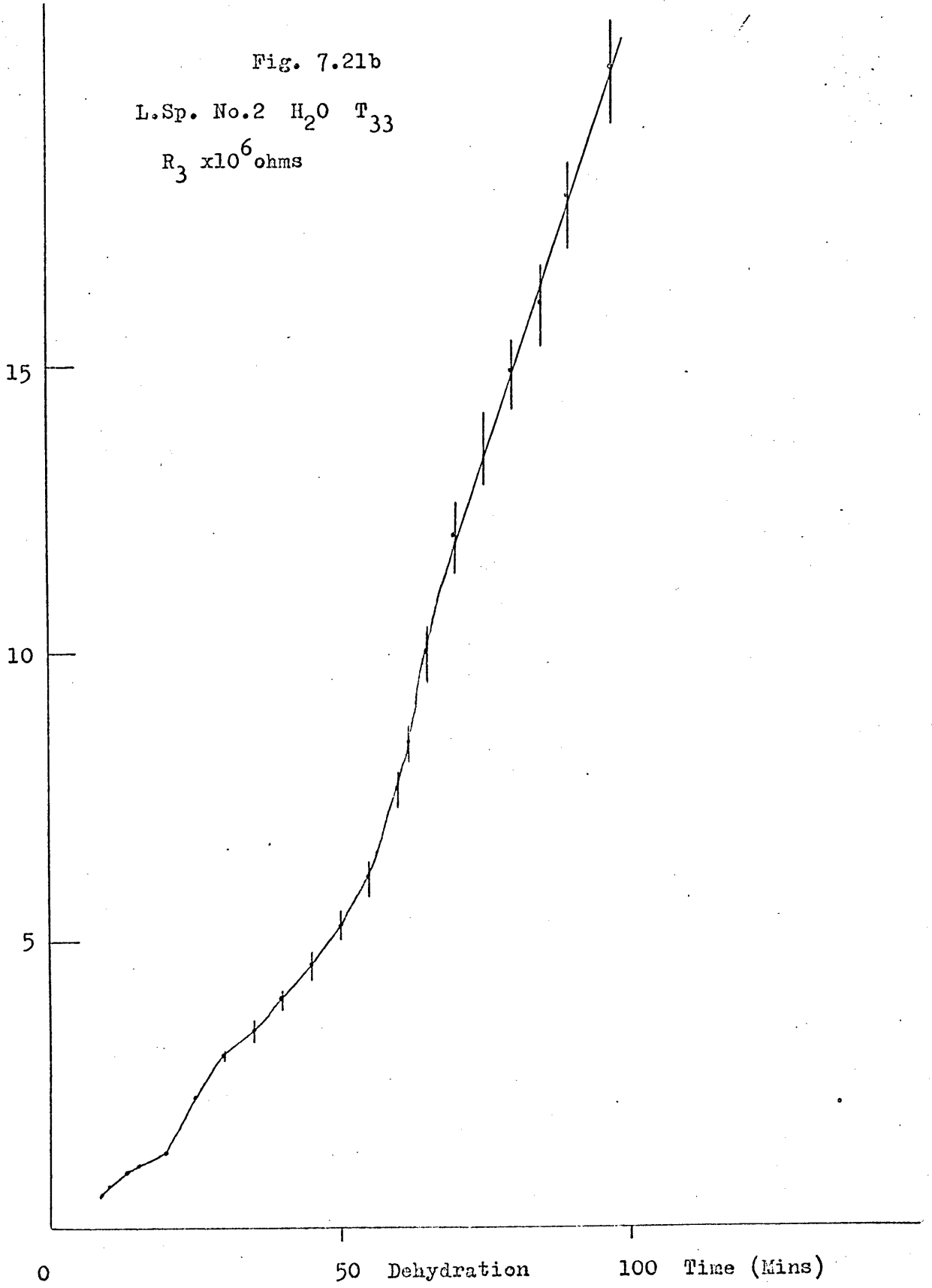

are not accurate to confirm this.They do however show that the main discontinuity does not occur in the labelled 2 direction for the stressed specimens.It thus appears that whereas the discontinuity for the unstressed specimens shows itself in the bone long direction or 3 direction, the application of certain stresses changes this so that it appears in the labelled 1 direction.Since the discontinuity in unstressed bone has been interpreted as showing that the collagen A band bound water is aligned in the fibre long direction unlike that in the B band , it is concluded that the application of stresses T_{11} and T_{33} on the two specimens causes the water in the Collagen A band to re-align itself from the 3 to the 1 direction.The stress and strain analysis carried out for the two bone specimens in which the fibres run obliquely to the bone long direction and are in the 13 plane shows, as expected, that only stresses T_{11} and T_{33} cause the protein fibres to shear against each other.(The analysis is given in the next section 7.18).This therefore indicates as a possible explanation, that the bound water molecules in the collagen A band only realign themselves when sheared.Since only the A bands of the collagen fibril are the regions where the individual collagen macromolecules are strongly bound together by lateral forces, it seems very plausible that it should be in these regions where a shearing strain has

the maximum effect of changing the water's contribution to the conductivity, and the result that the discontinuity appears in the labelled 1 direction and not the two direction is consistent with the existence of a shearing force in the 13 plane causing re-alignment of the water molecules.

If the results for these individual bone specimens are applied to living bone such as a human femur, then under normal everyday skeletal stresses the net orientation of the collagen A band water molecules will be perpendicular to the bone long direction. However for conditions of low bone stress such as exist for bed-ridden persons or astronauts, the resultant orientation will be along the bone long direction and therefore in the same direction as the blood flow through the bone. If some of the mineral crystals are bound to the protein in the collagen A band regions, it appears a possibility that the binding force between the mineral and protein would be decreased when the A band water molecules change their orientation so as to be along the fibre direction instead of perpendicular to it. This would account for the reported loss of bone calcium in bed-ridden patients and astronauts. If this process is correct, then it indicates that the A band water molecules play an important part in binding some of the mineral crystals to the protein. However, it is to be expected that the majority of the mineral

crystals will be bound to the more accessible B band regions where there is less lateral attraction between the collagen macromolecules.It is therefore likely that these crystals hold the neighbouring collagen molecules together in the transverse fibre direction, and are less affected by the reduction in bone stress.This might indicate that only a certain amount of mineral crystals can be lost through loss of stress.

It is reported that when the collagen fibres of connective tissue 'turn a corner' in the body, calcification starts to occur.If, as has been suggested, the protein - mineral binding force is increased when the protein fibres are sheared(due to reorientation of the A band water molecules),this binding force would be increased when the parallel collagen fibres suffered a large change in direction .This indicates that the initial seeding of the mineral may be in the vicinities of the collagen A bands.

We commented at the end of 7.14 that the bone collagen remains classically piezoelectric even for fully hydrated bone. This is because the B band region of the collagen fibril is expected to be responsible for its piezoelectric properties. The results of the first part of this chapter showed that the evaluated d'_{133} of wet bone(which partially arises from the bone collagen's piezoelectric properties) remains constant during

evaporation of the B band water.Hence the B band bone collagen must still be piezoelectric when the bone is fully wet.As expected, this indicates that the existence of water chains , with considerable resultant swelling of the fibres, is necessary to destroy collagen's piezoelectric properties.

7.18 Stress and Strain Analysis of the Bone Specimens.

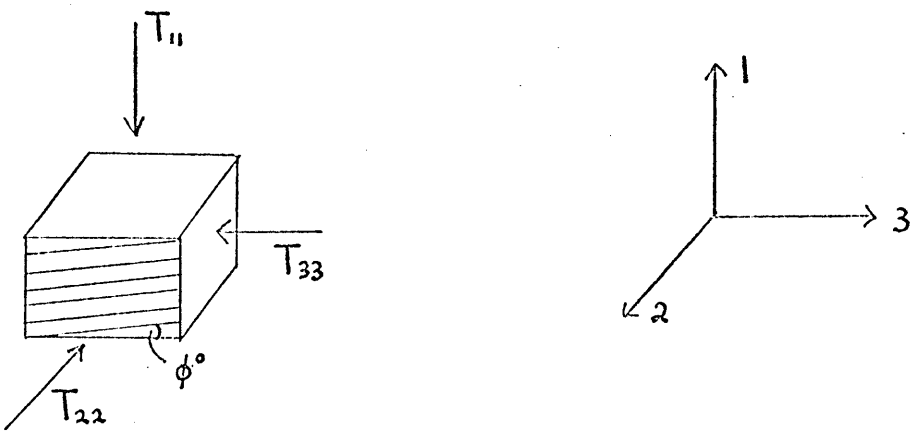

The nomenclature of Chapter 2 is used.The analysis is carried out for the bone specimen depicted above where the protein fibres are predominantly in the labelled 13 plane and make an angle of ϕ° with the 3 axis.We assume for the sake of simplicity that Young's Modulus is the same for the two transverse directions E_t , and that E_3 is the modulus in the bone long direction. Poisson's coefficients are denoted by μ_{mn} . The normal tensor

relations are used.The states of stress suffered by the fibres for the three simple compressive stresses T_{22} , T_{11} , T_{33} are shown below for the same applied stress .

$$T_{ij} = T_{22} \cdot \begin{matrix} 0 & 0 & 0 \\ 0 & 1 & 0 \\ 0 & 0 & 0 \end{matrix}$$

$$T_{ij} = T_{11} \cdot \begin{matrix} \cos^2\phi & 0 & \frac{1}{2}\sin 2\phi \\ 0 & 0 & 0 \\ \frac{1}{2}\sin 2\phi & 0 & \cos^2\phi \end{matrix}$$

$$T_{ij} = T_{33} \begin{matrix} 0 & 0 & -\frac{1}{2}\sin 2\phi \\ 0 & \sin^2\phi & 0 \\ -\frac{1}{2}\sin 2\phi & 0 & \cos^2\phi \end{matrix}$$

The application of stress T_{22} therefore produces no shearing stress on the collagen fibres.The equivalent strain tensors are shown below

$$\frac{S_{ij}}{T_{22}} = \begin{pmatrix} -\frac{\mu_{13}}{E_3} + \cos^2\phi\left(\frac{\mu_{13}}{E_3} - \frac{\mu_{12}}{E_t}\right) & 0 & \frac{1}{2}\sin 2\phi\left(\frac{\mu_{13}}{E_3} - \frac{\mu_{12}}{E_t}\right) \\ 0 & \frac{1}{E_t} & 0 \\ \frac{1}{2}\sin 2\phi\left(\frac{\mu_{13}}{E_3} - \frac{\mu_{12}}{E_t}\right) & 0 & -\frac{\mu_{12}}{E_t} + \cos^2\phi\left(\frac{\mu_{12}}{E_t} - \frac{\mu_{13}}{E_3}\right) \end{pmatrix}$$

$$S_{ij}/T_{11} = \begin{pmatrix} -\frac{\mu_{13}}{E_3} + \cos^2\phi\left(\frac{1}{E_t} + \frac{\mu_{13}}{E_3}\right) & 0 & \frac{1}{2}\sin 2\phi\left(\frac{1}{E_t} + \frac{\mu_{13}}{E_3}\right) \\ 0 & -\mu_{12}/E_t & 0 \\ \frac{1}{2}\sin 2\phi\left(\frac{1}{E_t} + \frac{\mu_{13}}{E_3}\right) & 0 & \frac{1}{E_t} - \cos^2\phi\left(\frac{1}{E_t} - \frac{\mu_{13}}{E_3}\right) \end{pmatrix}$$

$$\frac{S_{ij}}{T_{33}} = \begin{pmatrix} \frac{1}{E_3}\left(1 - \cos^2\phi(1+\mu_{13})\right) & 0 & -\frac{\sin 2\phi}{2E_3}\left(1+\mu_{13}\right) \\ 0 & -\frac{\mu_{13}}{E_3} & 0 \\ -\frac{\sin 2\phi}{2E_3}\left(1+\mu_{13}\right) & 0 & \frac{1}{E_3}\left(\cos^2\phi(1+\mu_{13}) - \mu_{13}\right) \end{pmatrix}$$

We therefore see that the shear strain of the collagen fibres produced by the application of T_{11} or T_{33} is much greater than than that due to T_{22}.

References

1.'On the Piezoelectric Effect of Bone.'E.Fukada.
J.Phys.Soc.Japan. Vol 12. No. 10. Oct 1957.

2.'Piezoelectric Effects in Collagen'. E.Fukada and I.Yasuda.
Jap.J.Appl.Phys. Vol.3 No.2 Feb. 1964.

3.'Piezoelectric Effect in Fibrous Proteins'. E.Fukada.
Reports on Polymer Physics in Japan. 1960. Vol.3 P.168

4.'Piezoelectricity in Polymers and Biological Materials'. E.Fukada.
(To be published)

5.'Piezoelectric Properties of Bone'. J.Dainora.
M.Sc. Thesis. West Virginia University.(U.S.A) 1964

6.'Electron Paramagnetic Resonance in Non-Irradiated Bone.' R.Becker.
Nature. Sep.28. 1963. Vol. 199

7.'Electron Paramagnetic Resonance Spectra of Bone and its Major
Components'. R.Beckerand A.AMarino. Nature. Vol.210. May 7th. 1966.

8.'Evidence For Direct Physical Bonding between the Collagen Fibres
and Apatite crystals in Bone.' A.A.Marino and R.Becker.
Nature. Vol. 213. Feb. 18th. 1967.

9.'Photoelectric Effects in Human Bone'. R.Becker and F.M.Brown.
Nature. Vol. 206.June 26th. 1965.

10.'Florescence of Bone.' C.H.Bachman and E.H.Ellis.
Vol.206. June 26th. 1965.

11 'Light Induced Effects in Bone.' G.M.Spruch and M.H.Shamos. Nature. Vol. 212. Dec. 31st. 1966.

12. 'Dielectric Determination of Bound Water of Bone.' A.A.Marino, R.O.Becker, and C.H.Bachman. Phys. Med. Biol. Vol. 12. No. 3. 1967.

13. 'Pyroelectric Effect in Bone and Tendon.' S.B.Lang. Nature. Vol. 212. Nov. 12th. 1966.

14. 'Generation of Electric Potentials by Bone in Response to Mechanical Stress.' C.A.L.Bassett and R.O.Becker. Science. Vol. 137. Jan 5th. 1963.

15. 'Piezoelectric Properties of Wood.' V.A.Bazhenov. Consultants Bureau. New York. 1961.

16. 'Piezoelectricity of Wood.' E.Fukada. J.Phys.Soc.Japan. Vol. 10. No.2. Feb. 1955.

17. 'Bioelectrical Factors Controlling Bone Structure.' R.O.Becker, C.A.Bassett, and C.H.Bachman. 'Bone Biodynamics' Little, Brown and Co. 1964.

18. 'Physical Bases for Bioelectric Effects in Mineralized Tissues.' M.H.Shamos, and L.S.Lavine. Clinical Orthopaedics. No.35. 1964.

19. 'Electrical and Piezoelectrical Properties of Dental Hard Tissues.' M.Braden, A.G.Bairstow, L.Baider, and B.G.Ritter. Nature. Vol. 212. Dec 31st .. 1966.

20. 'An X-Ray Diffraction Investigation of Swelling by Collagen.' M.A.Roughvie and R.S.Bear. J.Am. Leather. Chem. Assoc. Vol. 48. 1953 P.735

21.'The Structure and Assembly of Collagen Fibrils.' 1 and 2. R.W.Cox, R.A.Grant, and R.W.Horne. J.Roy.Microscop. Soc. Vol.87. June 1967 .

22. 'A Nuclear Magnetic Resonance Study of Collagen Hydration'. H.J.C.Berendsen. Ph.D thesis . Un'ty of Groningen. 1962.

23. 'The Electrical Effects in Bone.' C.A.Bassett. Scientific American. Nov. 1965.

24. 'Morphology of the Osteon.' Cooper, Robinson, et al. J.B.J.S Vol.48A No.7 Oct. 1966

25. 'Arrangement of Collagen Fibres in Secondary Osteons.' J.W.Smith. J.B.J.S 42B. No.3 1960.

26. A.Engström and J.B.Fincan. Nature. Vol. 171. 1953.

27. H.Fernandez-Moran and A.Engström . Biochem. Biophys. Acta. Vol.23.1957 P.264

28. M.J.Glimcher. Rev. Mod. Phys. Vol. 31. 1959. P. 359

29. S.Fitton-Jackson and J.Randall. Nature. Vol.178. 1956. P. 793.

30. Neuman, Toribara, and Mulryan. 1953. (from 12).

31. H.B.Bull. J.Amer.Chem.Soc. Vol 66. 1949.

32. 'The Electrical Properties of Wet Collagen'. J.C.Anderson and C.Eriksson. Nature. Vol. 218. April. 13th. 1968.

33. 'Textbook of Physical Chemistry'. S.Glasstone. New.York. 1947.

34.'Adsorption, Surface Area, and Porosity.'S.J.Gregg , and K.S.W.Sing.

35. H.T.S.Britton and R.A.Robinson. J.Chem.Soc. 1931. P.1456.

36. J.H.Bowes and R.H.Kenten. Biochem.J. Vol. 43. 1948.P.358

37.'The Chemistry and Reactivity of Collagen.' K.H.Gustavson. Academic Press. 1956.

38. 'Nature and Structure of Collagen.' Ed. J.T.Randall. Butterworths. 1953

39. J.Boek, A.M.Sookne. J.Res. Nat. Bur. Stands. Vol. 23 1939. P.271

40. 'A Modified Micro-Apparatus for Electrophoresis.' H.Douglas . J.Chem. Soc. Vol.24 April 1947 .

41.'Electrophoresis of Proteins.'A. Abraham , and M.Gorin. Rheinhold Co. 1942.

42. 'Buffer Solutions for Electrophoresis'. G.L.Miller and R.H.Golder. Archiv. Biochem and Biophys. Vol. 29. 1950. P.420

43. 'Advances in Protein Chemistry'. W.F.Harrington and P.H.Von Hippel. Vol. 16. 1961.

44. 'Collagen Hydration'. E.M.Bradbury, R.E.Burge, J.T.Randall, and G.R.Wilkinson. Disc. Far. Soc. Vol. 25. 1958. P173.

45. N.G.Esipova, N.S.Andreeva, and T.V.Gatovskaja.
Biofizika. Vol. 3 . 1958. P.530

46.W.Grassman, K.Hannig, and A.Nordwig. 'The Nonpolar region of the Collagen molecule Six Amino Acid sequences. Z.Physiol.Chem. Vol. 333. 1963.

47.A.Rich and F.H.C. Crick. 'The Molecular structure of Collagen, J.Mol.Biol. Vol.3 1961. P.483.

48. 'Piezoelectricity'.W.G.Cady. Dover Publ. New York. 1964

49. 'Piezoelectric Crystals and their Applications to Ultrasonics.' Van Nostrand. 1950. W.P. Mason .

50.'Comparative Studies of the Organic Matrices of Invertebrate Mineralized Tissues.' D.F.Travis, C.J.Francois, L.C.Bonar, and M.J.Glimcher. J.Ultrastr. Res. Vol. 18. 1967. P.550

51.'An Electron Microscope Study on Primary Periosteal Bone.' A.Ascenzi, E.Bonucci, and D.Steve Bocciarelli. J.Ultrastr.Res. Vol. 18. 1967. P.605

52. 'Coloured Symmetry.' A.V.Shubnikov, andN.V.Belov. Pergamon Press. 1964.

53. S.Brunaer, P.Emmett, and E.Teller. J.Amer.Chem.Soc. Vol. 60. 1938. P309.

(*Reprinted from Nature, Vol.* 218, *No.* 5137, *pp.* 166–168, *April* 13, 1968)

Electrical Properties of Wet Collagen

THE electrical properties of dried collagen and bone have been studied by Fukada and Yasuda[1,2]. Both were shown to be piezoelectric, producing a measurable potential between opposite faces when stressed and also deforming on application of a voltage. The piezoelectric coefficients d_{14} belonging to the polycrystalline point group ∞ were found for collagen, and the values reported for d_{14} were about the same as d_{11} in quartz. Because both tendon and bone are bathed in ionic fluid of high conductivity when *in vivo*, it was decided that the electrical activity of wet collagen should be examined.

The specimens chosen were human Achilles tendons which were stored in Ringer solution in a domestic refrigerator. This tendon consists of collagen fibres, largely parallel to the long axis of the tendon, which typically was 5 cm long and 8 mm in diameter. Because of this structure there is a large number of fine capillary channels throughout the length of the specimen, through which liquid can flow. When the tendon is stretched, liquid is squeezed out and will stream back into the specimen when it is relaxed. Such movement of ionic fluid gives rise to a streaming potential and it is necessary to design an experiment in which streaming potential can be separated from any piezoelectric potential that might be present.

The mechanism of streaming potential at its simplest depends on the absorption of one type of ion on the surface of the molecule, with an associated diffuse layer of ions of the opposite type extending out from the molecular surface. When the liquid streams past the molecule there is a net transport of one type of ion with a resulting potential gradient, which may be measured by means of electrodes placed in the stream. The magnitude of the streaming potential is dependent on the type of molecule and the *p*H of the solution. At a given *p*H, the isoelectric point, the concentration of ions is such that as many positive as negative ions are absorbed on the molecule and the streaming potential is then zero.

The piezoelectric potential is dependent only on the strain applied to the molecule and may be expected to be independent of the *p*H of the surrounding solution. If any charges appear on the surface of the strained fibre, caused by the piezoelectric effect, they will rapidly be cancelled by ions of opposite polarity absorbed from the solution. This would result in a change in the isoelectric point.

Thus, in order to separate the two effects experimentally, the tendon should be strained and the potential developed

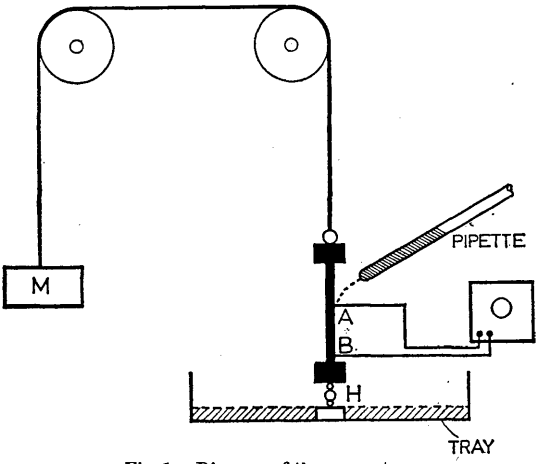

Fig. 1. Diagram of the apparatus.

between two electrodes buried into it measured, with the *p*H of the surrounding solution varied through the isoelectric point. If potentials were observed at the normal isoelectric *p*H for collagen they would be attributable to piezoelectric effects.

The apparatus is shown diagrammatically in Fig. 1. The tendon was anchored to a brass hook *H* by means of a stainless steel wire suture at the lower end. The upper end was attached to piano wire, also by stainless steel wire, which passed over two pulleys and was attached to the mass *M*. Freshly made Ag-AgCl electrodes were buried into the tendon, 3 cm apart, by injecting them through a fine glass capillary tube and subsequently withdrawing the tube. The leads from the electrodes were taken to an oscilloscope with a storage screen, having a sensitivity of 1 mV/cm^{-1}.

The tendon was prepared by allowing it to dry in a desiccator at room temperature until it was stiff, brittle and pale yellow in colour. It was then immersed in a solution of known *p*H, prepared from standard buffer solution (BDH), for a period of 24–48 h until it became completely flabby. When mounted in the apparatus a slow drip of the same solution was directed over it so that the whole length of the tendon was bathed in solution, to prevent it drying.

To obtain readings a standard impulse was applied to the specimen by allowing the mass *M*, 2–10 kg, to fall through a fixed distance of 1 in. The resulting electrical pulse was displayed on the oscilloscope. The value recorded was the steady pulse amplitude obtained after repeated loading at approximately 1 impulse s^{-1} for 10–15 s.

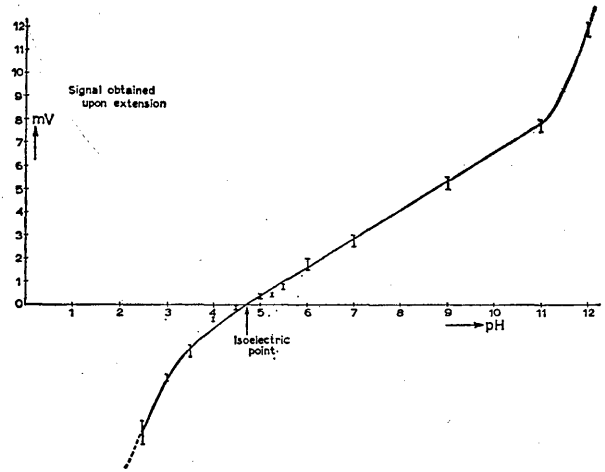

Fig. 2. The peak value of the voltage pulse as a function of the *p*H of the solution.

In agreement with ideas of a streaming potential the signal obtained was proportional to the load and at *p*H 4·7 no signal was obtained whatever the force applied. A graph of the peak value of voltage pulse against *p*H of the solution is shown in Fig. 2.

While isoelectric points for rat-tail and hide collagen have been reported in the literature[3–6], no information was available on human Achilles tendon collagen. Accordingly, measurements were carried out on the tendons used in the foregoing measurements by micro-cell electrophoresis using a commercial apparatus.

The tendon was dried and ground up, using fine glass-paper and a homogenizer. The mean particle size was estimated to be approximately 20μ, and specimen solutions were made up by adding powder to the recommended buffer solutions for electrophoresis[7], covering the range of *p*H values 3·5 to 10.

The cell was calibrated by plotting the particle velocity against depth using red blood cells in the bare cell and when the cell was coated with haemoglobin. The electrophoretic velocity of particles with a current of 5 mA passing through the solution cell is plotted against *p*H in Fig. 3 for an ionic strength of 0·05 M. Because an applied electric field has no effect on the particles at a *p*H value of 4·7, this is taken to be the isoelectric point for human Achilles tendon.

The coincidence of the isoelectric point with the *p*H for zero electrical impulse potential indicates that the impulse potentials involved are caused by streaming potentials only, there being no contribution from the piezoelectric effect. This is further supported by the general similarity

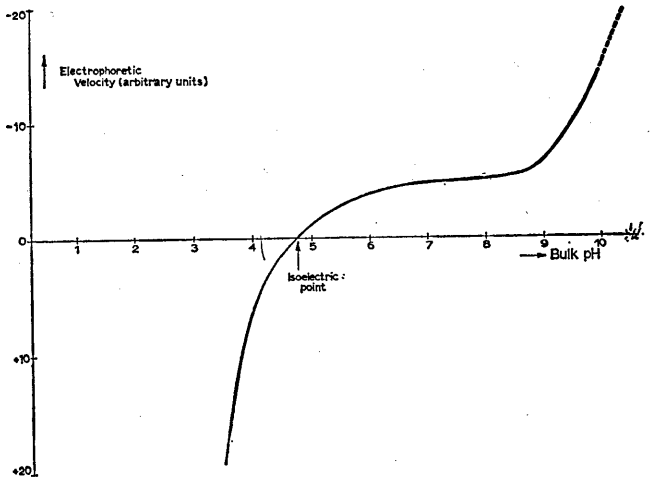

Fig. 3. The electrophoretic velocity of tendon particles, with a current of 5 mA passing through the cell, as a function of pH.

in the shapes of the curves of Figs. 2 and 3. It is therefore concluded that the piezoelectric effect is absent from the completely wet collagen.

The ability of a material to exhibit piezoelectricity is a function of its crystal symmetry.

Fukada[1] measured the piezoelectric coefficients d_{14} and d_{25} $(= -d_{14})$ for dried bone, defined by the equation

$$d_{ij} = \frac{\partial s_j}{\partial E_i}$$

where s is strain and E electric field; the subscripts denote the axes along which d is measured with respect to field and strain. The d coefficients found corresponded to the non-polar, polycrystalline point group $\infty : 2$ $(\infty/2)$. For dry Achilles tendon, Fukada found coefficients corresponding to the point group ∞. Of the seven possible point groups for polycrystalline materials, Sh'ubnikov[8] has shown that only the groups ∞, $\infty : 2$ and $\infty . m$ can exhibit piezoelectricity. (These correspond to point groups 6, $6mm$ and 622 and 4, $4mm$ and 422, respectively, in matrix notation.)

We thought it curious that bone should belong to a point group having a higher symmetry than that of its main constituent collagen, especially as its other constituent, hydroxyapatite, is centro-symmetrical and therefore is not piezoelectric. Accordingly, work was carried out to check the results on dry human bone using Fukada's method. Unlike Fukada's work, however, no heat was applied in drying the specimens; silica gel was used instead. It was found that the results could be

explained purely in terms of those coefficients found for tendon collagen if one took into account the orientation of the collagen fibres relative to the long axis of the human femur, which was used in the study. The result is that, statistically speaking, the collagen fibres may be said to exhibit conical symmetry with respect to the long direction of the bone femur. The apical angle depends on how many fibres lie parallel to the axis of the osteon and how many lie circumferentially, and whether the osteons themselves spiral along the direction of the long axis. Hence the coefficients found by Fukada for parallel tendon fibres were transferred to the new system of co-ordinates where the new 3′ axis spiralled around the old 3 axis. It was found that an apical angle of 13° gave the best agreement with the practical results. Thus both dry bone and dry collagen are allocated to the point group ∞.

These results with wet collagen imply that, because it exhibits no piezoelectric effect, it belongs to a group of higher symmetry than does the dry material. The structure of collagen has been described by Ramachandran[9]. The difference between dry and wet states is brought about by the incorporation of bound water in the wet material. Harrington and von Hippel[10] state that the crystallinity of collagen, as revealed by X-ray studies, is destroyed by dehydration, and Bradbury *et al.*[11] demonstrated that systematically disposed water molecules, in the collagen, constitute an important part of the diffracting structure. Esipova *et al.*[12] also found that hydration increased the crystallinity of collagen and inferred that the oxygen atoms of water, bound to the ordered portion of the collagen structure, lie close to the axis of the polypeptide chains and are arranged in a semi-regular fashion along the chains. It is thus reasonable to expect that the incorporation of water increases the symmetry of the collagen molecule. Until the precise arrangement of the water molecules within the collagen framework is known, however, it is not possible to allocate it to a particular symmetry group. The absence of piezoelectricity, however, indicates that it should belong to one of the groups $\infty : m$, $m.\infty : m$, ∞/∞, $\infty/\infty.m$, the first two groups being the most likely.

This work was supported by a grant from the Medical Research Council. We thank Dr Forester, of the Chester Beatty Research Institute, who carried out the electrophoretic measurements, Dr M. A. R. Freeman who supplied the specimens and Miss B. Rothberg who assisted with the early experimental work.

J. C. Anderson
C. Eriksson

Department of Electrical Engineering,
Imperial College of Science and Technology,
London.

Received March 5, 1968.

[1] Fukada. E., and Yasuda, I., *J. Phys. Soc. Japan*, **12**, 1159 (1957).
[2] Fukada, E., and Yasuda, I., *Jap. J. App. Physics*, **3**, 117 (1964).
[3] Bower, J. H., and Kenten, R. H., *Biochem. J.*, **43**, 358 (1948).
[4] Gustavson, K. H., *The Chemistry and Reactivity of Collagen* (Academic Press, 1956).
[5] Randall, J. T., *Nature and Structure of Collagen* (Butterworths, 1953).
[6] Beek, J., and Sookne, A. M., *J. Res. Nat. Bur. Stand.*, **23**, 271 (1939).
[7] Hiller, G. L., and Golder, R. H., *Arch. Biochem. Biophys.*, **29**, 420 (1950)
[8] Sh'ubnikov, A. V., and Belov, N. V., *Coloured Symmetry* (Pergamon Press, 1964).
[9] Ramachandran, G. N., *Intern. Rev. Connective Tissue Research*, **1**, 127 (1963).
[10] Harrington, W. F., and von Hippel, P. H. *Advances in Protein Chemistry*, **16**, 1 (1961).
[11] Bradbury, E. M., Burge, R. E., Randall, J. T and Wilkinson, G. R., *Disc. Faraday Soc.*, **25**, 173 (1958).
[12] Esipova, N. G., Andreeva, N. S., and Gatovskaja, T. V., *Biofizika*, **3**, 530 (1958).

Printed in Great Britain by Fisher, Knight & Co., Ltd., St. Albans.